

Thwarting Adversaries with Unpredictability:
Massive-scale Game-Theoretic Algorithms for Real-world Security Deployments

by

Manish Jain

A Dissertation Presented to the
FACULTY OF THE USC GRADUATE SCHOOL
UNIVERSITY OF SOUTHERN CALIFORNIA
In Partial Fulfillment of the
Requirements for the Degree
DOCTOR OF PHILOSOPHY
(COMPUTER SCIENCE)

August 2013

Acknowledgments

Today, I stand on the advise and support of many people. My research style, skills and direction has been forged after many discussions with my advisor, colleagues, friends and family. I would like to give a special thanks to my advisor Milind Tambe without whom I would not be the researcher I am today and this thesis would probably be non-existent. Milind, I thank you for your unending dedication to my progress and success, and for the countless hours you have spent on having discussions with me, advising me, debating with me, correcting my unpolished drafts and advertising my finished results. I have thoroughly enjoyed my PhD process, and a whole lot of credit goes to just you. You taught me what it meant to do research. You gave me the opportunity to work on a problem where I could see my research in action – a thought that still gives me goosebumps. I appreciate and thank you for how you sought out opportunities for awards, presentations and collaborations for me. I admire you for helping me grow as a presenter of my work. I still remember the rather embarrassing presentation at the Preference Handling Workshop at AAAI, 2008 when I was so nervous that I ran through my slides in about 10 minutes in a 25 minute slot – it has been a journey of progress since then. I also praise you for your efforts you put to maintain an active social life in the group with our coffees, lunches, dinners, boat cruises and retreats, and how you keep engaged with the alumni of our research group. I cannot even begin to

enumerate the things that I have learnt from you and would hopefully be emulating in my research career as I move forward.

I would also like to thank other members of my thesis committee, namely, Fernando Ordóñez, Vincent Conitzer, Bhaskar Krishnamachari and Mathew McCubbins for their helpful feedback and guidance. A special thanks to Fernando, since he was a tremendous guide to me when I started my research on developing scalable algorithms. You introduced me to large-scale optimization techniques of Operations Research, a tool that I have used extensively throughout my thesis work. We have collaborated since 2008 and I hope that our collaboration extends much further. Similarly, I would like to especially thank Vince for all his help through the years. You have been a part of multiple research efforts that have constituted my work, and this thesis would definitely not be in its current shape without you.

I would also like to thank the many collaborators I have had over the years. Apart from Milind, Fernando and Vince, I have been fortunate enough to work along with many researchers. I thank all of them whole-heartedly. This lists includes Sarit Kraus, Makoto Yokoo, Kevin Leyton-Brown, Christopher Kiekintveld, Matthew E. Taylor, Bo An, Albert Xin Jiang, James Pita, Jason Tsai, Eric Shieh, Ondřej Vaněk, Zhengyu Yin, Branislav Bošanský, Michal Pěchouček, Dmytro Korzhyk, Rong Yang, Erim Kardes and Jun-young Kwak, among others. I also thank all the students who worked on developing the software assistants ARMOR and IRIS, including Christopher Portway, Craig Western, Shyamsundar Rathi, Parth Parimal Shah, You Zhou and Ripple Goyal.

I would also like to thank CREATE and the Federal Air Marshals Service for help and support over the years. They provided me not just the real-world problems of research interest, but also with the unique opportunity of deploying my research. My special thanks goes to James Curren of the Federal Air Marshals Service for his continued support of my research. I also want to thank

Isaac Maya and Erroll Southers for their tireless promotion of game-theoretic randomization as the preferred approach for real-world security scheduling. I also thank my colleagues at USC and the entire Teamcore family. You have all helped make my PhD experience unique and fun for these many years. I especially thank James Pita, Jason Tsai, Jun-young Kwak, Zhengyu Yin, Rong Yang, Matthew Brown and Eric Shieh for you have all made my stay at USC special. I would also like to thank all the students I have advised for their inputs on my advising style and shortcomings.

Finally, I would like to thank my family and friends who have been a tremendous support for all these years. To my father Sudhir Jain, my mother Nilam Jain, my sister Mahima Jain and my grandma Nirmala Jain, you have all been always supportive of all my endeavors. Special thanks to my cousin Ripple Goyal for being there at USC for the past two years, you helped me especially in times when I was stressed and also treated me with great home-cooked food. I also would like to thank my friends William Yeoh, Nilesh Mishra, Vivek Kumar Singh and Megha Gupta who have all been a part of my life at USC. Thank you everyone for assisting me in pushing my limits and exploring the world around me. Without the unconditional love and support of all these people I would not have been able to get to where I am today.

Table of Contents

Acknowledgments	ii
List of Figures	viii
Abstract	xii
Chapter 1: Introduction	1
1.1 Problem Addressed	2
1.2 Contributions	6
1.2.1 ASPEN	7
1.2.2 RUGGED and SNARES	9
1.2.3 HBGS and HBSA	11
1.2.4 $d:s$ and Phase Transition	12
1.2.5 Real World Applications: ARMOR and IRIS	13
1.3 Guide to thesis	14
Chapter 2: Background	15
2.1 Motivating Domains	15
2.1.1 Los Angeles International Airport (LAX):	16
2.1.2 United States Federal Air Marshals Service (FAMS):	17
2.1.3 United States Transportation Security Agency (TSA):	17
2.1.4 United States Coast Guard:	18
2.2 Stackelberg Games	19
2.3 Strong Stackelberg Equilibrium (SSE)	21
2.4 Stackelberg Security Games	23
2.5 Security Problems with Arbitrary Scheduling Constraints (SPARS)	27
2.6 Security Problems with Patrolling Constraints (SPPC)	29
2.6.1 Payoff Structure	31
2.7 Game Model 1: Multiple Attackers	32
2.8 Network Security Domain	33
2.9 Baseline Algorithms	35
2.9.1 Multiple LPs approach	35
2.9.2 DOBS: Mixed Integer Linear Program	36
2.9.3 ERASER Mixed Integer Linear Program	38
2.9.4 RANGER solution approach	39

Chapter 3: Strategy Generation for One Player	40
3.1 SPARS domain	40
3.1.1 ASPEN Column Generation	43
3.1.1.1 Master Problem:	43
3.1.1.2 Slave Problem:	45
3.1.2 Improving Branching and Bounds	47
3.2 Column generation for joint patrolling schedules	51
3.3 SPPC Domain	53
3.3.1 Column Generation:	54
3.3.1.1 Master Formulation:	54
3.3.1.2 Slave Formulation:	55
3.4 Experimental Results	57
3.4.1 Comparison Results	57
3.4.2 ASPEN on Large SPARS Instances:	59
Chapter 4: Strategy generation for both players	63
4.1 RANGER Counterexample	63
4.2 RUGGED	67
4.2.1 Algorithm Description	67
4.2.2 CoreLP	69
4.2.3 Defender Oracle	70
4.2.4 Attacker Oracle	74
4.3 Evaluation of RUGGED	79
4.3.1 Comparison with RANGER	80
4.3.2 Scale-up and analysis	81
4.3.3 Algorithm Dynamics Analysis	83
4.4 SNARES	84
4.4.1 Algorithm Description	84
4.4.2 Warm-starting using mincut-fanout	87
4.4.3 Using "Better" Responses	88
4.4.3.1 Better Response for the Defender	88
4.4.3.2 Better Response for the Attacker	93
4.4.4 Evaluation of SNARES	95
4.4.4.1 Analysis of Components of SNARES	95
4.4.4.2 Scalability in Simulation:	98
4.4.4.3 Real Data	100
Chapter 5: Solving Bayesian Games	102
5.1 Solving Bayesian-SPNSC Problem Instances	102
5.1.1 Bayesian Game Computation	103
5.1.2 HBGS Solution Methodology	105
5.1.2.1 Hierarchical Type Trees	105
5.1.2.2 Pruning a Bayesian Game	107
5.1.2.3 HBGS Description	110
5.1.3 Experimental Results	113

5.1.3.1	HBS Scale-up	114
5.1.3.2	Approximations	117
5.2	Solving Bayesian-SPARS Problem Instances	118
5.2.1	Bayesian-ASPEN	118
5.2.1.1	Bayesian-ASPEN Column Generation	119
5.2.1.2	Improving Branching and Bounds	121
5.2.2	Experimental results	122
5.2.2.1	Scale-up in number of targets:	122
5.2.2.2	Scale-up in number of types:	123
5.2.2.3	Effects of using different hierarchies	123
5.2.2.4	Different arrangement of types in HBSA	125
5.3	Bayesian SPPC Domain	127
5.3.1	Master Formulation	128
5.3.2	Slave	129
Chapter 6: <i>d:s</i> and Phase Transition		131
6.1	Deployment to Saturation Ratio	134
6.1.1	SPNSC Domain	135
6.1.1.1	General sum representation.	135
6.1.1.2	Security game compact representation.	137
6.1.2	SPARS Domain	138
6.1.3	SPPC Domain	140
6.2	Implications of the findings	140
6.3	Phase Transitions	142
6.3.1	Phase Transitions in Security Games	144
Chapter 7: Related Work		149
7.1	Computation in Stackelberg Security Games	149
7.1.1	Efficient computation of Stackelberg equilibria	150
7.1.2	Stackelberg equilibria modeling humans	154
7.1.3	Computation of robust solutions	155
7.2	Stackelberg games in other security scenarios	155
7.3	Other optimization techniques for security domains	156
Chapter 8: Conclusions		158
8.1	Contributions	160
8.2	Future Plans	162
8.2.1	Scalable behavioral game theory	162
8.2.2	Stochastic coalitional game theory	163
8.2.3	Spatiotemporal game theory	164
Bibliography		166

List of Figures

1.1	The image shows examples of three domains which have inspired my research: in all these three domains, security agencies need to deploy limited resources to protect from potential adversaries.	2
1.2	The image shows examples of three security domains where my research has been successfully applied	7
1.3	The figure shows the screenshots of ARMOR and IRIS, the deployed software assistants.	14
2.1	Example 1	33
3.1	Working of Branch and Price for a non-Bayesian SPARS problem instance. . . .	41
3.2	Example Minimum Cost Network Flow Graph for a SPARS problem instance. . .	47
3.3	This figure shows an example network-flow based slave formulation. There are as many levels in the graphs as the number of targets. Each node represents a specific target. A path from the source to the sink maps to a tour taken by the defender. . .	57
3.4	Comparison between ERASER-C, ASPEN and BnP for SPARS problem instances with 10 resources. The number of schedules for these experiments was two times the number of targets. In this figure and others with y-axis on the log scale, error bars are not shown since they are not prominent because of the logarithmic axis. In this experiment, the difference in runtime for all pair-wise comparisons was statistically significant except between ERASER-C and ASPEN for 40 and 50 targets.	59
3.5	These figures present results comparing the runtime required by ASPEN, ASPEN without the ORIGAMI-S branch-and-bound heuristic (BnP) and ERASER-C with column generation on SPARS instances with 2 schedules per target. The y-axis shows the runtime in seconds in log scale, whereas the x-axis varies an input parameter, as specified in the figure. Again, we do not show the error bars because of the log scale of the y-axis, but ASPEN was the fastest algorithm with statistical significance.	60

3.6	These figures present the runtime results for ASPEN when the size of the input problem is scaled. The y-axis shows the runtime in seconds, whereas the x-axis varies an input parameter, as specified in the figure.	62
4.1	This example is solved <i>incorrectly</i> by RANGER. The variables a, b are the coverage probabilities on the corresponding edges.	64
4.2	The possible allocations of two resources to the four edges. The blocked edges are shown in bold. The probabilities (x or y) are shown next to each allocation. . . .	65
4.3	A <i>defender oracle</i> problem instance corresponding to the SET-COVER instance with $U = \{1, 2, 3\}$, $\mathcal{S} = \{\{1\}, \{2\}, \{3\}, \{1, 2\}, \{1, 3\}\}$. Here, the attacker's mixed strategy uses three paths: $(e_1, e_{1,2}, e_{1,3}, e'_1)$, $(e_2, e_{1,2}, e'_2)$, $(e_3, e_{1,3}, e'_3)$. Thus, the SET-COVER instance has a solution of size 2 (for example, using $\{1, 2\}$ and $\{1, 3\}$); correspondingly, with 2 resources, the defender can always capture the attacker (for example, by covering $e_{1,2}, e_{1,3}$).	71
4.4	An example graph corresponding to the CNF formula $(x_1 \vee \neg x_2 \vee \neg x_3) \wedge (x_1 \vee x_2 \vee x_4)$	75
4.5	Example graph of Southern Mumbai with 455 nodes. Sources are depicted as green arrows and targets are red bulls-eyes. Best viewed in color.	78
4.6	Results. Figure (a) shows the scale-up analysis on WFC graph of different sizes. Figure (b) shows the convergence of oracle values to the final game value and the anytime bounds. Figure (c) compares the runtimes of oracles and the core LP. . .	81
4.7	Comparison between SNARES and state-of-the-art: SNARES can now scale to solve problems the size of full cities where previous work could only scale to the southern tip of Mumbai.	85
4.8	Flow Chart for the SNARES Algorithm	85
4.9	The contributions of individual components of SNARES. RUGGED is used as a baseline.	95
4.10	The runtime required by SNARES as the input problem size is varied.	95
4.11	Varying Number of targets.	99
5.1	Example tree representing the pure strategies for the attacker in a Bayesian Stack-elberg security game.	104

5.2	Examples of possible hierarchical type trees generated in Hbgs. The root node is the original Bayesian-SPARS problem instance, $G(\Theta, \Psi^\Lambda)$. Every other node is a restricted Bayesian game. Figure 5.2(a) shows a depth-one partitioning, where $G(\Theta, \Psi^\Lambda)$ is decomposed into four restricted games $G(\Theta, \Psi^{\Lambda_i}), i \in \{1..4\}$. Figure 5.2(b), on the other hand, shows the full binary partitioning where the original $G(\Theta, \Psi^\Lambda)$ is decomposed into two restricted games, which are then further re-decomposed into two smaller restricted games.	107
5.3	This plot shows the comparisons in performance of the four algorithms when the size of the input problem is scaled.	114
5.4	This plot shows the comparisons of Hbgs and its approximation variants.	118
5.5	This plot shows the comparisons in performance of the three algorithms when the input problem is scaled.	122
5.6	A Depth-Two tree for 8 attacker types.	124
5.7	The figure shows the impact in runtime when the distribution of trees is varied in the hierarchy used in HBSA. These results are for 8 attacker types. While I do not show the error bars in this figure as well, depth-two hierarchy was faster for 10 and 15 targets whereas full binary hierarchy was faster for 20 targets with statistical significance.	126
5.8	The figure shows the impact in runtime when the distribution of types is varied in the hierarchy used in HBSA. We, again, do not show the error bars because of the log scale of the y-axis but the similar type arrangement was faster than the dissimilar type arrangement for 10, 15 and 20 targets with statistical significance.	128
6.1	Average running time of DOBSS, ASPEN and multiple-attacker branch-and-price algorithm for SPNSC, SPARS and SPPC domains respectively.	133
6.2	Average runtime of computing the optimal solution for a SPNSC problem instance. The vertical dotted line shows $d:s = 0.5$	136
6.3	Average runtime of computing the optimal solution for a SPARS game using ASPEN. The vertical dotted line shows $d:s = 0.5$	138
6.4	Average runtime for computing the optimal solution for a patrolling domain. The vertical dotted line shows $d:s = 0.5$	139
6.5	The difference between expected defender utilities from ERASER and a naïve randomization policy. The vertical line shows $d:s = 0.5$	143

6.6	Average runtime of computing the optimal solution for a SPNSC problem instance. The vertical dotted line shows $d:s = 0.5$	145
6.7	Average runtime of computing the optimal solution for a SPARS game using ASPEN. The vertical dotted line shows $d:s = 0.5$	146
6.8	Average runtime for computing the optimal solution for a patrolling domain. The vertical dotted line shows $d:s = 0.5$	147
6.9	ERASER results with varying number of attacker types.	147
6.10	Probability that the decision problem $SSE(D^*)$ is soluble for SPNSC instances of three problem sizes. The phase transition gets sharper as the problem size increases.	148

Abstract

Protecting critical infrastructure and targets such as airports, transportation networks, power generation facilities as well as critical natural resources and endangered species is an important task for police and security agencies worldwide. Securing such potential targets using limited resources against intelligent adversaries in the presence of the uncertainty and complexities of the real-world is a major challenge. My research uses a game-theoretic framework to model the strategic interaction between a defender (or security forces) and an attacker (or terrorist adversary) in security domains.

Game theory provides a sound mathematical approach for deploying limited security resources to maximize their effectiveness. While game theory has always been popular in the arena of security, unfortunately, the state of the art algorithms either fail to scale or to provide a correct solution for large problems with arbitrary scheduling constraints. For example, US carriers fly over 27,000 domestic and 2,000 international flights daily, presenting a massive scheduling challenge for Federal Air Marshal Service (FAMS).

My thesis contributes to a very new area that solves game-theoretic problems using insights from large-scale optimization literature towards addressing the computational challenge posed by real-world domains. I have developed new models and algorithms that compute optimal strategies for scheduling defender resources in large real-world domains. My thesis makes the following

contributions. First, it presents new algorithms that can solve for trillions of actions for both the defender and the attacker. Second, it presents a hierarchical framework that provides orders of magnitude scale-up in attacker types for Bayesian Stackelberg games. Third, it provides an analysis and detection of a phase-transition that identifies properties that makes security games hard to solve.

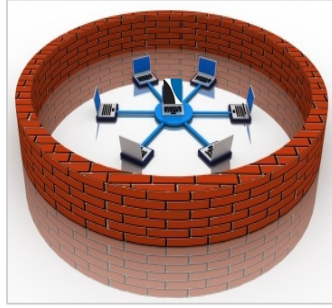
These new models have not only advanced the state of the art in computational game-theory, but have actually been successfully deployed in the real-world. My work represents a successful transition from game-theoretic advancements to real-world applications that are already in use, and it has opened exciting new avenues to greatly expand the reach of game theory. For instance, my algorithms are used in the IRIS system: IRIS has been in use by the Federal Air Marshals Service (FAMS) to schedule air marshals on board international commercial flights since October 2009.

Chapter 1: Introduction

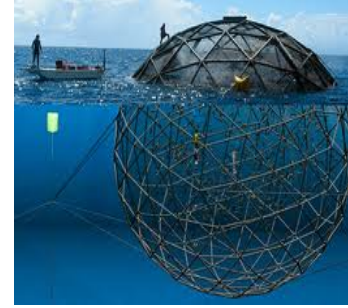
Protecting critical infrastructure and targets such as airports, transportation networks, power generation facilities as well as critical natural resources and endangered species is an important task for police and security agencies worldwide. Securing such potential targets using limited resources against intelligent adversaries in the presence of the uncertainty and complexities of the real-world is a major challenge. For example, in 2001, the 9/11 attack on the World Trade Center in New York City via commercial airliners resulted in \$27.2 billion of direct short term costs [Looney, "2002"] as well as a loss of 2,974 lives. The 2004 Madrid commuter train bombings resulted in 191 lives lost, 1755 wounded, and an estimated cost of 212 million Euros [Blanco et al., 2007]. Finally, the 2008 terrorist attacks in Mumbai resulted in 195 lives lost and nearly 300 wounded [Chandran and Beitchman, 29 November 2008]. Measures for protecting potential target areas include monitoring entrances and inbound roads, checking inbound traffic and patrolling aboard transportation vehicles. Whereas there are many more important security scenarios, the common problem among them is that security agencies have limited security resources to protect their critical infrastructure against an adaptive adversary who conducts surveillance and responds to the strategy followed by the security personnel.



(a) Transportation Networks



(b) Cyber-security



(c) Sustainable Fishing

Figure 1.1: The image shows examples of three domains which have inspired my research: in all these three domains, security agencies need to deploy limited resources to protect from potential adversaries.

1.1 Problem Addressed

Game theory provides a sound mathematical approach for deploying limited security resources to maximize their effectiveness. Indeed, my research uses game-theoretic techniques for computing optimal strategies deploying defender resources. While this connection between game theory and security has existed for last several decades, research on computational approaches to game theory in the past two decades has enabled very large-scale problems to be cast in game-theoretic contexts, thus providing the computational tools to address problems of security allocations.

My contributions have been at the forefront of this research applying game theory for security. I have been involved in the development of actual deployed applications of game theory for security. The ARMOR (Assistant for Randomized Monitoring Over Routes) software scheduling assistant [Pita et al., 2008], is successfully deployed at the Los Angeles International Airport (LAX) since 2007; in particular, ARMOR uses game theory to randomize allocation of police checkpoints and canine units. I also led the development and deployment of IRIS (Intelligent Randomization in Scheduling) [Jain et al., 2010c], which is used by the US Federal Air Marshal Service since 2009 to deploy air marshals on US air carriers. Success of ARMOR and IRIS have

paved the way for more deployed applications: GUARDS for the US Transportation Security Administration is getting evaluated for a national deployment across all airports [Pita et al., 2011b]. Similarly, PROTECT [Shieh et al., 2012], for the United States Coast Guard, is under deployment at the ports of Boston, New York and Los Angeles Long Beach and is expected to be taken nation-wide; TRUSTS [Yin et al., 2012b] is being used by the Los Angeles Sheriff’s department for conducting patrols on metro trains; and many other agencies around the globe are now looking to deploy these techniques.

This set of applications and associated algorithms has added to the already significant interest in game theory for security. They use the framework of Stackelberg games, which were first introduced to model leadership and commitment [von Stackelberg, 1934], to model the problem faced by the security agencies. While I provide a formal definition for Stackelberg games in Chapter 2, they are a natural model for such security problems because they model the commitment a defender (e.g., security agency) must make in allocating her resources before an attacker can conduct surveillance and choose his best attack strategy, *considering the action chosen by the defender*¹. Beyond the deployed real-world applications, Stackelberg games have been used to study security problems ranging from “police and robbers” scenarios [Gatti, 2008; Paruchuri et al., 2008b; Basilico et al., 2009] to computer network security [Lye and Wing, 2005], to missile defense systems [Brown et al., 2005a] and anti-terrorism policies [Sandler and M., 2003].

While Stackelberg games have been successfully used to model the security resource allocation problem, newer and more complex real-world application domains make it challenging for existing techniques for Stackelberg games to be applied, and thus novel techniques to solve large games are required. Real world problems, like scheduling air marshals to protect flights or protecting

¹By convention, I refer to the defender (leader) as *she* and attacker (follower) as *he*

computer networks, present trillions of pure strategies to either one player or to both the defender and the attacker. Such large problem instances cannot even be represented in modern computers, let alone solved using previous techniques. I have provided new models and algorithms that compute optimal defender strategies for massive real-world security domains. In particular, I have addressed the following problems:

1. *Compute optimal security scheduling strategies in domains with a very large number of pure strategies (up to trillions of actions) for the defender.* Let us use the problem faced by the Federal Air Marshals Service (FAMS) as an example domain where the number of pure strategies for the defender are very large. The FAMS schedules armed officers on-board passenger aircrafts. The enormity of the challenge faced by the FAMS can be revealed by a small example: an instance with 100 flights and 10 officers would have more than a billion possible assignments of air marshals to flights; in reality, there are an estimated 3,000–4,000 officers and about 30,000 flights [Keteyian, 2010].
2. *Compute optimal security scheduling strategies in domains with a very large number of pure strategies (up to billions of actions) for the defender as well as the attacker.* An example domain requiring algorithms that can scale in number of pure strategies for both players is the security resource allocation problem faced when protecting targets in a city. In response to the attacks in 2008, the Mumbai police have started to schedule a limited number of inspection checkpoints on the road network throughout the city. Since the police could schedule any combination of checkpoints on the roads, they have exponentially many choices. Similarly, the attacker has exponentially many choices: a path from any *source* to any *target* is a feasible attacker strategy. Similar problems are faced in other domains

like cyber-security as well, especially when there are multiple defender resources to be scheduled.

3. *Compute optimal security scheduling strategies in domains with a very large number of attacker types: A large number of attacker types are required to model uncertainty in the real-world.* For example, the police may be facing either a well-funded hard-lined terrorist or criminals from local gangs. These two groups may have different capabilities, and the police may not know which attacker group they will be facing on any given day. These different attacker preferences, or simply uncertainty over the attacker is modeled as different attacker types using a Bayesian Stackelberg game. The computational complexity of Bayesian Stackelberg games has already been proven to be NP-hard [Conitzer and Sandholm, 2006].
4. *Finally, broadly identifying properties that make Stackelberg game problem instances computationally challenging is an important problem.* The objective is to identify properties that are invariant to different domains, algorithms, solvers and even equilibrium computation methods, but impact the runtime required to compute solutions for a problem instance. An understanding of the runtime required by game-theoretic algorithms is critical to furthering the application of game theory to other real-world domains.

In summary, existing techniques to compute optimal defender strategies in security domains fail to scale to real-world domains. My Ph.D. thesis has focused on addressing these challenges, and has made contributions by developing scalable game theoretic algorithms.

1.2 Contributions

Game theoretic models for real-world problems can have trillions of pure strategies for both players. Such large models cannot even be stored in the memory of computers today, let alone be solved by existing algorithms. I have provided algorithms especially designed to scale-up to exponentially many pure strategies for both players, as required to compute solutions for large real-world domains. These algorithms avoid representing the entire game in memory, while computing optimal solutions for the *entire large problem*. These algorithms are built on the following insights: (i) Real-world domains have exponentially many *pure strategies for the defender* (e.g. a combination of checkpoints), and so, an incremental approach of generating pure strategies of the defender is required. This will avoid enumerating all the pure strategies, and will only add a pure strategy if the pure strategy would help increase defender payoff. (ii) In domains with exponentially many attacker pure strategies, an incremental approach to generate pure strategies for the attacker (e.g. attack paths) should be used to avoid enumeration of the pure strategy set of the attacker. (iii) A Bayesian Stackelberg game can be decomposed into *hierarchically*-organized smaller games, each with smaller number of attacker types, providing heuristics which can be used to eliminate the never-best-response (that is, dominated) pure strategies of the attacker.

These insights provide speed-ups by reducing the size of the game: while insights (i) and (ii) restrict the game size by efficiently generating sub-games that include a pure strategy only if it improves the player's payoff, insight (iii) pre-processes the input Bayesian Stackelberg game instance and removes the attacker pure strategies that cannot be part of the optimal solution. Additionally, all these techniques provide mathematical guarantees and can generate optimal as well as approximate solutions efficiently. Furthermore, I have investigated what properties of

Stackelberg security game instances make them hard to solve in practice, across different input sizes and different security domains. The algorithms developed in my thesis have also been deployed in the real-world. Specifically, the contributions of my thesis are as follows:



(a) Airport security domain: image shows placement of vehicular checkpoints at Los Angeles International Airport. (b) FAMS security domain: image shows all the international flights leaving Chicago O' Hare on a day. (c) Network security domain: image shows the entire road network of the city of Mumbai.

Figure 1.2: The image shows examples of three security domains where my research has been **successfully applied**.

1.2.1 ASPEN

The ASPEN algorithm computes optimal strategies for the defender in domains where the number of pure strategies of the defender can be prohibitively large. It provides the scale-up using the first insight mentioned above – namely, strategy generation for the defender [Jain et al., 2010b]. As an illustrative example for a real-world domain with exponentially many defender strategies, let us consider the problem faced by the Federal Air Marshals Service (FAMS). There are currently tens of thousands of commercial flights flying each day, and public estimates state that there are thousands of air marshals that are scheduled daily by the FAMS [Keteyian, 2010]. Air marshals must be scheduled on tours of flights that obey logistical constraints (e.g., the time required to

board, fly, and disembark). An example of a valid schedule is an air marshal assigned to a round trip tour from Los Angeles to New York and back.

The scale of the domain is massive, since there are billions of possible assignments of air marshals to flight tours. For example, in our illustrative example of the FAMS, the number of ways in which 10 air marshals can be scheduled over 100 flights is $\binom{100}{10} \approx 1.7 \times 10^4$ billion. Simply finding schedules for the marshals is a computational challenge. The task is made more difficult by the need to find an optimal strategy over these schedules that meets the scheduling constraints of the domain, while also accounting for an adaptive attacker and the different payoff values of each flight.

I cast this problem as a *security game*, described in Section 2.4, where the attacker can choose any of the flights to attack, and each air marshal can cover one schedule. Each schedule here is a feasible set of targets that can be covered together; in the FAMS example, each schedule would represent a flight tour which satisfies all the logistical constraints that an air marshal could fly. A *joint schedule* then would assign every air marshal to a flight tour, and there could be exponentially many joint schedules in the domain. A pure strategy for the defender in this security game is a joint schedule. Since all the defender pure strategies (or joint schedules) cannot be enumerated for such massive problems, ASPEN starts by representing only few pure strategies of the defender and then incrementally generating the required pure strategies [Jain et al., 2010b]. ASPEN decomposes the problem into a *master* problem and a *slave* problem, which are then solved iteratively, as described in Chapter 3. Given a limited number of pure strategies, the master solves for the defender and the attacker optimization constraints, while the slave is used to generate a new pure strategy for the defender in every iteration.

The master in ASPEN operates on the pure strategies (joint schedules) generated thus far; its objective is to compute the optimal mixed strategy of the defender over these pure strategies. The objective of the slave problem is to generate the best joint schedule to add to the set of generated pure strategies. The best joint schedule is identified using the concept of *reduced costs* [Bertsimas and Tsitsiklis, 1994], which measures if a pure strategy can potentially increase the defender’s expected utility (the details of the approach are provided in Chapter 3. While a naïve approach would be to iterate over all possible pure strategies to identify the pure strategy with the maximum potential, ASPEN uses a novel minimum-cost integer flow problem to efficiently identify the best pure strategy to add. ASPEN always converges on the optimal mixed strategy for the defender as described in Chapter 3.

Employing strategy generation for large optimization problems is not an “out-of-the-box” approach, the problem has to be formulated in a way that allows for domain properties to be exploited. The novel contribution of ASPEN is to provide a linear formulation for the master and a minimum-cost integer flow formulation for the slave, which enable the application of strategy generation techniques. Additionally, ASPEN also provides a branch-and-bound heuristic to reason over attacker actions. This branch-and-bound heuristic provides a further order of magnitude speed-up, allowing ASPEN to handle the massive sizes of real-world problems. Indeed, ASPEN is currently being used by the FAMS to schedule air marshals on international flights.

1.2.2 RUGGED and SNARES

RUGGED is designed for domains where the number of pure strategies of the players are exponentially large, and it does strategy generation for both the defender and the attacker [Jain et al., 2011b]. RUGGED then serves as a building block for SNARES, which improves on RUGGED by making novel

use of two approaches: *warm starts* and *greedy responses* [Jain et al., 2013]. SNARES can now efficiently compute solutions for extremely large problems with trillions of pure strategies for both players. I also evaluate the performance of SNARES in real-world networks illustrating a significant advance over state-of-the-art algorithms.

Let us consider the urban network security game as an illustrative example. In this domain, the pure strategies of the defender correspond to allocations of resources to edges in the network – for example, an allocation of police checkpoints to roads in the city. The pure strategies of the attacker correspond to paths from any source node to any target node – for example, a path from a landing spot on the coast to the airport. The pure strategy space of the defender grows exponentially with the number of available resources, whereas the pure strategy space of the attacker grows exponentially with the size of the network. For example, in a fully connected graph with 20 nodes and 190 edges, the number of defender pure strategies for only 5 resources is $\binom{190}{5} \approx 2$ billion, while the number of possible attacker paths without any cycles is $\approx 6.6e18$. The graphs representing real-world scenarios are significantly larger, e.g., a simplified graph representing the road network in the southern tip of Mumbai has more than 250 nodes (intersections) and 700 edges (streets), and the security forces can deploy tens of resources.

Here, strategy generation is required for both the defender and the attacker since the number of pure strategies of both the players are prohibitively large. RUGGED models the domain as a zero-sum game, and computes the minimax equilibrium, since the payoff of the minimax strategy is equivalent to the SSE payoff in zero-sum games [Yin et al., 2010a]. RUGGED decomposes the computation into three modules: a minimax module and best response modules for both the defender and the attacker, whereas the two best response modules generate new strategies for the two players respectively.

The contribution of RUGGED is to provide the mixed integer formulations for the best response modules which enable the application of such a strategy generation approach. These mixed integer formulations are provided in Chapter 4. RUGGED can compute the optimal solution for deploying up to 4 resources in real-city network with as many as 250 nodes within a reasonable time frame of 10 hours (the complexity of this problem can be estimated by observing that both the best response problems are NP-hard themselves [Jain et al., 2011b]).

The RUGGED algorithm serves as a building block for SNARES, which makes the following contributions: (1) It defines and uses `mincut-fanout`, a novel method for efficient warm-starting of the computation; (2) It exploits the submodularity property of the defender optimization in a greedy heuristic, which is used to generate “better-responses”; SNARES also uses a better-response computation for the attacker. I also evaluate the performance of SNARES in real-world networks illustrating a significant advance: for example, whereas state-of-the-art algorithms could only schedule resources of Mumbai police on just the southern tip of Mumbai, SNARES can compute optimal strategy for the entire urban road network of Mumbai.

1.2.3 HBGS and HBSA

The different preferences of different attacker types are modeled through Bayesian Stackelberg games. Computing the optimal leader strategy in Bayesian Stackelberg game is NP-hard [Conitzer and Sandholm, 2006], and polynomial time algorithms cannot achieve approximation ratios better than $O(types)$ [Letchford et al., 2009]. I have developed a new technique for solving large Bayesian Stackelberg games that decomposes the entire game into many hierarchically-organized *restricted* Bayesian Stackelberg games as suggested in insight (iii); it then utilizes the solutions of these restricted games to more efficiently solve the larger Bayesian Stackelberg game [Jain et al., 2011a].

The overarching idea of hierarchical structure is to improve the performance of branch-and-bound on the attacker action tree by pruning the search space. It decomposes the Bayesian Stackelberg game into many hierarchically-organized smaller games, as explained in detail in Chapter 5. Each of the restricted games consider only a few attacker types, and are thus exponentially smaller than the Bayesian Stackelberg game at the ‘parent’. The solutions obtained for the restricted games at the child nodes of the hierarchical game tree are used to provide: (i) pruning rules, (ii) tighter bounds, and (iii) efficient branching heuristics to solve the bigger game at the parent node faster.

Such hierarchical techniques have seen little application towards obtaining optimal solutions in Bayesian games, while Stackelberg settings have not seen any application of such hierarchical decomposition. I provide HBGS which applies the hierarchical framework to general Stackelberg games, and HBSA that combines the hierarchical decomposition with strategy generation of ASPEN. I have shown that both HBGS and HBSA are orders of magnitude faster than other Bayesian Stackelberg algorithms for the respective problem settings. Additionally, these algorithms are naturally designed for obtaining quality bounded approximations since they are based on branch-and-bound, and provide a further order of magnitude scale-up without any significant loss in quality if approximate solutions are allowed.

1.2.4 $d:s$ and Phase Transition

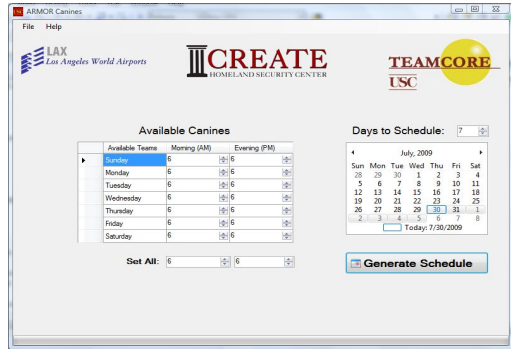
I have also identified the properties that make a *problem instance* computationally challenging. I formalized the concept of the *deployment-to-saturation* ($d:s$) ratio in Stackelberg security games, and showed that problem instances for which $d:s = 0.5$ are computationally harder than instances with other $d:s$ ratios for a wide range of different domains, algorithms, solvers or equilibrium

computation methods [Jain et al., 2012]. This work also provides evidence that the computationally hard region is also one where optimization is most beneficial to the real-world security agencies, thereby corroborating the need for algorithmic advances.

Furthermore, I use the concept of phase transitions to better understand this computationally hard region. I define a decision problem related to security games, and show that the probability that this problem has a solution exhibits a phase transition as the $d : s$ ratio crosses 0.5. This provides evidence that security games with $d : s = 0.5$ are indeed computationally more challenging.

1.2.5 Real World Applications: ARMOR and IRIS

Game-theoretic approaches for security scheduling have been successfully deployed in the real world, with applications like ARMOR and IRIS in use by the Los Angeles airport police and the FAMS since August 2007 and October 2009 respectively [Jain et al., 2010c]. I led the development of IRIS, I also made significant contributions to the development of ARMOR. While the algorithm of choice in ARMOR has been DOBSS [Paruchuri et al., 2008b] (the LAX domain is small compared to FAMS or urban network security since only 8 terminals need to be protected at LAX), IRIS uses the ASPEN algorithm mentioned before and described in Chapter 3. Currently, IRIS is used to schedule air marshals on-board international flights; FAMS is indeed working towards increasing the scope of IRIS towards domestic and other sectors. Furthermore, the success of IRIS and ARMOR systems has led to newer deployments of such algorithms in other real-world security domains, like the PROTECT system for the U.S. Coast Guard, and the TRUSTS system for the LA Sheriff Department.



(a) Screenshot of the ARMOR software assistant in use by the Los Angeles Airport Police.



(b) Screenshot of the IRIS software assistant in use by the Federal Air Marshals Service.

Figure 1.3: The figure shows the screenshots of ARMOR and IRIS, the deployed software assistants.

1.3 Guide to thesis

This thesis is organized in the following way. Chapter 2 introduces necessary background for the research presented in this thesis and Chapter 7 presents related work. Chapter 3 presents the algorithm ASPEN and corresponding experimental results. Chapter 4 presents the algorithms RUGGED and SNARES and corresponding experimental results. Chapter 5 describes the hierarchical decomposition technique for Bayesian Stackelberg games, whereas Chapter 6 describes the $d:s$ ratio and examines properties that make problem instances hard to solve. Finally, Chapter 8 concludes the thesis and presents issues for future work.

Chapter 2: Background

This chapter begins by introducing motivating examples of real world security applications in Section 2.1. The work in this thesis builds on Stackelberg games for modeling security domains, and so I then provide the background on the general Stackelberg game model and its Bayesian extension in Section 2.2. Section 2.3 introduces the standard solution concept known as the Strong Stackelberg Equilibrium (SSE). Section 2.4 then talks about the security game representation for Stackelberg games, whereas Section 2.5 describes security game models with arbitrary scheduling constraints. Section 2.6 then introduces security game model with patrolling constraints, followed by description of network security domains in Section 2.8. Finally, Section 2.9 overviews previous algorithms of relevance to this thesis.

2.1 Motivating Domains

Security scenarios addressed in this work exhibit the following important characteristics: there is a leader/follower dynamic between the security forces and terrorist adversaries, since the security forces commit to a security policy first while the adversaries conduct surveillance to exploit any weaknesses or patterns in the security strategies [Tambe, 2011]. A security policy here refers to some schedule to patrol, check or monitor the area under protection. There are limited security

resources available to protect a very large space of possible targets, so it is not possible to provide complete coverage at all times. Moreover, the targets in the real-world clearly have different values and vulnerabilities in each domain. Additionally, there is uncertainty over many adversary types. For example, the security forces may not know whether they would face a well-funded terrorist or a local gang member or some other threat. Typically, the security forces are interested in a randomized schedule, so that surveillance does not yield predictable patterns; yet they wish to ensure that more important targets have a higher protection and that they guard against an intelligent adversary's adaptive response to their randomized schedule. I now describe some concrete security domains which have motivated my research.

2.1.1 Los Angeles International Airport (LAX):

LAX is the fifth busiest airport in the United States, the largest destination airport in the United States, and serves 60-70 million passengers per year [LAWA, 2007; Stevens and et. al., 2006]. The LAX police use diverse measures to protect the airport, which include vehicular checkpoints, police units patrolling the roads to the terminals, patrolling inside the terminals (with canines), and security screening and bag checks for passengers. The application of game-theoretic approach is focused on two of these measures: (1) placing vehicle checkpoints on inbound roads that service the LAX terminals, including both location and timing (2) scheduling patrols for bomb-sniffing canine units at the different LAX terminals.

The eight different terminals at LAX have very different characteristics, like physical size, passenger loads, foot traffic or international versus domestic flights. These factors contribute to the differing risk assessments of these eight terminals. The numbers of available vehicle checkpoints and canine units are limited by resource constraints, so the key challenge is to apply

game-theoretic algorithms to intelligently allocate these resources – typically in a randomized fashion — to improve their effectiveness while avoiding patterns in the scheduled deployments.

2.1.2 United States Federal Air Marshals Service (FAMS):

The FAMS places undercover law enforcement personnel aboard flights of US air carriers originating in and departing the United States to dissuade potential aggressors and prevent an attack should one occur [TSA, 2008]. The exact methods used to evaluate the risks posed by individual flights is not made public by the service, and many factors might influence such an evaluation. For example, flights have different numbers of passengers, and some fly over densely populated areas while others do not [TSA, 2008]. International flights also serve different countries, which may pose different risks. Special events can also change the risks for particular flights at certain times [Wiki, 2008]. The scale of the domain is massive. There are currently tens of thousands of commercial flights scheduled each day, and public estimates state that there are thousands of air marshals [CNN, 2008]. Air marshals must be scheduled on tours of flights that obey various constraints (e.g., the time required to board, fly, and disembark). Simply finding schedules for the marshals that meet all of these constraints is a computational challenge. The task is made more difficult by the need to find a randomized policy that meets these scheduling constraints, while also accounting for the different values of each flight.

2.1.3 United States Transportation Security Agency (TSA):

The TSA is tasked with protecting the nation’s transportation systems [TSA, 2011a]. One set of systems in particular is the over 400 airports [TSA, 2011a] which services approximately 28,000 commercial flights and up to approximately 87,000 total flights [ATC, 2011] per day. To

protect this large transportation network, the TSA employs approximately 48,000 Transportation Security Officers [TSA, 2011a], who are responsible for implementing security activities at each individual airport. While many people are aware of common security activities, such as individual passenger screening, this is just one of many security layers TSA personnel implement to help prevent potential threats [TSA, 2011b,a]. These layers can involve hundreds of heterogeneous security activities executed by limited TSA personnel leading to a complex resource allocation challenge. While activities like passenger screening are performed for every passenger, the TSA cannot possibly run every security activity all the time. Thus, while the resources required for passenger screening are always allocated by the TSA, it must also decide how to appropriately allocate its remaining security officers among the layers of security to protect against a number of potential threats, while facing challenges such as surveillance and an adaptive adversary as mentioned before.

2.1.4 United States Coast Guard:

The US Coast Guard patrols harbors to safeguard the maritime and security interests of the country. The Coast Guard continues to face a challenging future with an evolving asymmetric threat within the maritime environment both within the Maritime Global Commons but also within the ports and waterways that make up the United States Maritime Transportation System (MTS). The Coast Guard can cover any subset of patrol areas in any patrol schedule. They can also perform many security activities at each patrol area. The challenge for the Coast Guard again is to design a randomized patrolling strategy given that they need to protect a diverse set of targets along the harbor and the attacker conducts surveillance and is adaptive.

2.2 Stackelberg Games

In a Stackelberg game, a leader commits to a strategy first, and then followers sequentially selfishly optimize their rewards, *considering the action chosen by the leader*. For the remainder of this thesis, I will refer to the leader as ‘her’ and the follower as ‘him’. To see the advantage of being the leader in a Stackelberg game, consider a simple game with the payoff table as shown in Table 2.1, which was first presented by [Conitzer and Sandholm, 2006]. The leader is the row player and the follower is the column player. The only pure-strategy Nash equilibrium for this game is when the leader plays a and the follower plays c , which gives the leader a payoff of 2; in fact, for the leader, playing b is strictly dominated. However, if the leader can commit to playing b before the follower chooses his strategy, then the leader will obtain a payoff of 3, since the follower would then play d to ensure a higher payoff for himself. If the leader commits to a uniform mixed strategy of playing a and b with equal (0.5) probability, then the follower will play d , leading to a payoff for the leader of 3.5.

	Target 1	Target 2
Target 1	2, 1	4, 0
Target 2	1, 0	3, 2

Table 2.1: Payoff table for example Stackelberg game.

The Stackelberg games I consider in this thesis have two agents, the leader (defender), Θ , and the follower (attacker/adversary), Ψ . Each player has a set of possible *pure strategies*, denoted $\sigma_\Theta \in \Sigma_\Theta$ and $\sigma_\Psi \in \Sigma_\Psi$. A *mixed strategy* allows a player to play a probability distribution over pure strategies, denoted \mathbf{x} and \mathbf{a} for the leader and the follower respectively. Payoffs for each player are defined over all possible joint pure-strategy outcomes: $U_\Theta : \Sigma_\Theta \times \Sigma_\Psi \rightarrow \mathcal{R}$ for the defender and similarly for each attacker. The payoff functions are extended to mixed strategies in

the standard way by taking the expectation over pure-strategy outcomes. The follower can observe the leader's strategy, and then act in a way to optimize its own payoffs. Formally, the attacker's strategy in a Stackelberg security game becomes a function that selects a strategy for each possible leader strategy: $F_\Psi : \mathbf{x} \rightarrow \mathbf{a}$.

The Bayesian extension to Stackelberg games allows for each player (leader or follower) to be one of multiple possible types, with each type associated with its own payoff values. In this thesis, the defender (leader), Θ , only has one type since she is considering her own personal resources. However, the attacker (follower) can be one of a set of possible types denoted by $\lambda \in \Lambda$. For example, a security force may be interested in protecting against potential terrorist attacks and catching potential drug smugglers, which represent two different types of adversaries. Each type is represented by a different and possibly uncorrelated payoff matrix for both the leader and follower. That is, the leader's payoffs will vary along with the follower's payoffs for each type of follower. At any time the leader does not know what follower type she will face, however, she is aware of the probability distribution over follower types (i.e., she knows how frequently she will face each follower type). The probability with which follower type $\lambda \in \Lambda$ appears is denoted by p^λ . The follower is always aware of his own type and thus always has perfect information about the leader's payoffs and his own payoffs. The notation used in this thesis when referring to Bayesian Stackelberg games is given in Table 2.2.

Given this formal model, the leader's goal is to determine the mixed strategy \mathbf{x} , such that her expected value is maximized given that each follower type will choose his expected-value-maximizing action with complete knowledge of the leader's mixed strategy. Such a commitment

Variable	Definition
Θ	Refers to the leader
Ψ	Refers to the follower
Λ	Set of follower types
Σ_{Θ}	Set of pure strategies of the leader
Σ_{Ψ}	Set of pure strategies of the follower
p^{λ}	Probability of follower type λ
$G(\Theta, \Psi^{\Lambda})$	Bayesian Stackelberg game
U_{Θ}	Payoffs for the leader
U_{Ψ}	Payoffs for the follower
\mathbf{x}	Leader's strategy
\mathbf{a}	Follower's strategy

Table 2.2: Notation

to a mixed strategy models a real-world situation where security forces commit to a randomized patrolling strategy first. Given this commitment, an adversary can conduct as much surveillance of this mixed strategy as he desires. Even with knowledge of this mixed strategy, the adversary has no specific knowledge of what the security force may do on a particular day however. He only has knowledge of the mixed strategy the security force will use to decide her resource allocations for that day. In this model, predictable defense strategies are vulnerable to exploitation by a determined adversary.

2.3 Strong Stackelberg Equilibrium (SSE)

The most common solution concept in game theory is a *Nash equilibrium*, which is a profile of strategies for each player in which no player can gain by unilaterally changing to another strategy [Osbourne and Rubinstein, 1994]. Stackelberg equilibrium is a refinement of Nash equilibrium specific to Stackelberg games. It is a form of sub-game perfect equilibrium in that it requires that each player select the best-response in any subgame of the original game (where subgames correspond to partial sequences of actions). The effect is to eliminate equilibrium profiles that

are supported by non-credible threats off the equilibrium path. Subgame perfection is a natural requirement, but it does not guarantee a unique solution in cases where the follower is indifferent among a set of strategies. The literature contains two form of Stackelberg equilibria that identify unique outcomes, first proposed by Leitmann [Leitmann, 1978], and typically called “strong” and “weak” after Breton et. al. [Breton et al., 1988]. The strong form assumes that the follower will always choose the optimal strategy for the leader in cases of indifference, while the weak form assumes that the follower will choose the worst strategy for the leader. Unlike the weak form, strong Stackelberg equilibria are known to exist in all Stackelberg games [Basar and Olsder, 1995]. A standard argument suggests that the leader is often able to induce the favorable strong form by selecting a strategy arbitrarily close to the equilibrium which causes the follower to strictly prefer the desired strategy [von Stengel and Zamir, 2004]. We adopt strong Stackelberg equilibrium as our solution concept in part for these reasons, but also because it is the most commonly used in related literature [Osbourne and Rubinstein, 1994; Conitzer and Sandholm, 2006; Paruchuri et al., 2008b].

Definition 1. *A set of strategies (δ_Θ, F_Ψ) form a Strong Stackelberg Equilibrium (SSE) if they satisfy the following:*

1. *The leader plays a best-response:*

$$U_\Theta(\mathbf{x}, F_\Psi(\mathbf{x})) \geq U_\Theta(\mathbf{x}', F_\Psi(\mathbf{x}')) \forall \mathbf{x}'.$$

2. *The follower plays a best-response:*

$$U_\Psi(\mathbf{x}, F_\Psi(\mathbf{x})) \geq U_\Psi(\mathbf{x}, \mathbf{a}) \forall \mathbf{a}.$$

3. *The follower breaks ties optimally for the leader:*

$U_{\Theta}(\mathbf{x}, F_{\Psi}(\mathbf{x})) \geq U_{\Theta}(\mathbf{x}, \mathbf{a}) \forall \mathbf{x}, \mathbf{a} \in \Sigma_{\Psi}^*(\mathbf{x})$, where $\Sigma_{\Psi}^*(\mathbf{x})$ is the set of follower best-responses, as above.

In the case of Bayesian games with many follower types Λ , the leader's best response is a weighted best response to the followers' responses, where the weights are based on the probability of occurrence of each type (p^{λ}). The strategy of each attacker type γ becomes: F_{Ψ}^{γ} , which still satisfies constraints 2 and 3 in Definition 1.

2.4 Stackelberg Security Games

In a security game, a defender must perpetually defend the site in question, whereas the attacker is able to observe the defender's strategy and attack when success seems most likely. This fits neatly into the description of a Stackelberg game if we map the attackers to the follower's role and the defender to the leader's role [Avenhaus et al., 2002; Brown et al., 2006; Kiekintveld et al., 2009]. The actions for the security forces represent the action of scheduling a patrol or checkpoint, e.g. a checkpoint at the LAX airport or a federal air marshal scheduled to a flight. The actions for an adversary represent an attack at the corresponding infrastructural entity. The strategy for the leader is a mixed strategy spanning the various possible actions.

There are two major problems with using conventional methods to represent security games in normal form. First, many solution methods require the use of a Harsanyi transformation when dealing with Bayesian games [Harsanyi and Selten, 1972]. The Harsanyi transformation converts a Bayesian game into a normal-form game, but the new game may be exponentially larger than the original Bayesian game. The compact representation of security games avoids this Harsanyi

transformation, and instead directly operates on the Bayesian game. Operating directly on the Bayesian representation is possible in security games because the evaluation of the leader strategy against a Harsanyi-transformed game matrix is equivalent to its evaluation against each of the game matrices for the individual follower types [Kiekintveld et al., 2009]. The second problem arises that the defender has many possible resources to schedule in the security policy. This can also lead to a combinatorial explosion in a standard normal-form representation. For example, if the leader has m resources to defend n entities, then normal-form representations model this problem as a single leader with $\binom{n}{m}$ rows, each row corresponding to a leader action of covering m targets with security resources. However, in the security game representation, the game representation would only include n rows, each row corresponding to whether the corresponding target was covered or not. Such a representation is equivalent to the normal form representation if *the defender does not face any scheduling constraints* (examples of domains with scheduling constraints will be given in Sections 2.5 to 2.8 – for the same reason, such problems are also referred to as **Security Problems with No Scheduling Constraints (SPNSC)** in this thesis). This compactness in SPNSC is possible because the payoffs for the leader in these games simply depend on whether the attacked target was covered or not, and not on what other targets were covered (or not covered). The representation we use here avoids both of these potential problems, using methods similar to other compact representations for games [Koller and Milch, 2003; Jiang and Leyton-Brown, 2006].

I now introduce this compact representation for security games. Let $T = \{t_1, \dots, t_n\}$ be a set of *targets* that may be attacked, corresponding to pure strategies for the attacker. The defender has a set of resources available to *cover* these targets, $R = \{r_1, \dots, r_m\}$ (for example, in the FAMS domain, targets could be flights and resources could be federal air marshals). Associated with

each target are four payoffs defining the possible outcomes for an attack on the target, as shown in Table 2.3. Similarly, 2.4 shows an example for an entire Bayesian security game with no scheduling constraints with two targets. There are two cases, depending on whether or not the target is covered by the defender. The defender's payoff for an uncovered attack when facing an adversary of type γ is denoted $U_{\Theta}^{\gamma,u}(t)$, and for a covered attack $U_{\Theta}^{\gamma,c}(t)$. Similarly, $U_{\Psi}^{\gamma,u}(t)$ and $U_{\Psi}^{\gamma,c}(t)$ are the payoffs of the attacker.

	Covered	Uncovered
Defender	5	-20
Attacker	-10	30

Table 2.3: Example payoffs for an attack on a target.

Attacker Type 1					Attacker Type 2				
	Defender		Attacker			Defender		Attacker	
Target	Cov.	Uncov.	Cov.	Uncov.	Target	Cov.	Uncov.	Cov.	Uncov.
t_1	10	0	-1	1	t_1	5	-4	-2	1
t_2	0	-10	-1	1	t_2	4	-5	-1	2

Table 2.4: Example Bayesian security game with two targets and two attacker types.

A crucial feature of the model is that payoffs depend only on the target attacked, and whether or not it is covered by the defender. The payoffs do *not* depend on the remaining aspects of the schedule, such as whether any unattacked target is covered or which specific defense resource provides coverage. For example, if an adversary succeeds in attacking Terminal 1, the penalty for the defender is the same whether the defender was guarding Terminal 2 or 3. Therefore, from a payoff perspective, many resource allocations by the defender are identical. We exploit this by summarizing the payoff-relevant aspects of the defender's strategy in a *coverage* vector, C , that gives the probability that each target is covered, c_t . The analogous attack vector A^γ gives the

probability of attacking a target by a follower of type γ . We restrict the attack vector for each follower type to attack a single target with probability 1. This is without loss of generality because a strong Stackelberg equilibrium (SSE) solution still exists under this restriction [Paruchuri et al., 2008b]. Thus, the follower of type γ can choose any pure strategy $\sigma_\Psi^\gamma \in \Sigma_\Psi^\gamma$, that is, attack any one target from the set of targets.

The payoff for a defender when a specific target t is attacked by an adversary of type γ is given by $U_\Theta^\gamma(t, C)$ and is defined in Equation 2.1. Thus, the expectation of $U_\Theta^\gamma(t, C)$ over t gives U_Θ^γ , which is the defender's expected payoff given coverage vector C when facing an adversary of type γ whose attack vector is A^γ . U_Θ^γ is defined in Equation 2.2. The same notation applies for each follower type, replacing Θ with Ψ . Thus, $U_\Psi^\gamma(t, C)$ gives the payoff to the attacker when a target t is attacked by an adversary of type γ . We also define the useful notion of the *attack set* in Equation 2.3, $\Lambda^\gamma(C)$, which contains all targets that yield the maximum expected payoff for the attacker type γ given coverage C . This *attack set* is used by the adversary to break ties when calculating a strong Stackelberg equilibrium. Moreover, in these security games, exactly one adversary is attacking in one instance of the game; however, the adversary could be of any type and the defender does not know the type of the adversary faced.

$$U_\Theta^\gamma(t, C) = c_t U_\Theta^{\gamma, c}(t) + (1 - c_t) U_\Theta^{\gamma, u}(t) \quad (2.1)$$

$$U_\Theta^\gamma(C, A^\gamma) = \sum_{t \in T} a_t^\gamma \cdot (c_t \cdot U_\Theta^{\gamma, c}(t) + (1 - c_t) U_\Theta^{\gamma, u}(t)) \quad (2.2)$$

$$\Lambda^\gamma(C) = \{t : U_\Psi^\gamma(t, C) \geq U_\Psi^\gamma(t', C) \forall t' \in T\}. \quad (2.3)$$

In a strong Stackelberg equilibrium, the attacker selects the target in the attack set with maximum payoff for the defender. Let t^* denote this optimal target. Then the expected SSE payoff for the defender when facing this adversary of type γ with probability p^γ is $\hat{U}_\Theta^\gamma(C) = U_\Theta^\gamma(t^*, C) \times p^\gamma$, and for the attacker $\hat{U}_\Psi^\gamma(C) = U_\Psi^\gamma(t^*, C)$.

2.5 Security Problems with Arbitrary Scheduling Constraints (SPARS)

I now introduce the SPARS domain, which includes arbitrary scheduling constraints for the defender. A SPARS game is a security game where each defender resource can be assigned to a *schedule* covering multiple targets, $s \subseteq T$, so the set of all legal schedules is defined as $S \subseteq \mathcal{P}(T)$. The defender has R resources, such that each defender resource r is restricted to a set of legal schedules, $S_r \subseteq S$ (note that this implies that defender resources are no longer identical). The defender's pure strategies are the set of *joint schedules* that assign each resource to at most one schedule. Additionally, we assume that a target may be covered by at most 1 resource in a joint schedule (though this can be generalized). A joint schedule \mathbf{j} can be represented by the vector $\mathbf{P}_\mathbf{j} = \langle P_{jt} \rangle \in \{0, 1\}^n$ where P_{jt} represents whether or not target t is covered in joint schedule \mathbf{j} . The set of all feasible joint schedules is denoted by \mathbf{J} . We define a mapping M from \mathbf{j} to $\mathbf{P}_\mathbf{j}$ as: $M(\mathbf{j}) = \langle P_{jt} \rangle$, where $P_{jt} = 1$ if $t \in \bigcup_{s \in \mathbf{j}} s$; 0 otherwise. The defender's mixed strategy \mathbf{x} specifies the probabilities of playing each $\mathbf{j} \in \mathbf{J}$, where each individual probability is denoted by x_j . Let $\mathbf{c} = \langle c_t \rangle$ be the vector of coverage probabilities corresponding to \mathbf{x} , where $c_t = \sum_{\mathbf{j} \in \mathbf{J}} P_{jt} x_j$ is the marginal probability of covering t .

A Bayesian-SPARS instance is an extension for the SPARS problem for many attacker types. Thus, each target in Bayesian-SPARS now has many sets of payoffs, one for each attacker type. For reference, Table 2.5 summarizes all of the notation introduced here, and builds on the notation presented in Table 2.2 for SPNSC problems.

Example: Consider a FAMS game with 5 targets (flights), $T = \{t_1, \dots, t_5\}$, and three marshals of the same type, $R = 3$, $S_1 = S_2 = S_3 = S$. Let the set of feasible schedules be $S = \{\{t_1, t_2\}, \{t_2, t_3\}, \{t_3, t_4\}, \{t_4, t_5\}, \{t_1, t_5\}\}$. The set of feasible joint schedules is shown below, where column \mathbf{j}_1 represents the joint schedule $\{\{t_1, t_2\}, \{t_3, t_4\}\}$.

$$\mathbf{P} = \begin{array}{c} t_1 : \\ t_2 : \\ t_3 : \\ t_4 : \\ t_5 : \end{array} \begin{array}{ccccc} \mathbf{j}_1 & \mathbf{j}_2 & \mathbf{j}_3 & \mathbf{j}_4 & \mathbf{j}_5 \\ \left[\begin{array}{ccccc} 1 & 1 & 1 & 1 & 0 \\ 1 & 1 & 1 & 0 & 1 \\ 1 & 1 & 0 & 1 & 1 \\ 1 & 0 & 1 & 1 & 1 \\ 0 & 1 & 1 & 1 & 1 \end{array} \right] \end{array}$$

Each joint schedule in \mathbf{J} assigns only 2 air marshals in this example, since no more than 1 air marshal is allowed on any flight. Thus, the third air marshal will remain unused. Suppose all of the targets have identical payoffs $U_{\Theta}^c(t) = 1$, $U_{\Theta}^u(t) = -5$, $U_{\Psi}^c(t) = -1$ and $U_{\Psi}^u(t) = 5$. In this case, the optimal strategy for the defender randomizes uniformly across the joint schedules, $\mathbf{x} = \langle .2, .2, .2, .2, .2 \rangle$, resulting in coverage $\mathbf{c} = \langle .8, .8, .8, .8, .8 \rangle$. All pure strategies have equal

payoffs for the attacker, given this coverage vector. Furthermore, for this example, ERASER-C incorrectly outputs the coverage vector $\mathbf{c} = \langle 1, 1, 1, 1, 1 \rangle$.¹

To summarize, a solution to the SPARS problem instance is the optimal mixed strategy over joint schedules, such that each joint schedule assigns every defender resource to a schedule (or a set of targets). This mixed strategy is indexed over joint schedules, where the number of joint schedules is combinatorial in the number of schedules S and the number of defender resources. In Chapter 3, I introduce the ASPEN algorithm that uses branch-and-price to compute solutions to SPARS instances with just one attacker type (non-Bayesian). This algorithm is extended to handle the Bayesian case in Chapter 5.

2.6 Security Problems with Patrolling Constraints (SPPC)

I now introduce a new domain: Security Problems with Patrolling Constraints (SPPC). This is a generalized security domain that allows us to consider many different facets of the patrolling problem. The defender needs to protect a set of targets, located geographically on a plane, using a limited number of resources. These resources start at a given target and then conduct a tour that can cover an arbitrary number of additional targets; the constraint is that the total tour length must not exceed a given parameter L . I consider two variants of this domain featuring different attacker models.

¹This coverage vector is incorrect since there does not exist a mixed strategy over joint schedules for the defender that can achieve these marginals.

Table 2.5: SPARS Notation

Variable	Definition
Θ	Refers to the defender
Ψ	Refers to the attacker
Λ	Set of attacker types
p^λ	Probability of attacker type
$G(\Theta, \Psi^\Lambda)$	Bayesian Stackelberg game
T	Targets
R	Defender Resources
S	Scheduling constraints for the defender
S_r	Set of feasible schedules for resource r
\mathbf{J}	Joint Schedules
\mathbf{P}	Mapping between Targets T and Joint Schedules \mathbf{J}
\mathbf{x}	Distribution over \mathbf{J} (mixed strategy of the defender)
\mathbf{a}_λ	Attack vector (pure strategy of the attacker type λ)
d_λ	Defender reward against type λ , when the defender has committed to mixed strategy \mathbf{x} and the attacker of type λ is playing his best response \mathbf{a}_λ
k_λ	Reward of attacker type λ , when the defender has committed to mixed strategy \mathbf{x} and the attacker of type λ is playing his best response \mathbf{a}_λ
\mathbf{d}_λ	Column vector of d_λ
\mathbf{k}_λ	Column vector of k_λ
\mathbf{q}_λ	Attack set of type λ
$U_{\lambda,\Theta}^u$	Utility for defender when target is uncovered
$U_{\lambda,\Theta}^c$	Utility for defender when target is covered
\mathbf{D}_λ	Diag. matrix of $U_{\lambda,\Theta}^c(t) - U_{\lambda,\Theta}^u(t)$
\mathbf{A}_λ	Diag. matrix of $U_{\lambda,\Psi}^c(t) - U_{\lambda,\Psi}^u(t)$
$\mathbf{U}_{\lambda,\Theta}^u$	Vector of values $\mathcal{U}_\Theta^u(t)$, similarly for Ψ
\mathbf{c}	Marginal coverage over targets
M	Huge Positive constant

1. There are multiple independent attackers, and each target can be attacked by a separate attacker. Each attacker can learn the probability that the defender protects a given target, and can then decide whether or not to attack it.
2. There is a single attacker with many types, modeled as a Bayesian game. The defender does not know the type of attacker she faces. The attacker attacks a single target.

Variable	Definition
\mathbf{S}	Set of sites (targets)
\mathbf{T}	Set of tours
L	Upper bound on the length of a defender tour
\mathbf{x}	Probability distribution over \mathbf{T}
\mathbf{q}	Attack vector
z_{st}	Binary value indicating whether or not $s \in T$
d	Defender reward
k	Adversary reward
P	Penalty to attacker
R_s	Reward to attacker at site s
τ_s	Defender reward for catching attacker on site s
M	Huge Positive constant

Table 2.6: Notation for the SPPC Domain

These variants were designed to capture properties of patrolling problems studied by researchers across many real-world domains [An et al., 2011; Bosansky et al., 2011; Vanek et al., 2011]. An example for the Bayesian single attacker setting is the US Coast Guard patrolling a set of targets along the port to protect against potential threats. The defender’s objective is to find the optimal mixed strategy \mathbf{x} over tours \mathbf{T} for all its resources in order to maximize her expected utility d . The notation used for this domain is described in Table 2.6.

2.6.1 Payoff Structure

With each target in the domain are associated payoffs, which specify the payoff to both the defender and the attacker in case of an successful or an unsuccessful attack. The attacker pays a high penalty for getting caught, where as the defender gets a reward for catching the attacker. On the other hand, if the attacker succeeds, the attacker gets a reward where as the defender pays a penalty. Both the players get a payoff of 0 if the attacker chooses not to attack. The payoff matrix for each target is given in Table 2.7. Thus, the defender gets a reward of τ_s units if she succeeds in protecting

the attack on target s , i.e. if the defender is *covering* the target s when it is attacked. On the other hand, the attacker pays a penalty of $-P$ on being caught. Similarly, the reward to the attacker is R_s for a successful attack on site s , whereas the corresponding penalty to the defender for leaving the target *uncovered* is $-R_s$.

	No Attack	Attack
Covered	0, 0	$\tau_s, -P$
Uncovered	0, 0	$-R_s, R_s$

Table 2.7: Payoff structure for each target: defender gets a reward of τ_s units for successfully preventing an attack, while the attackers pays a penalty $-P$. Similarly, on a successful attack, the attacker gains R_s and the defender loses $-R_s$. Both players get 0 in case there is no attack.

2.7 Game Model 1: Multiple Attackers

In this game model, there are as many attackers as the number of targets in the domain. Each attacker can choose to attack or not attack a distinct target. Each attacker can observe the net *coverage*, or probability of the target being on a defender's patrol, for the target that the attacker is interested in. In our formulation, we assume that the attackers are independent and do not coordinate or compete. Figure 2.1 shows an example problem and solutions for this example. There are just two targets, A and B, which are placed 5 units away from the home (starting) location of the defender's resources. There are two attackers, one for each target. The tour length allowed in this example was 10 units, that is, the defender can only patrol exactly one target in each patrol route. The penalty P was set to 70 units where as the reward R for a successful attack to the attacker was 100 units. For this particular example, the defender cannot protect the attacks

on both sites and the optimal defender strategy is to cover one target with probability 0.588, cover the other target with probability 0.412 with the optimal defender reward being -50.588 .

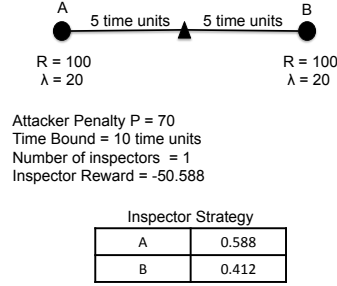


Figure 2.1: Example 1

2.8 Network Security Domain

I now introduce a **network security game**, where the number of actions for both the defender and the attacker can be exponential in number. A network security domain, as introduced by Tsai et al. [Tsai et al., 2010], is modeled using a graph $G = (N, E)$. The attacker starts at one of the source nodes $s \in S \subset N$ and travels along a path of his choosing to any one of the targets $t \in T \subset N$. The attacker's pure strategies are thus all the possible $s - t$ paths from any source $s \in S$ to any target $t \in T$. The defender tries to catch the attacker before he reaches any of the targets by placing k available (homogeneous) resources on edges in the graph. The defender's pure strategies are thus all the possible allocations of k resources to edges, so there are $\binom{|E|}{k}$ in total. Assuming the defender plays allocation $X_i \subseteq E$, and the attacker chooses path $A_j \subseteq E$, the attacker succeeds if and only if $X_i \cap A_j = \emptyset$. Additionally, a payoff $\mathcal{T}(t)$ is associated with each target t , such that the attacker gets $\mathcal{T}(t)$ for a successful attack on t and 0 otherwise. The defender receives $-\mathcal{T}(t)$ in case of a successful attack on t and 0 otherwise. The payoff structure used in network security domains of interest in this thesis is given in Table 2.8. The network security domain is modeled

as a **complete-information zero-sum** game, where the set S of sources, T of targets, the payoffs $U_{\lambda, \Psi}^u(t) = \mathcal{T}(t)$ for all the targets t and the number of defender resources R are known to both the players *a-priori*. The objective is to find the mixed strategy \mathbf{x} of the defender, corresponding to a Stackelberg equilibrium – equivalently, a Nash equilibrium strategy or a minimax strategy since in zero-sum games, Stackelberg equilibrium strategies are equivalent to Nash and minimax strategies [Yin et al., 2010b]. The notation used to describe a network security game is given in the Table 2.9.

	Covered	Uncovered
Defender	0	$-\mathcal{T}(t)$
Attacker	0	$\mathcal{T}(t)$

Table 2.8: Payoff structure for a network security game considered in this thesis.

$G(\mathbf{N}, \mathbf{E})$	Network
\mathbf{N}	Nodes (n iterates over \mathbf{N})
\mathbf{E}	Edges (e iterates over \mathbf{E})
\mathcal{T}	Target Payoffs
R	Defender resources
\mathbf{X}	Set of defender allocations, $\mathbf{X} = \{X_1, X_2, \dots, X_n\}$
X_i	i^{th} defender allocation. $X_i = \{X_{ie}\} \forall e, X_{ie} \in \{0, 1\}$
\mathbf{A}	Set of attacker paths, $\mathbf{A} = \{A_1, A_2, \dots, A_m\}$
A_j	j^{th} attacker path. $A_j = \{A_{je}\} \forall e, A_{je} \in \{0, 1\}$
z_{ij}	Boolean variable indicating whether A_j intersects with X_i
\mathbf{x}	Defender's mixed strategy over \mathbf{X}
\mathbf{a}	Adversary's mixed strategy over \mathbf{A}
$U_{\Theta}(\mathbf{x}, A_j)$	Defender's expected utility playing \mathbf{x} against A_j
σ_{Θ}^*	Defender's pure strategy best response
σ_{Ψ}^*	Attacker's pure strategy best response

Table 2.9: Notation

2.9 Baseline Algorithms

There is previous work on computing solutions for Bayesian Stackelberg games. These approaches have ranged from solving the normal form Stackelberg game, solving security games to solving the network security games. In this section, I briefly describe (i) MultipleLPs [Conitzer and Sandholm, 2006]; and (ii) DOBSS [Paruchuri et al., 2008b] for solving generic Bayesian Stackelberg games, (iii) ERASER [Kiekintveld et al., 2009] for Bayesian Security games (SPNSC); and (iv) RANGER [Tsai et al., 2010] for solving network security games. These approaches either do not scale or do not compute optimal solutions for the problems of interest in my thesis; however, I describe them here since they provide background for algorithm design and experimental evaluation.

2.9.1 Multiple LPs approach

The leader's strategy in the SSE is considered the optimal leader's strategy as it maximizes the leader's expected utility assuming the follower best responds. This section explains the baseline algorithms for finding the optimal leader's strategy of a Bayesian Stackelberg game. As shown by Conitzer and Sandholm [2006], the problem of computing the optimal leader's strategy \mathbf{x} is equivalent to finding a leader's mixed strategy \mathbf{x} and a follower's pure strategy response $\mathbf{a} = g(\mathbf{x})$ such that the three SSE conditions (refer Definition 1) are satisfied. Mathematically \mathbf{x} can be found by solving the following maximization problem:

$$(\mathbf{x}^*, \sigma_{\Psi}^*) = \arg \max_{\mathbf{x}, \sigma_{\Psi}^*} \{U_{\Theta}(\mathbf{x}, \sigma_{\Psi}^*) | U_{\Psi}^{\lambda}(\mathbf{x}, \sigma_{\Psi}^{\lambda*}) \geq U_{\Psi}^{\lambda}(\mathbf{x}, \sigma_{\Psi}^{\lambda'}), \forall \sigma_{\Psi}^{\lambda'} \in \Sigma_{\Psi}^{\lambda}\}. \quad (2.4)$$

Here, σ_{Ψ}^* is the pure strategy for the *Bayesian follower*, and consists of $\sigma_{\Psi}^* = \langle \sigma_{\Psi}^{\lambda*} \rangle$, i.e., pure strategy best responses for each follower type. \mathbf{x}^* refers to the optimal mixed strategy of the leader.

Equation (2.4) suggests the multiple linear program (LP) approach for finding \mathbf{x}^* as given in [Conitzer and Sandholm, 2006]. The idea is to enumerate all possible pure strategy responses of the follower $\sigma_{\Psi}^{\lambda}, \lambda \in \Lambda, \sigma_{\Psi}^{\lambda} \in \Sigma_{\Psi}^{\lambda}$. Furthermore, for each $\sigma_{\Psi} = \langle \sigma_{\Psi}^{\lambda} \rangle$, the optimal mixed strategy of the leader is chosen such that σ_{Ψ} is a best response of the follower, and can be found by solving the following LP:²

$$\begin{aligned}
& \max_{\mathbf{x}} \quad U_{\Theta}(\mathbf{x}, \sigma_{\Psi}) \\
& s.t. \quad \mathbf{x} \geq 0 \\
& \quad \mathbf{1}^T \mathbf{x} = 1 \\
& \quad U_{\Psi}^{\lambda}(\mathbf{x}, \sigma_{\Psi}^{\lambda}) \geq U_{\Psi}^{\lambda}(\mathbf{x}, \sigma_{\Psi}^{\lambda'}), \quad \forall \lambda \in \Lambda, \forall \sigma_{\Psi}^{\lambda'} \in \Sigma_{\Psi}^{\lambda'}
\end{aligned} \tag{2.5}$$

Some of the LPs may be infeasible but it can be shown that at least one LP will return a feasible solution. The optimal leader's strategy \mathbf{x}^* is then the optimal solution of the LP which has the highest objective value (i.e., the leader's expected utility) among all feasible LPs.

2.9.2 Dobss: Mixed Integer Linear Program

Since the followers of different types are mutually independent of each other, there can be at most $\prod_{\lambda} |\Sigma_{\Psi}^{\lambda}|$ possible combinations of follower best response actions over the follower types. The multiple LPs approach will then have to solve $\prod_{\lambda} |\Sigma_{\Psi}^{\lambda}|$ LPs and therefore its runtime complexity grows exponentially in the number of follower types. In fact, the problem of finding the optimal

²Note the formulation here is slightly different from and has fewer constraints in each LP than the original multiple LPs approach in [Conitzer and Sandholm, 2006] where a Bayesian game is transformed to a normal-form one using Harsanyi transformation [Harsanyi and Selten, 1972].

strategy for the leader in a Bayesian Stackelberg game with multiple follower types is NP-hard [Conitzer and Sandholm, 2006]. Nevertheless, researchers have continued to provide practical improvements. Dobss is an efficient general Stackelberg solver [Paruchuri et al., 2008b] and is in use for security scheduling at the Los Angeles International Airport in the ARMOR system [Pita et al., 2008]. Dobss obtains a decomposition scheme by exploiting the property that follower types are independent of each other and solves the entire problem as one mixed-integer linear program (MILP):

$$\begin{aligned}
& \max_{\mathbf{x}, \mathbf{d}, \mathbf{k}, \mathbf{a}} \quad \sum_{\lambda} p^{\lambda} d^{\lambda} \\
& s.t. \quad \mathbf{1}^T \mathbf{x} = 1, \mathbf{x} \geq 0 \\
& \quad \sum_{j=1}^{|\Sigma_{\Psi}^{\lambda}|} a_j^{\lambda} = 1, \quad \forall \lambda \\
& \quad a_j^{\lambda} \in \{0, 1\}, \quad \forall \lambda, \forall j = 1..|\Sigma_{\Psi}^{\lambda}| \\
& \quad d^{\lambda} \leq U_{\Theta}^{\lambda}(\mathbf{x}, j) + (1 - a_j^{\lambda}) \cdot M, \quad \forall \lambda, \forall j \\
& \quad 0 \leq k^{\lambda} - U_{\Psi}^{\lambda}(\mathbf{x}, j) \leq (1 - a_j^{\lambda}) \cdot M, \quad \forall \lambda, \forall j
\end{aligned} \tag{2.6}$$

Dobss effectively reduces the problem of solving an exponential number of LPs to a compactly represented MILP which can be solved much more efficiently via modern techniques in Operations Research. The key idea of the Dobss MILP is to represent the strategy of each follower type a^{λ} as a binary vector $a^{\lambda} = [\sigma_{\Psi_1}^{\lambda}, \sigma_{\Psi_2}^{\lambda}, \dots]$ where $\sigma_{\Psi_j}^{\lambda}$ is 1 if the follower type λ chooses pure strategy j and 0 otherwise. Here, $U_{\Theta}^{\lambda}(\mathbf{x}, j)$ is the expected utility for the leader when the leader is playing mixed strategy \mathbf{x} and the follower is playing its j^{th} pure strategy, i.e., $\sigma_{\Psi_j}^{\lambda}$. $U_{\Psi}^{\lambda}(\mathbf{x}, j)$ is also defined similarly for the follower. M is (conceptually) an infinitely large constant.

2.9.3 ERASER Mixed Integer Linear Program

The ERASER MILP is based on the same idea as DOBSS, however, it operates on security games. Thus, it exploits the compact representation of security games and avoids the enumeration of the exponentially many pure strategy combinations for the defender. The ERASER MILP is given as follows:

$$\begin{aligned}
& \max \quad \sum_{\lambda} d^{\lambda} \\
& a_t^{\lambda} \in \{0, 1\} \quad \forall t \in T, \lambda \in \Lambda \\
& \sum_{t \in T} a_t^{\lambda} = 1 \quad \forall \lambda \in \Lambda \\
& c_t \in [0, 1] \quad \forall t \in T \\
& \sum_{t \in T} c_t \leq R \\
& d^{\lambda} - U_{\Theta}^{\lambda}(t, C) \leq (1 - a_t^{\lambda}) \cdot M \quad \forall t \in T, \lambda \in \Lambda \\
& 0 \leq k^{\lambda} - U_{\Psi}^{\lambda}(t, C) \leq (1 - a_t^{\lambda}) \cdot M \quad \forall t \in T, \lambda \in \Lambda
\end{aligned} \tag{2.7}$$

Here, the defender's strategy is represented as the *coverage vector* C instead of the traditional probability distribution \mathbf{x} , and it represents the marginal coverage of the defender on each target. Like in DOBSS, the strategy of the attacker of type λ , \mathbf{a}^{λ} , is an indicator vector and is 1 for target t only if t is the best response of attacker type λ to the coverage C of the defender. $U_{\Theta}^{\lambda}(t, C)$ and $U_{\Psi}^{\lambda}(t, C)$ represent the expected utilities to the defender and the attacker respectively given attacker type λ when the defender is playing the coverage vector C and the attacker of type λ attacks target t . R is the total number of available defender resources. M , again, is (conceptually) an infinitely large constant.

2.9.4 RANGER solution approach

RANGER [Tsai et al., 2010] provides approximate solutions to the network security game. It approximates the strategy space of the players, using an efficient shortest-path based linear program to perform the computation of the optimal defender allocation in the network. Tsai et. al [Tsai et al., 2010] then provide two sampling schemes to sample from the mixed strategy computed by RANGER to schedule the actual allocation of defender resources. The RANGER linear program is given as follows:

$$\begin{aligned}
& \max \quad d^* \\
& s.t. \quad d^* \leq (1 - d_t) \cdot \mathcal{T}(t) \\
& \quad d_s = 0 \\
& \quad d_v \leq \min(1, d_u + x_e) \quad \forall e = (u, v) \in E \\
& \quad 0 \leq x_e \leq 1 \quad \forall e \in E \\
& \quad \sum_{e \in E} x_e \leq R
\end{aligned} \tag{2.8}$$

In this RANGER linear program, d^* is the defender reward computed by RANGER. x_e is the marginal probability of placing a checkpoint on edge e . The d_v are, for each vertex v , the *minimum* sum of checkpoint probabilities along any path from the source s to vertex v . The RANGER solution overestimates the optimal defender reward, and as I show, in Chapter 4, the solution quality of RANGER is unbounded.

Chapter 3: Strategy Generation for One Player

In this chapter, I show how strategy generation for one player can be used in domains where the number of pure strategies for one player are extremely large. I will use two domains to demonstrate the point: the SPARS domain as well as the SPPC domain. I will also show how strategy generation can be used in *conjunction* with previously published algorithms to compute optimal defender strategies in the SPARS domain. I conclude this section with experimental results in Section 3.4.

3.1 SPARS domain

In this section, I present *Accelerated SPARS ENgine*, ASPEN, an algorithm that solves an instance of the SPARS problem without having to enumerate all the pure strategies of the defender. ASPEN focuses on the non-Bayesian case (and so I omit the usage of the subscript λ in this section) – I will describe the Bayesian extension in Chapter 5. ASPEN formulates the SPARS problem as a mixed-integer program in which the pure strategies of the attacker are represented by integer variables \mathbf{a} with $a_t = 1$ if target t is attacked and 0 otherwise. Two key computational challenges arise in such a formulation. First, the space of possible strategies (joint schedules) for the defender suffers from combinatorial explosion: a FAMS problem with 100 flights, schedules with 3 flights, and 10 air marshals has up to 100,000 schedules and $\binom{100000}{10}$ joint schedules. Second, integer

variables are a well-known challenge for optimization, since linear problems without integer variables can be solved in polynomial time, while versions with integer variables are NP-hard. ASPEN overcomes these challenges using the framework of Branch and Price [Barnhart et al., 1994], which is used to solve very large optimization problems. It combines branch and bound search with column generation to mitigate both of the problems described above. The use of column generation decomposes the problem in such a way that one pure strategy (joint schedule) of the defender is generated in each iteration, thereby allowing the computation of the optimal strategy without explicitly enumerating the entire pure strategy space of the defender. This method operates on joint schedules (and not marginal probabilities, like ERASER-C), so it is able to handle scheduling constraints directly.

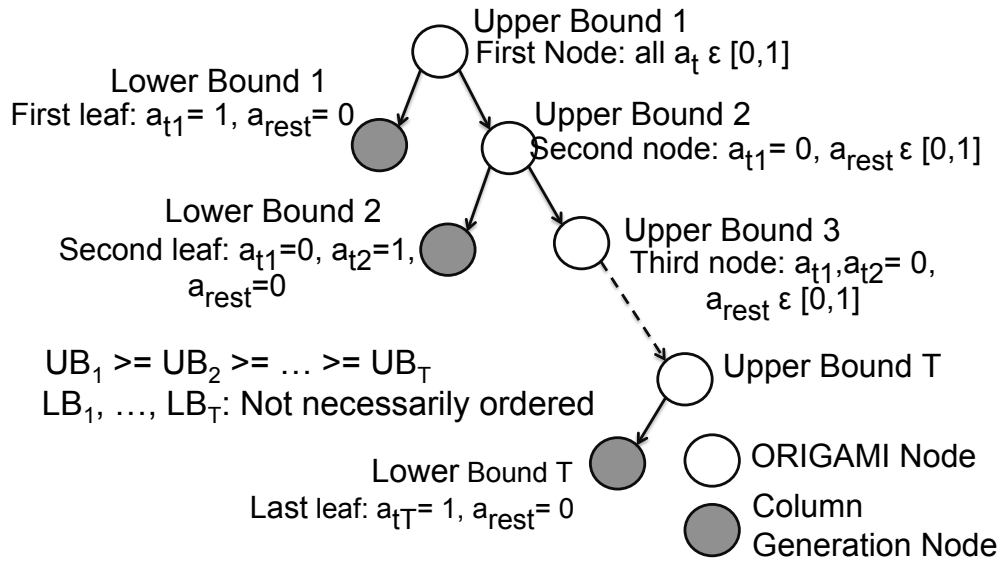


Figure 3.1: Working of Branch and Price for a non-Bayesian SPARS problem instance.

An example of branch and price for our problem is shown in Figure 3.1, with the root node representing the original problem. Every branch of this tree represents a pure strategy choice for the attacker. Branches to the left (gray nodes, labeled ‘Column Generation Node’) set exactly one

variable t_i in \mathbf{a} to 1 and the rest to zero, resulting in a linear program that gives a lower bound on the overall solution quality. Branches to the right fix that same variable t_i to zero, leaving the remaining variables unconstrained. An upper bound on solution quality computed for each white node (labeled as ‘ORIGAMI Node’) can be used to terminate execution without exploring all of the possible integer assignments. This upper bound can be computed both naïvely as well as using heuristics. In Section 3.1.2 we describe a heuristic based on the ORIGAMI algorithm that we use in ASPEN.

Solving the linear programs in each gray node normally requires enumerating all possible joint schedules for the defender. Column generation (i.e., pricing) avoids this by iteratively solving a restricted *master problem*, which includes only a small subset of the variables, and a *slave problem* that identifies new variables to include in the master problem. The new variables added by the slave problem are the ones that will maximally improve the objective value in the master problem. The algorithm terminates when the slave problem cannot identify any new variables that will improve the objective for the master problem.

Branch and price is not an “out of the box approach” and it has only recently begun to be applied in game-theoretic settings [Halvorson et al., 2009a]. To apply the technique here, we design a novel master-slave decomposition to facilitate column generation for SPARS, including a network flow formulation of the slave problem. A standard technique for generating upper bounds is to use a linear programming relaxation of the problem, but this approach performs poorly for these problems based on our experimental results. Instead, we propose new methods for bounding and selecting branches based on fast algorithms for security games without scheduling constraints.

3.1.1 ASPEN Column Generation

The linear programs at each leaf in Figure 3.1 are decomposed into *master* and *slave* problems for column generation (see Algorithm 1). The master solves for the defender strategy \mathbf{x} , given a restricted set of columns (i.e., joint schedules) \mathbf{P} , such that the attacker's best response \mathbf{a} is consistent with the leaf node from Figure 3.1. The objective function for the slave is updated in each iteration based on the current solution of the master problem. The slave problem is then solved to identify the best new column to add to the master problem, using *reduced costs* (explained later). If no column can improve the solution the algorithm terminates.

Algorithm 1 Column generation

1. Initialize P
 2. Solve Master Problem
 3. Calculate reduced cost coefficients from solution
 4. Update objective of slave problem with coefficients
 5. Solve Slave Problem
 - if** Optimal solution obtained **then**
 6. Return (\mathbf{x}, \mathbf{P})
 - else**
 7. Extract new column and add to \mathbf{P}
 8. Repeat from Step 2
-

3.1.1.1 Master Problem:

The master problem (Equations 3.1 to 3.6) solves for the probability vector \mathbf{x} that maximizes the defender reward (Table 2.5 in the Chapter 2 succinctly lists the notation).¹ This master problem operates directly on columns of \mathbf{P} , and the coverage vector \mathbf{c} is computed from these columns as $\mathbf{P}\mathbf{x}$. d represents the expected defender utility that is to be maximized, whereas \mathbf{d} is a column vector of d of dimension $|T|$. Similarly, k represents the attacker's expected utility whereas \mathbf{k}

¹The actual algorithm minimizes the negative of the defender reward for correctness of *reduced cost* computation used in the Slave Problem; we show maximization of defender reward for expository purposes.

is a column vector of k of dimension $|T|$. The vectors \mathbf{d} and \mathbf{k} are introduced for dimensional consistency in the matrix notation of the mixed integer linear program described below. While the payoffs U_{Θ}^u and U_{Θ}^c for the defender are defined as before, \mathbf{D} here is a diagonal matrix of $U_{\Theta}^c(t) - U_{\Theta}^u(t)$ of dimension $|T| \times |T|$. Similarly, U_{Ψ}^u and U_{Ψ}^c represent the payoffs for the attacker and \mathbf{A} is a diagonal matrix of $U_{\Psi}^c(t) - U_{\Psi}^u(t)$, again of dimension $|T| \times |T|$.

Constraints 3.2–3.4 enforce the SSE conditions that the players choose mutual best responses. Constraints 3.3 and 3.4 ensure that the assignment $a_t = 1$ can generate a feasible solution if and only if target t is the best response of the attacker (note that this assignment is done when resolving the branch of the branch-and-bound tree given in Figure 3.1). The defender expected payoff (Equation 2.1) for target t is given by the t^{th} component of the column vector $\mathbf{D}\mathbf{P}\mathbf{x} + \mathbf{U}_{\Theta}^u$ and denoted $(\mathbf{D}\mathbf{P}\mathbf{x} + \mathbf{U}_{\Theta}^u)_t$. Similarly, the attacker payoff for target t is given by $(\mathbf{A}\mathbf{P}\mathbf{x} + \mathbf{U}_{\Psi}^u)_t$. Constraints 3.2 and 3.3 are active only for the single target t^* attacked ($a_{t^*} = 1$). This target must be a best-response, due to Constraint 3.4. The pure strategy of the attacker \mathbf{a} is an input to the column generation procedure and not a variable for the formulation below.

$$\max \quad d \quad (3.1)$$

$$\text{s.t.} \quad \mathbf{d} - \mathbf{D}\mathbf{P}\mathbf{x} - \mathbf{U}_{\Theta}^u \leq (\mathbf{1} - \mathbf{a})M \quad (3.2)$$

$$\mathbf{k} - \mathbf{A}\mathbf{P}\mathbf{x} - \mathbf{U}_{\Psi}^u \leq (\mathbf{1} - \mathbf{a})M \quad (3.3)$$

$$\mathbf{A}\mathbf{P}\mathbf{x} + \mathbf{U}_{\Psi}^u \leq \mathbf{k} \quad (3.4)$$

$$\sum_{j \in J} x_j = 1 \quad (3.5)$$

$$\mathbf{x} \geq 0 \quad (3.6)$$

3.1.1.2 Slave Problem:

The slave problem finds the best column to add to the current columns in \mathbf{P} . This is done using *reduced costs*, which captures the rate of change in the defender payoff if a candidate column is added to \mathbf{P} . The candidate column with minimum reduced cost improves the objective value the most [Bertsimas and Tsitsiklis, 1994]. The reduced cost \bar{c}_j of variable x_j (associated with column \mathbf{P}_j) is given in Equation 3.7, where $\mathbf{w}, \mathbf{y}, \mathbf{z}$ and h are dual variables of master constraints 3.2, 3.3, 3.4 and 3.5 respectively. The dual variable measures the influence of the associated constraint on the objective, and can be calculated using standard techniques.

$$\bar{c}_j = \mathbf{w}^T(\mathbf{D}\mathbf{P}_j) + \mathbf{y}^T(\mathbf{A}\mathbf{P}_j) - \mathbf{z}^T(\mathbf{A}\mathbf{P}_j) - h \quad (3.7)$$

An inefficient approach would be to iterate through all of the columns and calculate each reduced cost to identify the best column to add. Indeed, this would defeat the whole point of column generation. Instead, we formulate a minimum cost network flow (MCNF) problem that efficiently finds the optimal column. Feasible flows in the network map to feasible joint schedules in the SPARS problem, so the scheduling constraints are captured by this formulation. The procedure to construct the MCNF graph for a given SPARS instance is given below, followed by an example.

We start by creating a sink node with demand $|R|$. A source node source_r with supply 1 is created for each defender $r \in R$.² The rest of the MCNF graph is constructed such that the flow from source_r to the sink will provide the schedule $s \in S_r$ that this resource shall undertake. Next, we construct a set of paths for each resource r from the source source_r to the sink node.

²In fact, resources r with the same set of scheduling constraints S_r are combined and connected to one source node with supply equal to the number of these resources with the same set of scheduling constraints S_r .

A path is added between source_r and sink for each schedule $s_r \in S_r$. We represent targets in schedule s for resource r using a pair of nodes $(a_{s_r,t}, b_{s_r,t})$ with a forward directed edge. Each target t is represented multiple times in the MCNF graph by a pair of nodes $(a_{s_r,t}, b_{s_r,t})$ for every schedule s_r it appears in. Then, for the schedule $s_r \in S_r$, we add a path from the source to the sink: $\langle \text{source}_r, a_{s_r,t_{i_1}}, b_{s_r,t_{i_1}}, a_{s_r,t_{i_2}}, \dots, b_{s_r,t_{i_L}}, \text{sink} \rangle$. The capacities on all edges are set to 1, and the default costs to 0. A dummy flow with infinite capacity is added to represent the possibility that some resources are unassigned. The number of resources assigned to t in a column \mathbf{P}_j is computed as:

$$\text{assigned}(t) = \sum_{s \in S} \text{flow}[\text{edge}(a_{s,t}, b_{s,t})].$$

Constraints are added to this slave problem so that

$$\text{assigned}(t) \leq 1$$

for all targets t . Thus, the value of 1 for $\text{assigned}(t)$ represents that the target t is covered by the defender, while 0 represents that no defender resource was allocated to target t .

A partial MCNF graph for our earlier example is shown in Figure 3.2, showing paths for 3 of the 5 schedules. The paths correspond to schedules $\{t_1, t_2\}$, $\{t_2, t_3\}$ and $\{t_1, t_5\}$. The supply and demand are both 3, corresponding to the number of available FAMS. Double-bordered boxes mark the flows used to compute $\text{assigned}(t_1)$ and $\text{assigned}(t_2)$. Every joint schedule corresponds to a feasible flow in G . For example, the joint schedule $\{\{t_2, t_3\}, \{t_1, t_5\}\}$ has a flow of 1 unit each through the paths corresponding to schedules $\{t_2, t_3\}$ and $\{t_1, t_5\}$, and a flow of 1 through the dummy. Similarly, any feasible flow through the graph G corresponds to a feasible joint schedule, since all resource constraints are satisfied.

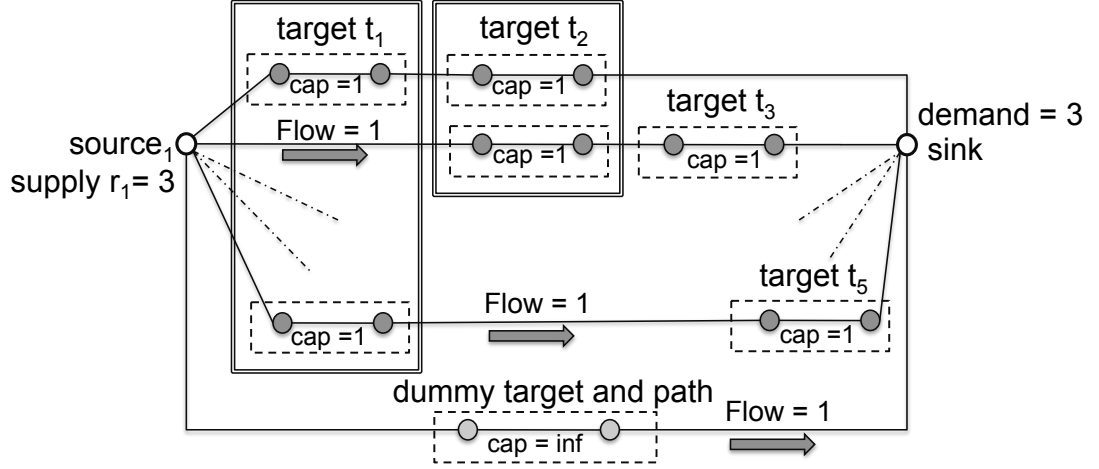


Figure 3.2: Example Minimum Cost Network Flow Graph for a SPARS problem instance.

It remains to define link costs such that the cost of a flow is the reduced cost for the joint schedule. We decompose \bar{c}_j into a sum of cost coefficients per target, \hat{c}_t , so that \hat{c}_t can be placed on links $(a_{s,t}, b_{s,t})$ for all targets t . \hat{c}_t is defined as $w_t \cdot D_t + y_t \cdot A_t - z_t \cdot A_t$ where w_t, y_t and z_t are t^{th} components of \mathbf{w}, \mathbf{y} and \mathbf{z} . D_t is equal to $U_{\Theta}^c(t) - U_{\Theta}^u(t)$ and $A_t = U_{\Psi}^c(t) - U_{\Psi}^u(t)$. The overall objective given below for the MCNF problem sums the contributions of the reduced cost from each individual flow and subtracts the dual variable h . If this is non-negative, no column can improve the master solution, otherwise the optimal column (identified by the flow) is added to the master and the process iterates.

$$\min_{\text{flow}} \sum_{(a_{s,t}, b_{s,t})} \hat{c}_t \cdot \text{flow}[(a_{s,t}, b_{s,t})] - h$$

3.1.2 Improving Branching and Bounds

ASPEN uses branch and bound to search over the space of possible attacker strategies. A standard technique in branch and price is to use LP relaxation, which allows the integer variables to take on arbitrary values (rather than just integers) to give an optimistic bound on the objective value of the original MIP. Our experimental results (Section 3.4) show that this generic method is ineffective in

our domain. We introduce ORIGAMI-S, a novel branch and bound heuristic for SPARS based on ORIGAMI [Kiekintveld et al., 2009], which is an efficient solution method for security games *without scheduling constraints* and heterogeneous resources. We use ORIGAMI-S to solve a relaxed version of SPARS that optimistically ignores scheduling constraints and integrate this with ASPEN.

The ORIGAMI-S model is given in Equations 3.8–3.16. It minimizes the attacker’s maximum payoff (Equations 3.8–3.10). The vector \mathbf{q} represents the *attack set*, and is 1 for every target that gives the attacker maximal expected payoff (Equation 3.10). The remaining non-trivial constraints restrict the coverage probabilities. ORIGAMI-S defines a set of probabilities $\tilde{c}_{t,s}$ that represent the coverage of each target t in each schedule $s \in S_r$. The total coverage c_t of target t is the sum of coverage on t across individual schedules (Equation 3.11). We define a set T_r which contains one target from each schedule $s \in S_r$ (e.g., choosing the first target from every schedule). The total coverage assigned for every resource r is bounded from above by 1 (Equation 3.12), analogous to the constraint that the total flow from the source_r in the MCNF network flow graph cannot be greater than the available supply of 1 resource.³ Total coverage is also bounded by multiplying the number of resources by the *maximum* size of any schedule (L) in Equation 3.13. The defender can

³Again, as in the MCNF graph, resources with the same set of constraints S_r are combined into one constraint, with the available supply equal to the number of equivalent resources.

never benefit by assigning coverage to nodes outside of the attack set, so these are constrained to 0 (Equation 3.14).

$$\min \quad k \quad (3.8)$$

$$\mathbf{U}_\Psi(\mathbf{c}) = \mathbf{A}\mathbf{c} + \mathbf{U}_\Psi^u \quad (3.9)$$

$$\mathbf{0} \leq \mathbf{k} - \mathbf{U}_\Psi(\mathbf{c}) \leq (\mathbf{1} - \mathbf{q}) \cdot M \quad (3.10)$$

$$c_t = \sum_{s \in S} \tilde{c}_{t,s} \quad \forall t \in T \quad (3.11)$$

$$\sum_{s \in S_r} \tilde{c}_{T_r(s),s} \leq 1 \quad \forall r \in R \quad (3.12)$$

$$\sum_{t \in T} c_t \leq L \cdot |R| \quad (3.13)$$

$$\mathbf{c} \leq \mathbf{q} \quad (3.14)$$

$$\mathbf{q} \in \{0, 1\}, \quad (3.15)$$

$$\mathbf{c}, c_{t,s} \in [0, 1] \quad \forall t \in T, s \in S \quad (3.16)$$

ORIGAMI-S is solved once at the start of ASPEN, and targets in the attack set are sorted by expected defender reward. The maximum value is an initial upper bound on the defender reward. The first leaf node that ASPEN evaluates corresponds to this maximum valued target (i.e, setting its attack value to 1), and a solution is found using column generation. This solution is a lower bound of the optimal solution, and the algorithm stops if this lower bound meets the ORIGAMI-S upper bound. Otherwise, a new upper bound from the ORIGAMI-S solution is obtained by choosing the second-highest defender payoff from targets in the attack set, and ASPEN evaluates the corresponding leaf node. This process continues until the upper bound is met, or the available nodes in the search tree are exhausted.

Theorem 1. *The defender payoff, computed by ORIGAMI-S, is an upper bound on the defender's payoff for the corresponding SPARS problem. For any target not in the attack set of ORIGAMI-S, the restricted SPARS problem in which this target is attacked is infeasible.*

Proof Sketch: ORIGAMI and ORIGAMI-S both minimize the maximum attacker payoff over a set of feasible coverage vectors. If there are no scheduling constraints, this also maximizes the defender's policy [Kiekintveld et al., 2009]. Briefly, the size of the attack set in the solution is maximized, and the coverage probability on each target in the attack set is also maximal. Both of these weakly improve the defender's payoff because adding coverage to a target is strictly better for the defender and worse for the adversary.

ORIGAMI-S makes optimistic assumptions about the coverage probability the defender can allocate by taking the maximum that could be achieved by *any* legal joint schedule and allowing it to be distributed arbitrarily across the targets, ignoring the scheduling constraints. To see this, consider the marginal probabilities \mathbf{c}^* of any legal defender strategy for SPARS. There is at least one feasible coverage strategy for ORIGAMI that gives the same payoff for the defender. Constraints 3.11 and 3.16 are satisfied by \mathbf{c}^* , because they are also constraints of SPARS. Each variable $\tilde{c}_{T_r(s),s}$ in the set defined for Constraint 3.12 belongs to a single schedule associated with resource r , and at most 1 of these can be selected in any feasible joint schedule, so this constraint must also hold for \mathbf{c}^* . Constraint 3.13 must be satisfied because it assumes that each available resource covers the largest possible schedule, so it generally allows excess coverage probability to be assigned. Finally, constraint 3.14 may be violated by \mathbf{c}^* for some target t . However, the coverage vector with coverage identical to \mathbf{c}^* for all targets in the ORIGAMI-S attack set and 0 coverage outside the attack set has identical payoffs, since these targets are never attacked.

3.2 Column generation for joint patrolling schedules

Several previous algorithms, most notably ERASER-C [Kiekintveld et al., 2009], directly reason about the marginal coverage probabilities on targets C as opposed to mixed strategies of the defender (refer Section 2.9.3). Using marginals avoids the necessity to represent the entire pure-strategy space of the defender, which can be prohibitively large. However, marginal probabilities cannot be used directly to sample a specific schedule for the defender to implement. Computing a full mixed strategy for the defender that can be used to sample a specific schedule in the general case has not been addressed in previous work (some limiting cases are addressed by [Korzhyk et al., 2010]). Furthermore, it may not be feasible to compute mixed strategies from the marginal distributions computed by an algorithm since some constraints cannot be represented in a formulation based only on marginals. For example, ERASER-C only correctly computes solutions to SPARS problem instances when each schedule in the problem instance contains only 2 targets, and they can be organized in a bipartite graph, like a federal air marshal taking a departure flight and an arrival flight. We show here how the same column generation approach used in ASPEN can also be used to generate joint schedules from the marginals output of such algorithms. This provides a competing approach to ASPEN, which we will evaluate experimentally in the following section.

The objective of the following program is to find joint schedules \mathbf{P} and a probability distribution \mathbf{x} such that the coverage vector $\mathbf{P}\mathbf{x}$ is as close as possible to the marginals \mathbf{c} provided as input. We use L1 norm to determine the distance between the coverage vector obtained by this approach and the marginals, since it may not always be feasible to convert marginals into implementable

mixed strategies. The procedure below will return an objective of 0 only when the marginals \mathbf{c} are implementable as a mixed strategy \mathbf{x} over joint schedules \mathbf{P} by the defender.

$$\begin{aligned} \min_x \quad & \|\mathbf{P}\mathbf{x} - \mathbf{c}\|_1 \\ \sum_j x_j &= 1 \\ x_j &\geq 0 \end{aligned} \tag{3.17}$$

The associated master problem is:

$$\min_{x, \gamma} \sum_{t \in T} \gamma_t \tag{3.18}$$

$$s.t. \quad \mathbf{P}\mathbf{x} - \gamma \leq \mathbf{c} \tag{3.19}$$

$$\mathbf{P}\mathbf{x} + \gamma \geq \mathbf{c} \tag{3.20}$$

$$\sum_{t \in T} x_t = 1 \tag{3.21}$$

$$x \geq 0 \tag{3.22}$$

The slave problem in this case is the same as the one used in ASPEN, where the reduced cost of a joint schedule is:

$$\bar{c}_j = -(\mathbf{w}_1 - \mathbf{w}_2)^T \mathbf{P}_j - \sigma \tag{3.23}$$

where $\mathbf{w}_1, \mathbf{w}_2, \sigma$ are the optimal dual variables of the current master problem associated constraints 3.19, 3.20, and 3.21. Again, the reduced cost \bar{c}_j can be decomposed into reduced cost coefficients per target \hat{c}_t , which can be computed using Equation 3.24 as follows:

$$\hat{c}_t = -(w_{1t} - w_{2t}) \quad (3.24)$$

Thus, the column generation approach of ASPEN can be combined with any algorithm that computes marginal probabilities, producing a mixed strategy for the defender consistent with scheduling constraints in the domain.

3.3 SPPC Domain

I propose a branch-and-price based formulation to compute optimal defender strategies in this domain as well. Again, branch and bound search is used to address the integer variables: each branch sets the values for some integer variable, whereas column generation is used to scale up the computation to very large input problems. There is a binary variable associated with each attacker: either an attacker chooses to attack or he does not. The binary variables are assigned values using a branch and bound tree, where each branch of this tree assigns a specific value to each attacker variable. Thus, each leaf of this tree assigns a value for every attacker, that is, for every binary variable. I now present the algorithm for the case with multiple attackers; the formulation for a Bayesian single attacker is presented in Chapter 5. As mentioned above, I use branch-and-price to compute solutions for this problem, and the column generation procedure used here is presented next.

3.3.1 Column Generation:

Column generation is used to solve each node of the above branch and bound tree. The problem at each leaf is formulated as a linear program, which is then decomposed into a *Master* problem and a *Slave* problem. The master solves for the defender strategy \mathbf{x} , given a restricted set of tours T . The objective function for the slave is updated based on the solution of the master, and the slave is solved to identify the best new column to add to the master problem, using reduced costs (explained later). If no tour can improve the solution further, the column generation procedure terminates.

3.3.1.1 Master Formulation:

The master problem solves for the best probability distribution \mathbf{x} that maximizes the defender's expected utility given a limited number of patrol tours \mathbf{T} . The defender's expected utility is a sum of defender utilities d_s over all the targets s . The master formulation is given in Equations (3.25) to (3.31). The notation is described in Table 2.6. Equations (3.27) and (3.28) capture the payoff to the defender. They ensure that d_s is upper bounded by the payoff to the defender at target s , Equation (3.27) capturing the payoff when the attacker chooses to attack s (i.e. $q_s = 1$) whereas (3.28) captures the defender's payoff when the attacker chooses to not attack s (i.e. $q_s = 0$). Similarly, Equations (3.29) and (3.30) capture the payoff of the attacker. They ensure that the assignment $q_s = 1$ is feasible if and only if the payoff to the attacker for attacking the target s , $(\sum_{t \in T} x_t z_{st})(-P - R_s) + R_s$, is greater than 0, the attacker's payoff for not attacking target s . Equations (3.26) and (3.31) ensure that the strategy \mathbf{x} is a valid probability distribution.

$$\min_{x,y,d,q} - \sum_{s \in S} d_s \quad (3.25)$$

$$\text{s.t.} \quad \sum_{t \in T} x_t \leq 1 \quad (3.26)$$

$$d_s - \sum_{t \in T} x_t z_{st} (\tau_s + R_s) + Mq_s \leq M - R_s \quad (3.27)$$

$$d_s - Mq_s \leq 0 \quad (3.28)$$

$$Mq_s(P + R_s) + \sum_{t \in T} x_t z_{st}(P + R_s) \leq M + R_s \quad (3.29)$$

$$-Mq_s(P + R_s) - \sum_{t \in T} x_t z_{st}(P + R_s) \leq -R_s \quad (3.30)$$

$$x_t \in [0, 1] \quad (3.31)$$

3.3.1.2 Slave Formulation:

The slave problem find the best patrol tour to add to the current set of tours \mathbf{T} . This is done using reduced cost, which captures the total change in the defender payoff if a tour is added to the set of tours \mathbf{T} . The candidate tour with the minimum reduced cost improves the objective value the most [Bertsimas and Tsitsiklis, 1994]. The reduced cost \bar{c}_t of variable x_t , associated with tour T , is given in Equation 3.32, where w , y , v and h are dual variables of master constraints (3.27), (3.29), (3.30) and (3.26) respectively. The dual variable measures the influence of the associated constraint on the objective, and can be calculated using standard techniques:

$$\bar{c}_t = \sum_{s \in S} (w_s(\tau_s + R_s) + (v_s - y_s)(P + R_s))z_{st} - h \quad (3.32)$$

One approach to identify the tour with the minimum reduced cost would be to iterate through all possible tours, compute their reduced costs, and then choose the one with the least reduced

cost. However, we propose a minimum-cost integer network flow formulation that efficiently finds the optimal column (tour). Feasible tours in the domain map to feasible flows in the network flow formulation and vice-versa. The minimum cost network flow graph is constructed in the following manner. A virtual source and virtual sink are constructed to mark the beginning and ending locations, i.e. home base, for a defender tour. These two virtual nodes are directly connected by an edge signifying the "Not attack" option for the attacker. As many levels of nodes are added to the graph as the number of targets. Each level contains nodes for every target. There are links from every node on level i to every node on level $i + 1$. Each node on every level i is also directly connected to the sink. Additionally, the length of the edge between any two nodes is the Euclidean distance between the two corresponding targets. Constraints are added to the slave problem to disallow a tour that covers two nodes corresponding to the same target (i.e. a network flow going through node (1,1) and (2,1) in the figure would be disallowed since both these nodes correspond to target 1). An additional constraint is added to the slave to ensure that the total length of every flow (i.e. sum of lengths of edges with a non-zero flow) is less than the specified upper bound L . Thus, the slave is setup such that there exists a one-to-one correspondence between a flow generated by the slave problem and patrol route that the defender can undertake. Figure 3.3 shows an example graph for the slave.

Each node representing a target is split into two dummy nodes with an edge between them. Link costs are put on these edges. The costs on these graphs are defined by decomposing the reduced cost of a tour, \bar{c}_t , into reduced costs over individual targets, \hat{c}_s . We decompose \bar{c}_t into

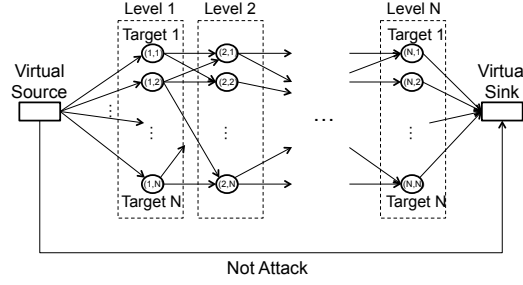


Figure 3.3: This figure shows an example network-flow based slave formulation. There are as many levels in the graphs as the number of targets. Each node represents a specific target. A path from the source to the sink maps to a tour taken by the defender.

a sum of cost coefficients per target \hat{c}_s , so that \hat{c}_s can be placed on the edges between the two dummy nodes of each target. \hat{c}_s are defined as follows:

$$\bar{c}_t = \sum_{s \in S} \hat{c}_s z_{st} - h \quad (3.33)$$

$$\hat{c}_s = (w_s(\tau_s + R_s) + (v_s - y_s)(P + R_s)) \quad (3.34)$$

3.4 Experimental Results

3.4.1 Comparison Results

This section presents detailed results of using strategy generation for computing solutions for domains with large number of pure strategies for one player. The results in this section focus solely on results on the SPARS domain (the trends for the SPPC domain are similar and are analyzed in more depth in Chapter 6). Here, I compare the performance of ASPEN (Section 3.1.1), ASPEN without the branch-and-bound heuristic of ORIGAMI-S (henceforth referred to as BnP), and the total runtime of ERASER-C [Kiekintveld et al., 2009]. In our results, we present runtimes

for ERASER-C that include the generation of the defender’s mixed strategy using our column generation approach (refer Section 3.2) in order to provide a fair comparison with ASPEN. For this experiment, we generate random instances of SPARS problems [Kiekintveld et al., 2009] with schedules of size two organized in a bipartite graph, e.g. with one departure flight and one arrival flight drawn from disjoint sets (this ensures that ERASER-C can find a correct optimal solution). We vary the number of targets, defender resources, and schedules.

All experiments are based on 30 sample games, and problem instances that took longer than 30 minutes to run were terminated. The results of the first experiment are shown in Figure 3.4. The y-axis shows the runtime in seconds on the log scale. The x-axis shows the number of resources. These results shows that for low number of targets (less than 100), ERASER-C is the fastest algorithm. However, ERASER-C starts to lose its performance advantage when the number of targets is increased. BnP is the slowest (as expected), and scales much poorly as compared to the other algorithms. To further examine the advantage offered by ASPEN, we increased the number of targets to 200 and beyond in the second set of experiments. The results varying the number of defender resources for 200 targets are shown in Figure 3.5(a).

As seen in Figure 3.5, ASPEN is the fastest of the three algorithms for large number of targets. The effectiveness of the ORIGAMI-S bounds and branching are clear in the comparison with standard BnP method. Since ASPEN solves a far more general set of security games (SPARS), we would not expect it to be competitive with ERASER-C in its specialized domain. However, ASPEN was 6 times faster than ERASER-C in some instances. This improvement over ERASER-C was an unexpected trend, and can be attributed to the number of columns generated by the two approaches (Table 3.1). We observe similar results in the second and third data sets presented in Figures 3.5(b) and 3.5(c).

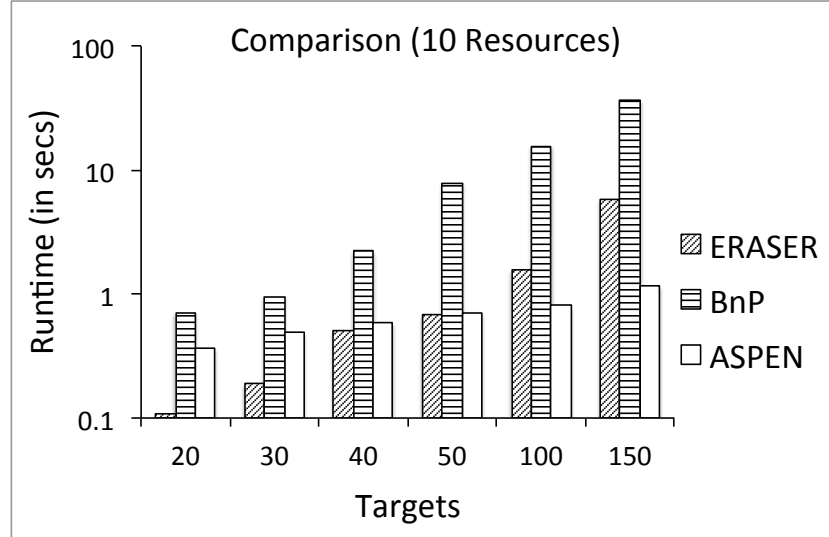


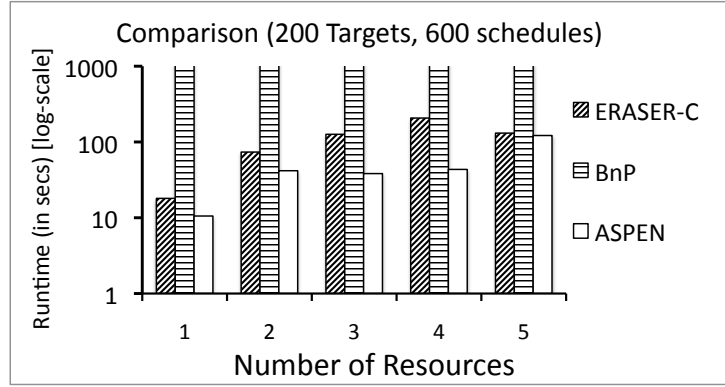
Figure 3.4: Comparison between ERASER-C, ASPEN and BnP for SPARS problem instances with 10 resources. The number of schedules for these experiments was two times the number of targets. In this figure and others with y-axis on the log scale, error bars are not shown since they are not prominent because of the logarithmic axis. In this experiment, the difference in runtime for all pair-wise comparisons was statistically significant except between ERASER-C and ASPEN for 40 and 50 targets.

Resources	ASPEN	ERASER-C	BnP (max. 30 mins)
10	126	204	1532
20	214	308	1679
30	263	314	1976
40	227	508	1510
50	327	426	1393

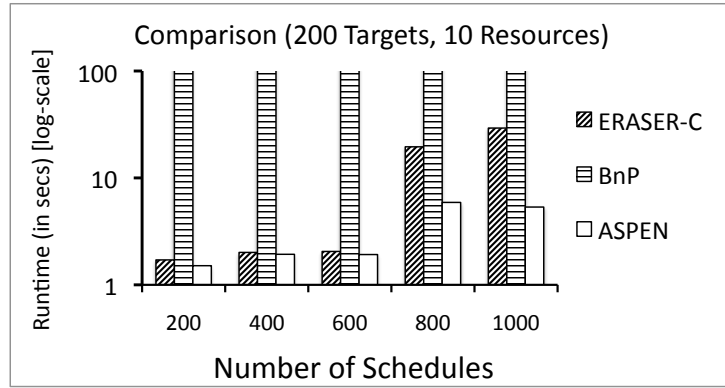
Table 3.1: This table shows the average number of columns (pure strategies for the defender) generated by the column generation approach for all the three algorithms: ASPEN, BnP, and column generation on marginals generated by ERASER-C. These results are averaged over 30 SPARS problem instances, with 200 targets and 600 schedules where each schedule is of size 2. These results confirm the presence of small support sets in such problem instances: the number of targets in these experiments was 200 which implies that the maximum number of pure strategies can be of the order of 10^{16} for 10 resources up to 10^{47} for 50 resources.

3.4.2 ASPEN on Large SPARS Instances:

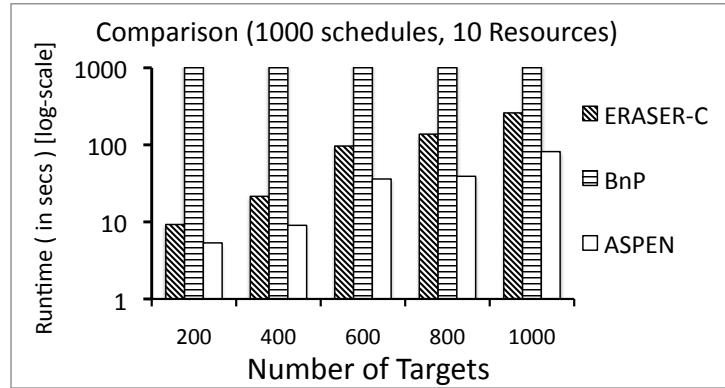
We also evaluate the performance of ASPEN on arbitrary scheduling problems as the size of the problem is varied to include very large instances. No comparisons could be made because ERASER-C does not handle arbitrary schedules and the only correct algorithms known, DOBSS [Paruchuri



(a) Resources



(b) Schedules



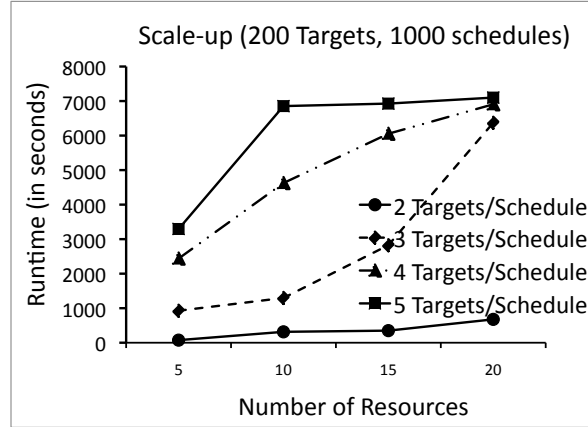
(c) Targets

Figure 3.5: These figures present results comparing the runtime required by ASPEN, ASPEN without the ORIGAMI-S branch-and-bound heuristic (BnP) and ERASER-C with column generation on SPARS instances with 2 schedules per target. The y-axis shows the runtime in seconds in log scale, whereas the x-axis varies an input parameter, as specified in the figure. Again, we do not show the error bars because of the log scale of the y-axis, but ASPEN was the fastest algorithm with statistical significance.

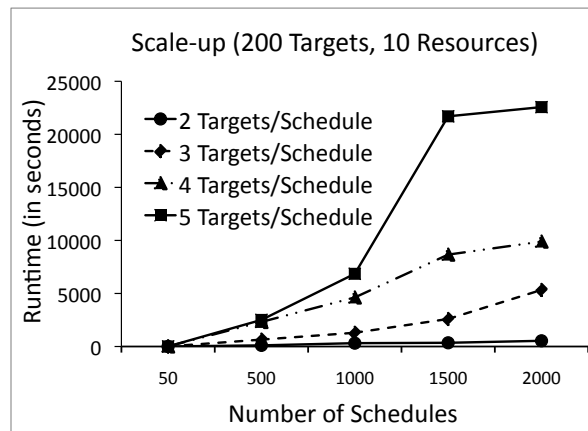
et al., 2008a] and BnP (ASPEN without the ORIGAMI-S branch-and-bound heuristic), do not scale to these problem sizes. We vary the number of resources, schedules, and targets as before. In addition, we vary the number of targets per schedule for each of the three cases to test more complex scheduling problems. Figure 3.6(a) shows the runtime results with 1000 feasible schedules and 200 targets, averaged over 10 samples. The x-axis shows the number of resources, and the y-axis shows the runtime in seconds. Each line represents a different number of schedules per target. The number of joint schedules in these instances can be as large as 10^{23} ($\binom{1000}{10} \approx 2.6 \times 10^{23}$). Interestingly, the runtime does not increase much when the number of resources is increased from 10 to 20 when there are 5 targets per schedules. Column 4 of Table 3.2 illustrates that the key reason for constant runtime is that the average number of generated columns remains similar. For a fixed number of resources, we observe an increase in runtime for more complex schedules that corresponds with an increase in the number of columns generated. The other two experiments, Figure 3.6(b) and 3.6(c) also show similar trends.

Resources	3 Targets / schedule	4 Targets / schedule	5 Targets / schedule
5	456	518	658
10	510	733	941
15	649	920	1092
20	937	1114	1124

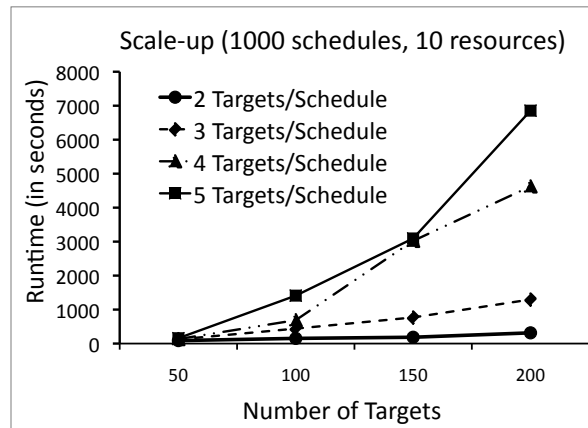
Table 3.2: This table shows the average number of columns (pure strategies for the defender) generated by the column generation approach for ASPEN. These results are averaged over 30 SPARS problem instances, with 200 targets and 1000 schedules.



(a) Resources



(b) Schedules



(c) Targets

Figure 3.6: These figures present the runtime results for ASPEN when the size of the input problem is scaled. The y-axis shows the runtime in seconds, whereas the x-axis varies an input parameter, as specified in the figure.

Chapter 4: Strategy generation for both players

This chapter focuses on the network security domain (NSD), and shows how strategy generation for both players can be used to compute solutions for extremely large problems with exponentially many pure strategies for both the players. However, before I proceed to describe my algorithms, RUGGED and SNARES, I first describe why RANGER, the best previous approach, failed to generate correct solutions for NSD problem instances. The RANGER algorithm as used in this chapter is described in Section 2.9.4.

4.1 RANGER Counterexample

RANGER was introduced by Tsai et al. [Tsai et al., 2010] and was designed to obtain approximate solutions for the defender for the network security game. Its main component is a polynomial-sized linear program that, rather than solving for a distribution over allocations, solves for the *marginal* probability with which the defender covers each edge. It does this by approximating the capture probability as the sum of the marginals along the attacker’s path. It further presents some sampling techniques to obtain a distribution over defender allocations from these marginals. What was known before was that the RANGER solution (regardless of the sampling method used) is suboptimal in general, because it is not always possible to find a distribution over allocations such

that the capture probability is indeed the sum of marginals on the path. In this paper, we show that RANGER's error can be arbitrarily large.

Let us consider the example graph shown in Figure 4.1. This multi-graph¹ has a single source node, s , and two targets, t_1 and t_2 ; the defender has 2 resources. Furthermore, the payoffs \mathcal{T} of the targets are defined to be 1 and 2 for targets t_1 and t_2 respectively.

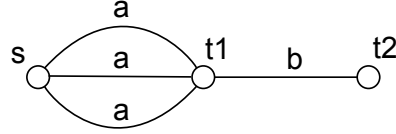


Figure 4.1: This example is solved *incorrectly* by RANGER. The variables a , b are the coverage probabilities on the corresponding edges.

RANGER solution:

Suppose RANGER puts marginal coverage probability a on each of the three edges between s and t_1 ,² and probability b on the edge between t_1 and t_2 , as shown in Figure 4.1. RANGER estimates that the attacker gets caught with probability a when attacking target t_1 and probability $a + b$ when attacking target t_2 . RANGER will attempt to make the attacker indifferent between the two targets to obtain the minimax equilibrium. Thus, RANGER's output is $a = 3/5$, $b = 1/5$, obtained from the following system of equations:

$$1(1 - a) = 2(1 - (a + b)) \quad (4.1)$$

$$3a + b = 2 \quad (4.2)$$

¹We use a multi-graph for simplicity. This counterexample can easily be converted into a similar counterexample that has no more than one edge between any pair of nodes in the graph.

²We can assume without loss of solution quality that symmetric edges will have equal coverage.

However, there can be no allocation of 2 resources to the edges such that the probability of the attacker being caught on his way to t_1 is $3/5$ and the probability of the attacker being caught on his way to t_2 is $4/5$. (The reason is that in this example, the event of there being a defensive resource on the second edge in the path cannot be disjoint from the event of there being one on the first edge.) In fact, for this RANGER solution, the attacker cannot be caught with a probability of more than $3/5$ when attacking target t_2 , and so the defender utility cannot be greater than $-2(1 - 3/5) = -4/5$.

Optimal solution:

Figure 4.2 shows the six possible allocations of the defender's two resources to the four edges. Three of them block some pair of edges between s and t_1 . Suppose that each of these three allocations is played by the defender with probability x .³ Each of the other three allocations blocks one edge between s and t_1 as well as the edge between t_1 and t_2 . Suppose the defender chooses these allocations with probability y each (refer Figure 4.2). The probability of the attacker being

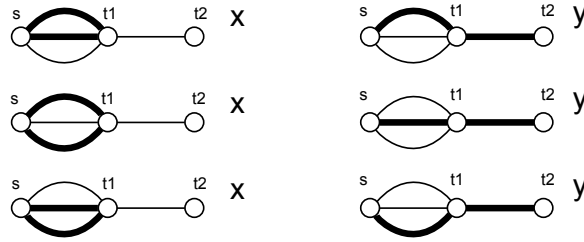


Figure 4.2: The possible allocations of two resources to the four edges. The blocked edges are shown in bold. The probabilities (x or y) are shown next to each allocation.

caught on his way to t_1 is $\frac{2}{3}3x + \frac{1}{3}3y$, or $2x + y$. Similarly, the probability of the attacker being

³Again, this can be assumed without loss of generality for symmetric edges.

caught on his way to t_2 is $2x + 3y$. Thus, a minimax strategy for this problem is the solution of Equations (4.3) and (4.4), which make the attacker indifferent between targets t_1 and t_2 .

$$1(1 - 2x - y) = 2(1 - 2x - 3y) \quad (4.3)$$

$$3x + 3y = 1 \quad (4.4)$$

The solution to the above system is $x = 2/9$, $y = 1/9$, so that the expected attacker utility is $4/9$. Thus, the expected defender utility is $-4/9$, which is higher than the expected defender utility of at most $-4/5$ resulting from using RANGER.

RANGER sub-optimality:

Suppose the payoff $\mathcal{T}(t_2)$ of target t_2 in the example above was H , $H > 1$. The RANGER solution in this case, again obtained using Equations 4.1 and 4.2, would be $a = \frac{(H+1)}{(2H+1)}$, $b = \frac{(H-1)}{(2H+1)}$.

Then, consider an attacker who attacks the target t_2 by first going through one of the three edges from s to t_1 uniformly at random (and then on to t_2). The attacker will fail to be caught on the way from t_1 to t_2 with probability $(1 - b)$, given that the defender's strategy is consistent with the output of RANGER. Even conditional on this failure, the attacker will fail to be caught on the way from s to t_1 with probability at least $1/3$, because the defender has only 2 resources. Thus, the probability of a successful attack on t_2 is at least $(1 - b)(1/3)$, and the attacker's best-response utility is at least:

$$\frac{H(1 - b)}{3} = \frac{H(H + 2)}{3(2H + 1)} > \frac{H(H + 0.5)}{3(2H + 1)} = \frac{H}{6} \quad (4.5)$$

Thus, the true defender utility for any strategy consistent with RANGER is at most $-\frac{H}{6}$.

Now, consider another defender strategy in which the defender always blocks the edge from t_1 to t_2 , and also blocks one of the three edges between s and t_1 uniformly at random. For such a defender strategy, the attacker can reach t_1 with probability $2/3$, but cannot reach target t_2 at all. Thus, the attacker's best-response utility in this case is $2/3$. Therefore, the optimal defender utility is at least $-2/3$. Therefore, any solution consistent with RANGER is at least $\frac{H}{6}/\frac{2}{3} = \frac{H}{4}$ suboptimal. Since H is arbitrary, RANGER solutions can be arbitrarily suboptimal. This motivates our exact, double-oracle algorithm, RUGGED.

4.2 RUGGED

In this section, I present RUGGED, a double-oracle based algorithm for network security games. We also analyze the computational complexity of determining best responses for both the defender and the attacker, and, to complete the RUGGED algorithm, we give algorithms for computing the best responses.

4.2.1 Algorithm Description

The algorithm RUGGED is presented as Algorithm 2. \mathbf{X} is the set of defender allocations generated so far, while \mathbf{A} is the set of attacker paths generated so far. $\text{CoreLP}(\mathbf{X}, \mathbf{A})$ finds an equilibrium (and hence, minimax and maximin strategies) of the two-player zero-sum game consisting of the sets of pure strategies, \mathbf{X} and \mathbf{A} , generated so far. CoreLP returns \mathbf{x} and \mathbf{a} , which are the current equilibrium mixed strategies for the defender and the attacker over \mathbf{X} and \mathbf{A} respectively. The *defender oracle* (DO) generates a defender allocation Λ that is a best response for the defender

against \mathbf{a} . (This is a best response among *all* allocations, not just those in \mathbf{X} .) Similarly, the *attacker oracle* (AO) generates an attacker path Γ that is a best response for the attacker against \mathbf{x} .

Algorithm 2 Double Oracle for Urban Network Security

1. Initialize \mathbf{X} by generating arbitrary candidate defender allocations.
 2. Initialize \mathbf{A} by generating arbitrary candidate attacker paths.
 - repeat**
 3. $(\mathbf{x}, \mathbf{a}) \leftarrow \text{CoreLP}(\mathbf{X}, \mathbf{A})$.
 - 4a. $\Lambda \leftarrow DO(\mathbf{a})$.
 - 4b. $\mathbf{X} \leftarrow \mathbf{X} \cup \{\Lambda\}$.
 - 5a. $\Gamma \leftarrow AO(\mathbf{x})$.
 - 5b. $\mathbf{A} \leftarrow \mathbf{A} \cup \{\Gamma\}$.
 - until** convergence
 7. Return (\mathbf{x}, \mathbf{a})
-

The double oracle algorithm thus starts with a small set of pure strategies for each player, and then grows these sets in every iteration by applying the best-response oracles to the current solution. Execution continues until convergence is detected. Convergence is achieved when the best-response oracles of both the defender and the attacker do not generate a pure strategy that is better for that player than the player's strategy in the current solution (holding the other player's strategy fixed). In other words, convergence is obtained if, for both players, the reward given by the best-response oracle is no better than the reward for the same player given by the *CoreLP*.

The correctness of best-response-based double oracle algorithms for two-player zero-sum games has been established by McMahan et al [McMahan et al., 2003]; the intuition for this correctness is as follows. Once the algorithm converges, the current solution must be an equilibrium of the game, because each player's current strategy is a best response to the other player's current strategy—this follows from the fact that the best-response oracle, which searches over all possible strategies, cannot find anything better. Furthermore, the algorithm must converge, because at worst, it will generate all pure strategies.

4.2.2 CoreLP

The purpose of *CoreLP* is to find an equilibrium of the restricted game consisting of defender pure strategies \mathbf{X} and attacker pure strategies \mathbf{A} . Below is the standard formulation for computing a maximin strategy for the defender in a two-player zero-sum game.

$$\max_{U_d^*, \mathbf{x}} U_d^* \quad (4.6)$$

$$\text{s.t. } U_d^* \leq U_d(\mathbf{x}, A_j) \quad \forall j = 1, \dots, |\mathbf{A}| \quad (4.7)$$

$$\mathbf{1}^T \mathbf{x} = 1 \quad (4.8)$$

$$\mathbf{x} \in [0, 1]^{|X|} \quad (4.9)$$

The defender's mixed strategy \mathbf{x} , defined over \mathbf{X} , and utility U_d^* are the variables for this problem. Inequality (4.7) is family of constraints; there is one constraint for every attacker path A_j in \mathbf{A} . The function $U_d(\mathbf{x}, A_j)$ is the expected utility of the attacker path A_j . Given A_j , the probability that the attacker is caught is the sum of the probabilities of the defender allocations that would catch the attacker. (We can sum these probabilities because they correspond to disjoint events.) More precisely, let z_{ij} be an indicator for whether allocation X_i intersects with path A_j , that is,

$$z_{ij} = \begin{cases} 1 & \text{if } X_i \cap A_j \neq \emptyset \\ 0 & \text{otherwise} \end{cases} \quad (4.10)$$

These z_{ij} are not variables of the linear program; they are parameters that are determined at the time the best responses are generated. Then, the probability that an attacker playing path A_j is caught is $\sum_i z_{ij} x_i$, and the probability that he is *not* caught is $\sum_i (1 - z_{ij}) x_i$. Thus, the payoff function

$U_d(\mathbf{x}, A_j)$ for the defender for choosing a mixed strategy \mathbf{x} when the attacker chooses path A_j is given by Equation (4.11), where $\mathcal{T}(t_j)$ is the attacker's payoff for reaching t_j .

$$U_d(\mathbf{x}, A_j) = -\mathcal{T}(t_j) \cdot \left(\sum_i (1 - z_{ij})x_i \right) \quad (4.11)$$

The dual variables corresponding to Inequality (4.7) give the attacker's mixed strategy \mathbf{a} , defined over \mathbf{A} . The expected utility for the attacker is given by $-U_d^*$.

4.2.3 Defender Oracle

This section concerns the best-response oracle problem for the defender. The *Defender Oracle* problem is stated as follows: generate the defender pure strategy (resource allocation) Λ allocating k resources over the edges E that maximizes the defender's expected utility against a given attacker mixed strategy \mathbf{a} over paths \mathbf{A} .

Defender Oracle problem is NP-hard: We show this by reducing the set cover problem to it.

The Set-Cover problem: Given are a set U , a collection \mathcal{S} of subsets of U (that is, $\mathcal{S} \subseteq 2^U$), and an integer k . The question is whether there is a cover $C \subseteq \mathcal{S}$ of size k or less, that is, $\bigcup_{c \in C} c = U$ and $|C| \leq k$. We will use a modification of this well-known NP-hard problem so that \mathcal{S} always contains all singleton subsets of U , that is, $x \in U$ implies $\{x\} \in \mathcal{S}$. This modified problem remains NP-hard.

Theorem 2. *The Defender Oracle problem is NP-hard, even if there is only a single source and a single target.*

Proof. **Reduction from Set-Cover to Defender Oracle:** We convert an arbitrary instance of the set cover problem to an instance of the defender oracle problem by constructing a graph G with

just 3 nodes, as shown in Figure 4.3. The graph G is a multi-graph⁴ with just three nodes, so that $\mathbf{N} = \{s, v, t\}$, where s is the only source and t is the only target (with arbitrary positive value). There are up to $|\mathcal{S}|$ loop edges adjacent to node v ; each loop edge corresponds to a unique non-singleton subset in \mathcal{S} . There are $|U|$ edges between s and v , each corresponding to a unique element in U . There are also $|U|$ edges between v and t , each corresponding to a unique element in U . The attacker's paths correspond to the elements in U . A path that corresponds to $u \in U$ starts with the edge between s and v that corresponds to u , then loops through all the edges that correspond to non-singleton subsets in \mathcal{S} that contain u , and finally ends with the edge between v and t that corresponds to u . Hence, any two paths used by the attacker can only intersect at the loop edges. The probabilities that the defender places on these paths are arbitrary positive numbers. We now

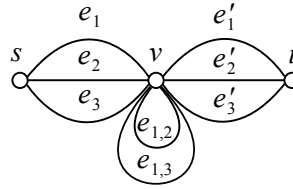


Figure 4.3: A *defender oracle* problem instance corresponding to the SET-COVER instance with $U = \{1, 2, 3\}$, $\mathcal{S} = \{\{1\}, \{2\}, \{3\}, \{1, 2\}, \{1, 3\}\}$. Here, the attacker's mixed strategy uses three paths: $(e_1, e_{1,2}, e_{1,3}, e'_1)$, $(e_2, e_{1,2}, e'_2)$, $(e_3, e_{1,3}, e'_3)$. Thus, the SET-COVER instance has a solution of size 2 (for example, using $\{1, 2\}$ and $\{1, 3\}$); correspondingly, with 2 resources, the defender can always capture the attacker (for example, by covering $e_{1,2}, e_{1,3}$).

show that set U can be covered with k subsets in $\mathcal{S} \subseteq 2^U$ if and only if the defender can block all of the attacker's paths with k resources in the corresponding defender oracle problem instance.

The “if” direction: If the defender can block all the paths used by the attacker with k resources, then the set U can be covered with $C \subseteq \mathcal{S}$, where $|C| = k$ and is constructed as follows.

If the defender places a resource on a loop edge, then C includes the non-singleton subset in \mathcal{S}

⁴Having a multi-graph is not essential to the NP-hardness reduction.

that corresponds to that loop edge. If the defender blocks any other edge then C includes the corresponding singleton subset.

The “only if” direction: If there exists a cover C of size k , then the defender can block all the paths by placing a defensive resource on every loop edge that corresponds to a non-singleton subset in C , and placing a defensive resource on the corresponding edge out of s for every singleton subset in C . \square

Formulation: The defender oracle problem, described below, can be formulated as a mixed integer linear program (*MILP*). The objective of the MILP is to identify the allocation that *covers* as many attacker paths as possible, where paths are weighted by the product of the payoff of the target attacked by the path and probability of attacker choosing it. (In this formulation, probabilities a_j are not variables; they are provided by *CoreLP*.) In the formulation, $\lambda_e = 1$ indicates that we assign a resource to edge e , and $z_j = 1$ indicates that path A_j (refer Table 2.9) is blocked by the allocation.

$$\max_{z, \lambda} \quad - \sum_j (1 - z_j) a_j \mathcal{T}_{t_j} \quad (4.12)$$

$$\text{s.t.} \quad z_j \leq \sum_e A_{je} \lambda_e \quad (4.13)$$

$$\sum_e \lambda_e \leq k \quad (4.14)$$

$$\lambda_e \in \{0, 1\} \quad (4.15)$$

$$z_j \in [0, 1] \quad (4.16)$$

Theorem 3. *The MILP described above correctly computes a best-response allocation for the defender.*

Proof. The defender receives a payoff of $-\mathcal{T}(t_j)a_j$ if the attacker successfully attacks target t_j using path A_j , and 0 in the case of an unsuccessful attack. Hence, if we make sure that $1 - z_j = 1$ if path A_j is not blocked, and 0 otherwise, then the objective function (4.12) correctly models the defender's expected utility. Inequality (4.13) ensures this: its right-hand side will be at least 1 if there exists an edge on the path A_j that defender is covering, and 0 otherwise. z_j need not be restricted to take an integer value because the objective is increasing with z_j and if the solver can push it above 0, it will choose to push it all the way up to 1. Therefore, if we let Λ correspond to the set of edges covered by the defender, z_j will be set by the solver so that:

$$z_j = \begin{cases} 1 & \text{if } \Lambda \cap A_j \neq \emptyset \Leftrightarrow \exists e \mid \lambda_e = A_{je} = 1 \\ 0 & \text{otherwise} \end{cases} \quad (4.17)$$

Inequality (4.14) enforces that the defender covers at most as many edges as the number of available resources k , and thus ensures feasibility. Hence, the above MILP correctly captures the best-response oracle problem for the defender. \square

Proposition 1. *For any attacker mixed strategy, the defender's expected utility from the best response provided by the defender oracle is no worse than the defender's equilibrium utility in the full zero-sum game.*

Proof. In any equilibrium, the attacker plays a mixed strategy that minimizes the defender's best-response utility; therefore, if the attacker plays any other mixed strategy, the defender's best-response utility can be no worse. \square

4.2.4 Attacker Oracle

This section concerns the best-response oracle problem for the attacker. The *Attacker Oracle* problem is to generate the attacker pure strategy (path) Γ from some source $s \in S$ to some target $t \in T$ that maximizes the attacker expected utility given the defender mixed strategy \mathbf{x} over defender allocations \mathbf{X} .

Attacker Oracle is NP-hard: We show that the attacker oracle problem is also NP-hard by reducing 3-SAT to it.

Theorem 4. *The Attacker Oracle problem is NP-hard, even if there is only a single source and a single target.*

Proof. **Reduction from 3-SAT to Attacker Oracle:** We convert an arbitrary instance of 3-SAT to an instance of the *attacker oracle* problem as follows. Suppose the 3-SAT instance contains n variables x_i , $i = 1, \dots, n$, and k clauses. Each clause is a disjunction of three literals, where each *literal* is either a variable or the negation of the variable. Consider the following example:

$$E = (x_1 \vee \neg x_2 \vee \neg x_3) \wedge (x_1 \vee x_2 \vee x_4) \quad (4.18)$$

The formula E contains $n = 4$ variables and $k = 2$ clauses.

We construct a multi-graph G^5 with $n + k + 1$ nodes, v_0, \dots, v_{n+k} so that the source node is $s = v_0$, and the target node is $t = v_{n+k}$. Every edge connects some pair of nodes with consecutive indices, so that every simple path from s to t contains exactly $n + k$ edges. Each edge corresponds to a literal in the 3-SAT expression (that is, either x_i or $\neg x_i$). There are exactly three edges that connect nodes v_{i-1} and v_i for $i = 1, \dots, k$. Those three edges correspond to the three literals in the

⁵We use a multi-graph for simplicity; having a multi-graph is not essential for the NP-hardness reduction.

i -th clause. There are exactly two edges that connect nodes v_{k+j-1} and v_{k+j} for $j = 1, \dots, n$. Those two edges correspond to literals x_j and $\neg x_j$. An example graph that corresponds to the expression (4.18) is shown in Figure 4.4.

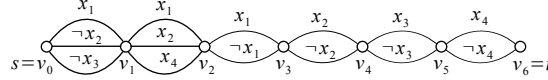


Figure 4.4: An example graph corresponding to the CNF formula $(x_1 \vee \neg x_2 \vee \neg x_3) \wedge (x_1 \vee x_2 \vee x_4)$

There are $2n$ defender pure strategies (allocations of resources), each played with equal probability of $1/(2n)$. Each defender pure strategy corresponds to a literal, and the edges that correspond to that literal are blocked in that pure strategy. In the example shown in Figure 4.4, the defender plays 8 pure strategies, each with probability $1/8$. Three edges are blocked in the pure strategy that corresponds to the literal x_1 (namely, the top edge between v_0 and v_1 , the top edge between v_1 and v_2 , and the top edge between v_2 and v_3); only one edge is blocked in the pure strategy that corresponds to the literal $\neg x_4$ (the bottom edge between v_5 and v_6). (If it is desired that the defender always use the same number of resources, this is easily achieved by adding dummy edges.) We now show that there is an assignment of values to the variables in the 3-SAT instance so that the formula evaluates to *true if and only if* there is a path from s to t in the corresponding attacker oracle problem instance which is blocked with probability at most $1/2$.

The “if” direction: Suppose there is a path Γ from s to t that is blocked with probability at most $1/2$. Note that any path from s to t is blocked by at least one of the strategies $\{x_i, \neg x_i\}$, for all $i = 1, \dots, n$, so the probability that the path is blocked is at least $n/(2n) = 1/2$. Moreover, if for some i , the path passes through both an edge labeled x_i and one labeled $\neg x_i$, then the probability that the path is blocked is at least $(n + 1)/(2n) > 1/2$ —so this cannot be the case for Γ . Hence, we can assign the *true* value to the literals that correspond to the edges on the path Γ , and *false* to all

the other literals. This must correspond to a solution to the 3-SAT instance, because each clause must contain a literal that corresponds to an edge on the path, and is thus assigned a *true* value.

The “only if” direction: Suppose there is an assignment of values to the variables such that the 3-SAT formula evaluates to *true*. Consider a simple path Γ that goes from s to t through edges that correspond to literals with *true* values in the assignment. Such a path must exist because by assumption the assignment satisfies every clause. Moreover, this path is blocked only by the defender strategies that correspond to *true* literals, of which there are exactly n . So the probability that the path is blocked is $n/(2n) = 1/2$. \square

Formulation: The attacker oracle problem can be formulated as a set of mixed integer linear programs, as described below. For every target in T , we solve for the best path to that target; then we take the best solution overall. Below is the formulation when the attacker is attacking target t_m . (In this formulation, probabilities x_i are not variables; they are values produced earlier by *CoreLP*.) In the formulation, $\gamma_e = 1$ indicates that the attacker passes through edge e , and $z_i = 1$

indicates that the allocation X_i blocks the attacker path. Equations (4.20) to (4.22) represent the flow constraints for the attacker for every node $n \in \mathbf{N}$.

$$\max_{z, \gamma} \quad \mathcal{T}_{t_m} \sum_i x_i (1 - z_i) \quad (4.19)$$

$$\text{s.t.} \quad \sum_{e \in \text{out}(n)} \gamma_e = \sum_{e \in \text{in}(n)} \gamma_e \quad n \neq s, t_m \quad (4.20)$$

$$\sum_{e \in \text{out}(s)} \gamma_e = 1 \quad (4.21)$$

$$\sum_{e \in \text{in}(t_m)} \gamma_e = 1 \quad (4.22)$$

$$z_i \geq \gamma_e + X_{ie} - 1 \quad \forall e \forall i \quad (4.23)$$

$$z_i \geq 0 \quad (4.24)$$

$$\gamma_e \in \{0, 1\} \quad (4.25)$$

Theorem 5. *The MILP described above correctly computes a best-response path for the attacker.*

Proof. The flow constraints are represented in Equations (4.20) to (4.22). The sink for the flow is the target t_m that we are currently considering for attack. To deal with the case where there is more than one possible source node, we can add a virtual source (s) to G that feeds into all the real sources. $\text{in}(n)$ represents the edges coming into n , $\text{out}(n)$ represents those going out of n . The flow constraints ensure that the chosen edges indeed constitute a path from the (virtual) source to the sink.

The attacker receives a payoff of $\mathcal{T}(t_m)$ if he attacks target t_m successfully, that is, if the path does not intersect with any defender allocation. Hence, if we make sure that $1 - z_i = 1$ if allocation X_i does not block the path, and 0 otherwise, then the objective function (4.19) correctly models the attacker's expected utility. Inequality (4.23) ensures this: if the allocation X_i covers some e for

which $\gamma_e = 1$, then it will force z_i to be set at least to 1; otherwise, z_i only needs to be set to at least 0 (and in each case, the solver will push it all the way down to this value, which also explains why the z_i variables do not need to be restricted to take integer values). Therefore, if we let Γ correspond to the path chosen by the attacker, z_i will be set by the solver so that

$$z_i = \begin{cases} 1 & \text{if } X_i \cap \Gamma \neq \emptyset \Leftrightarrow \exists e \mid \gamma_e = X_{ie} = 1 \\ 0 & \text{otherwise} \end{cases} \quad (4.26)$$

It follows that the MILP objective is correct. Hence, the above MILP captures the best-response oracle problem for the attacker. \square

Proposition 2. *For any defender mixed strategy, the attacker's expected utility from the best response provided by the attacker oracle is no worse than the attacker's equilibrium utility in the full zero-sum game.*

Proof. In any equilibrium, the defender plays a mixed strategy that minimizes the attacker's best-response utility; therefore, if the defender plays any other mixed strategy, the attacker's best-response utility can be no worse. \square



Figure 4.5: Example graph of Southern Mumbai with 455 nodes. Sources are depicted as green arrows and targets are red bulls-eyes. Best viewed in color.

4.3 Evaluation of RUGGED

In this section, we describe the results I achieved with RUGGED. We conducted experiments on graphs obtained from road network GIS data for the city of Mumbai (inspired by the 2008 Mumbai incidents [Chandran and Beitchman, 29 November 2008]), as well as on artificially generated graphs. We provide two types of results: (1) Firstly, we compare the solution quality obtained from RUGGED with the solution quality obtained from RANGER. These results are shown in Section 4.3.1. (2) Secondly, we provide runtime results showing the performance of RUGGED when the input graphs are scaled up.⁶ The following three types of graphs were used for the experimental results:

(1) *Weakly fully connected (WFC)* graphs, denoted $G^{\text{WFC}}(N, E)$, are graphs where N is an ordered set of nodes $\{n_1, \dots, n_m; S = \{n_1\}, T = \{n_m\}\}$. For each node n_i , there exists a set of directed edges, $\{(n_i, n_j) | n_i < n_j\}$, in E . These graphs were chosen because of the extreme size of the strategy spaces for both players. Additionally, there are no *bottleneck* edges, so these graphs are designed to be computationally challenging for RUGGED.

(2) *Braid-type* graphs, denoted $G^B(N, E)$, are graphs where N is a sequence of nodes n_1 to n_m such that each pair n_{i-1} and n_i is connected by 2 to 3 edges. Node n_1 is the source node. Any following node is a target node with probability 0.2, with payoff \mathcal{T} randomly chosen between 1 and 100. These graphs have a similar structure as the graph in Figure 4.1, and were motivated by the counterexample in Section 4.1.

(3) *City* graphs of different sizes were extracted from the southern part of Mumbai using the GIS data provided by OpenStreetMaps. The placement of 2-4 targets was inspired by the Mumbai incidents from 2008 [Chandran and Beitchman, 29 November 2008]; 2-4 sources were placed

⁶All experiments were run on standard desktop 2.8GHz machine with 2GB main memory.

on the border of the graph,⁷ simulating an attacker approaching from the sea. We ran the test for graphs with the following numbers of nodes: 45, 129 and 252. Figure 4.5 shows a sample Mumbai graph with 252 nodes, 4 sources and 3 targets.

4.3.1 Comparison with RANGER

This section compares the solution quality of RUGGED and RANGER. Although we have already established that RANGER solutions can be arbitrarily bad in general, the objective of these tests is to compare the actual performance of RANGER with RUGGED. The results are given in Table 4.1, which shows the average and maximum *error* from RANGER. We evaluated RANGER on the three types of graphs — city graphs, braid graphs and weakly fully connected graphs of different sizes, fixing the number of defender resources to 2 and placing 3 targets, with varied values from the interval $[0, 1000]$. The actual defender utility from the solution provided by RANGER⁸ is computed by using the best-response oracle for the attacker with the RANGER defender strategy as input. The error of RANGER is then expressed as the difference between the defender utilities in the solutions provided by RANGER and by RUGGED.

Table 4.1 shows the comparison results between RANGER and RUGGED, summarized over 30 trials. It shows the percentage of trials in which RANGER gave an incorrect solution (denoted “pct”). It also shows the average and maximum error of RANGER (denoted as *avg* and *max* respectively) over these trials. It shows that while RANGER was wrong only about 1/3 of the time for Braid graphs, it gave the wrong answer in *all* the runs on the fully connected graphs. Furthermore, it was wrong 90% of the time on city graphs, with an average error of 215 units and a maximum error of

⁷We placed more sources and targets into larger graphs.

⁸Because RANGER provides a solution in the form of marginal probabilities of defender allocations along edges, we used *Comb sampling* [Tsai et al., 2010] to convert this into a (joint) probability distribution over defender allocations.

721 units. Given an average target value of 500, these are high errors indeed — indicating that RANGER is unsuitable for deployment in real-world domains.

	City		Braid		WFC	
nodes	45	129	10	20	10	20
avg error	215	250	210	259	191	80
max error	721	489	472	599	273	117
pct	90%	100%	30%	37%	100%	100%
avg \mathcal{T}	500	500	500	500	500	500

Table 4.1: RANGER average and maximum error and percent of samples where RANGER provided a suboptimal solution. Target values \mathcal{T} were randomly drawn from the interval $[1, 1000]$.

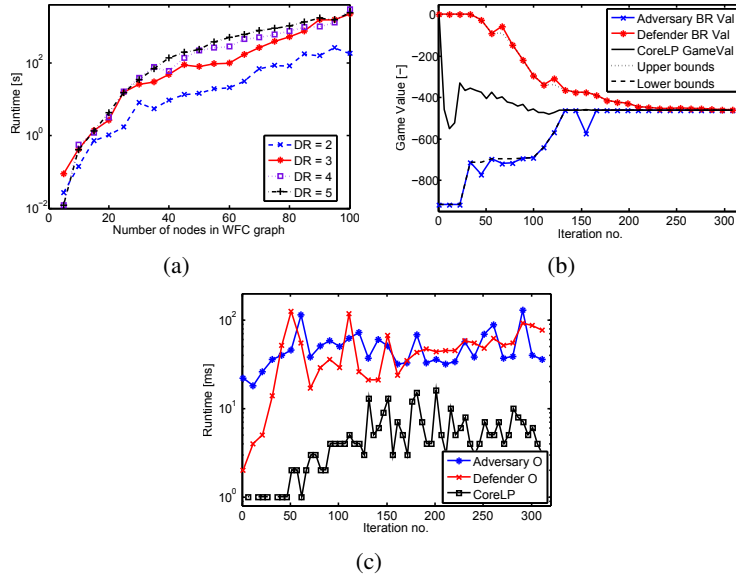


Figure 4.6: Results. Figure (a) shows the scale-up analysis on WFC graph of different sizes. Figure (b) shows the convergence of oracle values to the final game value and the anytime bounds. Figure (c) compares the runtimes of oracles and the core LP.

4.3.2 Scale-up and analysis

This section concerns the performance of RUGGED when the input problem instances are scaled up. The experiments were conducted on graphs derived directly from portions of Mumbai’s road network. The runtime results are shown in Table 4.2, where the rows represent the size of the

	1	2	3	4
45	0.91	6.43	22.58	33.42
129	6.63	32.55	486.48	3140.23
252	17.19	626.25	2014.14	34344.70

Table 4.2: Runtime (in seconds) of RUGGED when the input problem instances are scaled up. These tests were done on graphs extracted from the road network of Mumbai. The rows correspond to the number of nodes in the graph whereas the columns correspond to the number of defender resources.

graph and the columns represent the number of defender resources that need to be scheduled. As an example of the complexity of the graph, the number of attacker paths in the Mumbai graph with 252 nodes is at least a 10^{12} , while the number of defender allocations is approximately 10^{10} for 4 resources. The game matrix for this problem cannot even be represented, let alone solved. The ability of RUGGED to compute optimal solutions in such situations, while overcoming NP-hardness of both oracles, marks a significant advance in the state of the art in deploying game-theoretic techniques.

Figure 4.6(a) examines the performance of RUGGED when the size of the strategy spaces for both players is increased. These tests were conducted on WFC graphs, since they are designed to have large strategy spaces. These problems have 20 to 100 nodes and up to 5 resources. The x-axis in the figure shows the number of nodes in the graph, while the y-axis shows the runtime in seconds. Different number of defender resources are represented by different curves in the graph. For example for 40 nodes, and 5 defender resources, RUGGED took 108 seconds on average.

To speed up the convergence of RUGGED, we tried to *warm-start* the algorithm with an initial defender allocation such as min-cut-based allocations, target- and source-centric allocations, RANGER allocations and combinations of these. No significant improvement of runtime was measured; in some cases, the runtime increased because of the larger strategy set for the defender.

4.3.3 Algorithm Dynamics Analysis

This section analyzes the anytime solution quality and the performance of each of the three components of RUGGED: the defender oracle, the attacker oracle, and the *CoreLP*. When we solve the best-response oracle problems, they provide lower and upper bounds on the optimal defender utility, as shown in Propositions 1 and 2. Figure 4.6(b) shows the progress of the bounds and the *CoreLP* solution for a sample problem instance scheduling 2 defender resources on a fully connected network with 50 nodes. The x-axis shows the number of iterations and the y-axis shows the expected defender utility. The graph shows that a good solution (i.e., one where the difference in the two bounds is less than ϵ) can be computed reasonably quickly, even though the algorithm takes longer to converge to the optimal solution. For example, a solution with an allowed approximation of 10 units⁹ can be computed in about 210 iterations, whereas 310 iterations are required to find the optimal solution. The difference between these two bounds gives an upper bound on the error in the current solution of the *CoreLP*; this also provides us with an *approximation* variant of RUGGED.

Figure 4.6(c) compares the runtime needed by the three modules in every iteration. The x-axis shows the iteration number and the y-axis shows the runtime in seconds in logarithmic scale. As expected, *CoreLP* — solving a standard linear program — needs considerably less time in each iteration than both the oracles, which solve mixed-integer programs. The figure also shows that the modules scale well as the number of iterations increases.

⁹10 units is 1% of the maximum target payoff (1000).

4.4 SNARES

The focus of this section is to present SNARES (Securing Networks by Applying a Randomized Emplacement Strategy), a new algorithm for computing the optimal solution for much larger network security domains. SNARES builds on the double-oracle approach of RUGGED, and has two novel features. First, SNARES uses greedy heuristics to compute “better” (rather than “best”) responses for *both players*. I show that the best-response problem for the defender has a submodularity property, and exploiting this provide a bound for the solution quality of our better response. Second, SNARES uses a novel “mincut-fanout” technique to warm-start the computation by initializing the game matrix with pure strategies for both the players. We show that naïve ways of warm-starting the computation can actually *increase* the runtime, and that our novel technique is effective. We extensively analyze these individual components of SNARES in this paper. Finally, I demonstrate SNARES’s significant advance over the state-of-the-art (i.e., RUGGED): whereas state-of-the-art was restricted to the southern tip of Mumbai, with SNARES, optimal strategies for the entire road network of the city of Mumbai (refer Figure 4.7) can be obtained in a reasonable amount of time.

4.4.1 Algorithm Description

I now present SNARES in detail. The flow chart for SNARES is presented in Figure 4.8. The boxes with double lines are the three novel features in SNARES, and I will describe them in detail in this section, while modules also present in RUGGED are shown in boxes with single-line borders. The formal algorithm is given as Algorithm 3.

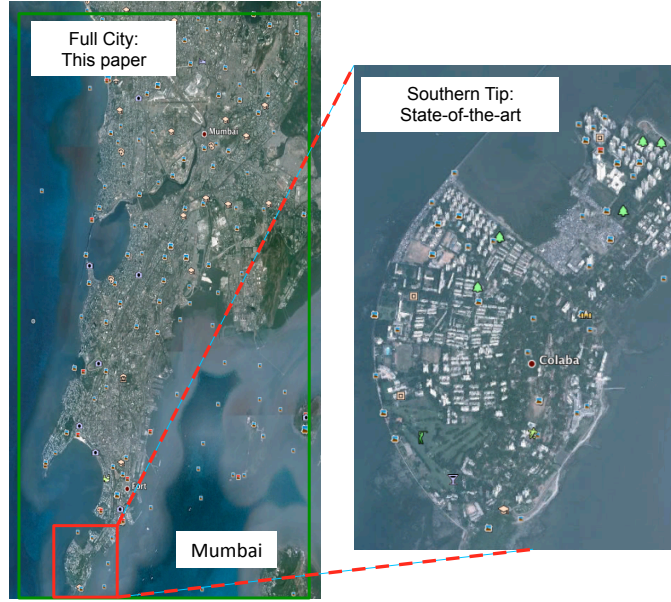


Figure 4.7: Comparison between SNARES and state-of-the-art: SNARES can now scale to solve problems the size of full cities where previous work could only scale to the southern tip of Mumbai.

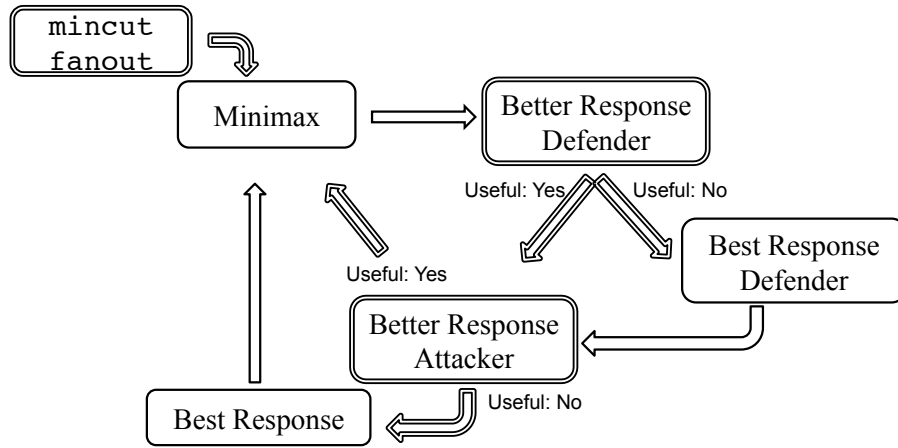


Figure 4.8: Flow Chart for the SNARES Algorithm

SNARES warm starts the computation with the pure strategies obtained using the mincut-fanout procedure, which will be explained next. DBO and ABO in Lines 4 and 8 refer to the defender better response and attacker better response oracles respectively, while DO and AO in Lines 6 and 10 are the best response oracles for both players respectively. In Line 4, DBO

Algorithm 3 $\text{SNARES}(G, k)$

```
1: Initialize  $\mathbf{X}, \mathbf{A}$  using mincut-fanout
2: repeat
3:    $(\mathbf{x}, \mathbf{a}) \leftarrow \text{CoreLP}(\mathbf{X}, \mathbf{A})$ .
4:    $X \leftarrow \text{DBO}(\mathbf{a})$ .
5:   if  $U_d(X, \mathbf{a}) - U_d(\mathbf{x}, \mathbf{a}) \leq \epsilon$  then
6:      $X \leftarrow \text{DO}(\mathbf{a})$ .
7:    $\mathbf{X} \leftarrow \mathbf{X} \cup \{X\}$ .
8:    $A \leftarrow \text{ABO}(\mathbf{x})$ .
9:   if  $U_a(A, \mathbf{x}) - U_a(\mathbf{a}, \mathbf{x}) \leq \epsilon$  then
10:     $A \leftarrow \text{AO}(\mathbf{x})$ .
11:    $\mathbf{A} \leftarrow \mathbf{A} \cup \{A\}$ .
12: until convergence
13: return  $(\mathbf{x}, \mathbf{a})$ 
```

returns a heuristic response X of the defender (we call this heuristic response as a “better” response as opposed to the “best” response; here X may not be strictly better than existing strategies). Line 5 checks whether this utility $U_d(X, \mathbf{a})$ is higher than the utility $U_d(\mathbf{x}, \mathbf{a})$ obtained from minimax by at least ϵ , i.e., whether X is at least ϵ -better than all strategies present in \mathbf{X} against \mathbf{a} . If $U_d(X, \mathbf{a})$ is not at least ϵ higher than $U_d(\mathbf{x}, \mathbf{a})$, then the best response DO is invoked (Line 6). Line 7 guarantees that each iteration adds an improving pure strategy to \mathbf{X} , should one exist. Similarly computation is performed for the attacker in Lines 8–11. Line 12 states that the computation proceeds until convergence, which is obtained when the utility obtained from the best response of each player is not better than the corresponding player’s utility from the minimax strategy. In other words, convergence is obtained when $U_d(X, \mathbf{a}) - U_d(\mathbf{x}, \mathbf{a}) \leq \tau$ and $U_a(A, \mathbf{x}) - U_a(\mathbf{a}, \mathbf{x}) \leq \tau$, where τ defines the tolerance.¹⁰ Finally, SNARES is guaranteed to converge on the global optimal solution since convergence can be obtained only when the best responses for both the players are unable to generate an improving strategy.

¹⁰In all our experiments, we fix both ϵ and τ to 0.001.

4.4.2 Warm-starting using mincut-fanout

The objective of warm-starting is to generate pure strategies for both the defender and the attacker before the computation of the minimax strategy is started. Given the setup of the game, the best response of the attacker will choose to attack the highest-valued target \hat{t} with probability 1.0, if there exists a $s - \hat{t}$ path in $G(N, E)$ that does not intersect with any of the defender's allocations. Consequently, strategies considering the most-valued target get generated by the iterative procedure of the double-oracle based algorithm in the first few iterations. The objective of warm-starts here is to generate such strategies for both players and add them before the start of the double-oracle iterative procedure. This will reduce the number of iterations that are required by the algorithm.

Thus, we construct a game with just one target: \hat{t} . Solution for this game can be computed in polynomial-time: it is to uniformly distribute the defender's resources on the $s - \hat{t}$ min-cut [Washburn and Wood, 1995]. Thus, mincut-fanout will sample pure strategies for the defender, or defender allocations, from the $s - \hat{t}$ min-cut, such that each allocation covers k edges. We then compute pure strategies for the attacker, or attacker paths, which are best responses to each individual defender allocation. This is done using Dijkstra's shortest path computation, such that each edge e in the defender allocation X has weight \inf , while the other edges have a weight of 1. This also prefers short attacker paths over long ones, the intuition being that shorter paths should be preferred by the attacker since longer paths are more likely to be intercepted.

We also generalized the above idea to consider all the targets and not just the highest valued target \hat{t} . However, as we show in Section 4.4.4.1, our choice of using only the highest valued target in mincut-fanout performs better against considering all the targets. We also show that it performs better against other potential strategies for warm starting the computation.

4.4.3 Using "Better" Responses

SNARES presents heuristics to compute "better responses" for both players. Each better response module aims to compute a strategy for the corresponding player that is better than any strategy already in the mix against the other player's current equilibrium strategy. If successful, this guarantees that CoreLP will compute a different equilibrium when this strategy is added. If the better response heuristic fails to generate such a strategy, then the best-response module is called. The objective is to reduce the number of invocations of the best response modules, both of which solve an NP-hard problem [Jain et al., 2011b] and consume significant runtime when the problem size gets bigger. On the other hand, the better response solutions used by SNARES can be computed in polynomial time. Furthermore, even with the use of better responses, SNARES still converges on the global equilibrium since the best responses modules are called if the better response modules do not generate an improving strategy. We now present the better response algorithms for both players.

4.4.3.1 Better Response for the Defender

In this section, we first present a greedy approach to generate the better response X_g of the defender. This approach greedily maximizes a "normalized" defender utility function $f(X, \mathbf{a})$. We next show that this utility function is a non-negative sub-modular function, and then establish a bound on the solution quality of our greedy better response solution. This bound suggests that our greedy approach generates good solutions.

The defender payoffs are always negative in our domain: the defender gets a payoff of $-\mathcal{T}(t)$ when the attacker successfully attacks target t and 0 otherwise. To facilitate analysis, we define a *non-negative normalized utility* function f for the defender, where

$$U_d(X, \mathbf{a}) = -\sum_{A_j \in \mathbf{A} | X \cap A_j = \emptyset} a_j \mathcal{T}(t_j) \quad (4.27)$$

$$f_{\mathbf{a}}(X) = U_d(X, \mathbf{a}) - U_d(\emptyset, \mathbf{a}) \quad (4.28)$$

More specifically, f gives the added benefit of the defender allocation X over the defender not protecting any edges. Furthermore, using Equation 4.27,

$$f_{\mathbf{a}}(X) = -\sum_{A_j \in \mathbf{A} | X \cap A_j = \emptyset} a_j \mathcal{T}(t(j)) - U_d(\emptyset, \mathbf{a}) = \sum_{A_j \in \mathbf{A} | X \cap A_j \neq \emptyset} a_j \mathcal{T}(t_j) \quad (4.29)$$

The greedy better response algorithm is described as Algorithm 4, where in each iteration, the objective is to add an edge e to the greedy defender allocation X_g that maximizes $f_{\mathbf{a}}(X \cup \{e\})$. Here, X_g (Line 1) is the computed better response of the defender. \mathbf{a} is the mixed strategy of the attacker over the set of paths \mathbf{A} that is input to the better response oracle. \mathbf{A}_r in Line 2 is used to keep track of attacker paths that not already covered by the defender's allocation. w_e (initialized in Line 4) represents the weight of each edge. These weights are updated in Lines 5–7, such that w_e represents the total marginal usage of edge e in the attacker's mixed strategy \mathbf{a} , weighted by the payoff of the target attacked by the attacker when traversing through e . The defender, following the greedy approach, chooses an edge e^* with the highest weight in Line 8. Finally, all the paths intersecting with edge e^* are removed from the set of paths considered in subsequent iterations,

i.e., from \mathbf{A}_r (Lines 10–12). Lines 13–15 are invoked only if the allocation X_g already intersects with all the attacker paths $A_j \in \mathbf{A}$, and ensures that the defender chooses k edges in its allocation.

Algorithm 4 Defender Better Response: $DBO(\mathbf{A}, \mathbf{a})$

```

1: Initialize  $X_g \leftarrow \emptyset$  (defender allocation)
2: Initialize  $\mathbf{A}_r \leftarrow \mathbf{A}$ 
3: while  $|X_g| < k$  and  $\mathbf{A}_r \neq \emptyset$  do
4:    $w_e = 0 \quad \forall e \in E$ 
5:   for all  $A_j \in \mathbf{A}_r$  do
6:     for all  $e \in A_j$  do
7:        $w_e \leftarrow w_e + a_j \mathcal{T}(t(j))$ 
8:    $e^* \leftarrow \arg \max_e w_e$ 
9:    $X_g \leftarrow X_g \cup \{e^*\}$ 
10:  for all  $A_j \in \mathbf{A}_r$  do
11:    if  $e^* \in A_j$  then
12:       $\mathbf{A}_r \leftarrow \mathbf{A}_r - \{A_j\}$ 
13: while  $|X_g| < k$  do
14:   Choose  $e$  arbitrarily from  $E$ 
15:    $X_g \leftarrow X_g \cup e$ 
16: return  $X_g$ 

```

Theorem 6. *The normalized defender utility, $f_{\mathbf{a}}(X)$, is sub-modular in X .*

Proof. We show here that the gain in defender utility when adding an edge e to an existing defender allocation X exhibits diminishing returns. Let X_1 and X_2 be two defender allocations such that $X_1 \subseteq X_2 \subseteq E$. Furthermore, let $\mathbf{A}_1 = \{A_j | A_j \cap X_1 = \emptyset\}$, i.e., the set of attacker paths that are **not** covered by X_1 . Similarly, let $\mathbf{A}_2 = \{A_j | A_j \cap X_2 = \emptyset\}$. Furthermore, $X_1 \subseteq X_2$, therefore, $\mathbf{A}_2 \subseteq \mathbf{A}_1$ since every path that is covered by X_1 is covered by X_2 .

Moreover, using Equation 4.29,

$$f_{\mathbf{a}}(X_i) = - \sum_{A_j \in \mathbf{A}_i} a_j \mathcal{T}(t(j)) - U_d(\emptyset, \mathbf{a}), \quad i \in \{1, 2\} \quad (4.30)$$

Let us now consider the addition of an edge e . Let e intersect with attacker paths $A_{12}^e \cup A_2^e \cup A_\emptyset^e$ where $A_{12}^e = \{A_j | e \in A_j, A_j \in \mathbf{A}, A_j \cap X_1 \neq \emptyset\}$ (and thus, paths in A_{12}^e also intersect with X_2), $A_2^e = \{A_j | e \in A_j, A_j \in \mathbf{A}, A_j \cap X_1 = \emptyset, A_j \cap X_2 \neq \emptyset\}$, and $A_\emptyset^e = \{A_j | e \in A_j, A_j \in \mathbf{A}, A_j \cap X_2 = \emptyset\}$ (and thus, paths in A_\emptyset^e also do not intersect with X_1). Here, \mathbf{A} represents all the possible exponentially many attacker paths possible in the input network security game. Therefore,

$$f_{\mathbf{a}}(X_1 \cup \{e\}) - f_{\mathbf{a}}(X_1) \quad (4.31)$$

$$= \sum_{A_j \in A_{12}^e \cup A_\emptyset^e} a_j \mathcal{T}(t(j)) \quad (4.32)$$

$$= \sum_{A_j \in A_{12}^e} a_j \mathcal{T}(t(j)) + \sum_{A_j \in A_\emptyset^e} a_j \mathcal{T}(t(j)) \quad (4.33)$$

$$= \sum_{A_j \in A_{12}^e} a_j \mathcal{T}(t(j)) + (f_{\mathbf{a}}(X_2 \cup \{e\}) - f_{\mathbf{a}}(X_2)) \quad (4.34)$$

$$\geq f_{\mathbf{a}}(X_2 \cup \{e\}) - f_{\mathbf{a}}(X_2) \quad (4.35)$$

Hence, the normalized defender utility $f_{\mathbf{a}}(X)$ is a non-negative sub-modular function. \square

Letting X^* to be the best response of the defender,

$$f_{\mathbf{a}}(X_g) \geq (1 - \frac{1}{e}) f_{\mathbf{a}}(X^*) \quad (4.36)$$

since we compute an incrementally maximizing greedy solution to a non-negative sub-modular function [Nemhauser et al., 1978].

We now establish the relationship between a global minimax equilibrium solution $\langle \mathbf{x}^*, \mathbf{a}^* \rangle$ and the solution $\langle \mathbf{x}_c, \mathbf{a}_c \rangle$ obtained when using just this greedy response *DBO* to compute pure

strategies for the defender, i.e., we never call DO but we do call AO by taking out Lines 5 and 6 from Algorithm 3 to arrive at $\langle \mathbf{x}_c, \mathbf{a}_c \rangle$.

Theorem 7. *The defender utility $U_d(\mathbf{x}_c, \mathbf{a}_c)$ is lower bounded by $(1 - \frac{1}{e})U_d(\mathbf{x}^*, \mathbf{a}^*) + \frac{1}{e}U_d(\emptyset, \mathbf{a}_c)$.*

Proof. Firstly, given that $\langle \mathbf{x}^*, \mathbf{a}^* \rangle$ is a minimax solution,

$$U_d(\mathbf{x}^*, \mathbf{a}^*) \geq U_d(\mathbf{x}, \mathbf{a}^*) \quad \forall \mathbf{x} \quad (4.37)$$

$$U_d(\mathbf{x}^*, \mathbf{a}) \geq U_d(\mathbf{x}^*, \mathbf{a}^*) \quad \forall \mathbf{a} \quad (4.38)$$

Furthermore, defining

$$f_{\mathbf{a}}(\mathbf{x}) = \sum_{X_i \in \mathbf{X}} x_i f_{\mathbf{a}}(X_i) \quad (4.39)$$

and using Equations (4.28), (4.37), (4.38) and (4.39), we have:

$$f_{\mathbf{a}^*}(\mathbf{x}^*) \geq f_{\mathbf{a}^*}(\mathbf{x}) \quad \forall \mathbf{x} \quad (4.40)$$

$$f_{\mathbf{a}}(\mathbf{x}^*) \geq f_{\mathbf{a}^*}(\mathbf{x}^*) + (U_d(\emptyset, \mathbf{a}^*) - U_d(\emptyset, \mathbf{a})) \quad \forall \mathbf{a} \quad (4.41)$$

Therefore, using Equations (4.36) and (4.41),

$$f_{\mathbf{a}_c}(\mathbf{x}_c) = f_{\mathbf{a}_c}(DBO(\mathbf{a}_c)) \quad (4.42)$$

$$\geq (1 - \frac{1}{e})f_{\mathbf{a}_c}(DO(\mathbf{a}_c)) \quad (4.43)$$

$$\geq (1 - \frac{1}{e})f_{\mathbf{a}_c}(\mathbf{x}^*) \quad (\text{by definition of } DO) \quad (4.44)$$

$$\geq (1 - \frac{1}{e})[f_{\mathbf{a}^*}(\mathbf{x}^*) + (U_d(\emptyset, \mathbf{a}^*) - U_d(\emptyset, \mathbf{a}_c))] \quad (4.45)$$

Therefore, $U_d(\mathbf{x}_c, \mathbf{a}_c) \geq (1 - \frac{1}{e})U_d(\mathbf{x}^*, \mathbf{a}^*) + \frac{1}{e}U_d(\emptyset, \mathbf{a}_c)$. \square

Thus, not only is the better response defender utility bounded in each iteration, but the solution quality for using just the better response is also bounded at convergence. Furthermore, $U_d(\mathbf{x}_c, \mathbf{a}_c) \geq U_d(\mathbf{x}_c, \mathbf{a}) \forall \mathbf{a}$. Thus, $U_d(\mathbf{x}_c, \mathbf{a}_c)$ is the utility that \mathbf{x}_c guarantees the defender. Also, naturally, $U_d(\emptyset, \mathbf{a}_c) \geq -\max_{t \in T} \mathcal{T}(t)$. So the greedy solution does at least as well as doing nothing $\frac{1}{e}$ of the time and playing optimally the rest of the time. This proof suggests that the better response oracle can produce good solutions efficiently, a hypothesis which we experimentally validate in Section 4.4.4.

4.4.3.2 Better Response for the Attacker

We now describe the better response heuristic for the attacker. We use a shortest path based approach to generate better responses for the attacker, which is given as Algorithm 5. This algorithm is designed to accurately determine the defender's coverage probability when estimating the attacker's utility of the better response, even if the attacker chooses two edges in his path which are covered in the same defender allocation. For example, if in the attacker's better response, the attacker traverses through the edges e_1 and e_2 , and there exists a defender allocation $X_i | e_1, e_2 \in X_i$, then Algorithm 5 will not double count the probability x_i associated with allocation X_i when computing the attacker's reward. This is different from previous greedy approaches for computing the attacker's response, which defined the cost of the edge e as the defender's marginal coverage of e [Tsai et al., 2010], and suffered from over-estimation of the defender's coverage. Algorithm 5 below assumes the presence of only one source s ; if there are multiple sources, then a virtual source is added which then connects to all the existing sources.

Lines 1–15 of Algorithm 5 follow the Dijkstra's algorithm. Here, path distances are computed using $\text{caught}[u]$, which gives the probability of the attacker's $s - u$ path getting intercepted by

Algorithm 5 Attacker Better Response: $ABO(\mathbf{X}, \mathbf{x})$

```
1: for all  $n \in N$  do
2:    $\text{caught}[n] \leftarrow \infty$ 
3:  $\text{caught}[s] \leftarrow 0$ 
4:  $\overline{\mathbf{X}}_s \leftarrow \mathbf{X}$ 
5: Add  $s$  to Priority Queue PQ
6: while PQ is not empty do
7:    $u \leftarrow \arg \min_{n \in \text{PQ}} \text{caught}[n]$ 
8:   Remove  $u$  from PQ.
9:   for  $e(u, v) \in \text{out-edges}(u)$  do
10:     $c_e \leftarrow \sum_{X_i \in \overline{\mathbf{X}}_u | e \in X_i} x_i$ 
11:    if  $\text{caught}[u] + c_e \leq \text{caught}[v]$  then
12:       $\text{caught}[v] \leftarrow \text{caught}[u] + c_e$ 
13:       $\text{prev}[v] \leftarrow u$ 
14:       $\overline{\mathbf{X}}_v \leftarrow \overline{\mathbf{X}}_u - \{X_i | e \in X_i\}$ 
15:      Add  $v$  to PQ
16: for  $t \in T$  do
17:    $\text{payoff}[t] \leftarrow (1 - \text{caught}[t]) \cdot \mathcal{T}(t)$ 
18:    $t^* \leftarrow \arg \max_t \text{payoff}[t]$ 
19:  $A_g \leftarrow \text{path}(s - t^*)$  constructed using  $\text{prev}[t^*]$ 
20: return  $A_g$ 
```

the defender. To ensure the correct computation of $\text{caught}[u]$, the algorithm keeps track of $\overline{\mathbf{X}}_u$, or the set of allocations that the attacker has *not* encountered along the $s - u$ path. $\overline{\mathbf{X}}_v$ is updated once the attacker moves to node v using the edge $e : (u, v)$ (Line 14), by removing all the allocations from $\overline{\mathbf{X}}_u$ that contributed to the cost c_e of edge e . c_e (Line 10) gives the probability of the attacker getting intercepted by the defender on this particular edge, only considering allocations in $\overline{\mathbf{X}}_u$. Lines 16 to 18 then find highest expected utility target to attack for the attacker, and the greedy path A_g is then constructed using the stored predecessor information (Lines 13 and 19). As opposed to the defender's pure strategies, the edges for the attacker *cannot* be chosen independently, because they should define a valid path from s to a target t . Such a restriction prevents us from conducting a sub-modularity analysis similar to the defender case; and we focus on experimental validation of this approach. The results are presented in Section 4.4.4.

4.4.4 Evaluation of SNARES

I now experimentally evaluate the performance of SNARES, both on simulated graphs as well as on real urban road networks. I first present the analysis of the components of SNARES, followed by scalability results.

4.4.4.1 Analysis of Components of SNARES

In this section, we evaluate the performance boost provided by each component of the SNARES algorithm. Specifically, we compare the performance with and without the use of `mincut-fanout` strategies for warm starts as well as with and without the better responses. These experiments were conducted on a machine with 16 GB main memory and a 2.3 GHz processor.

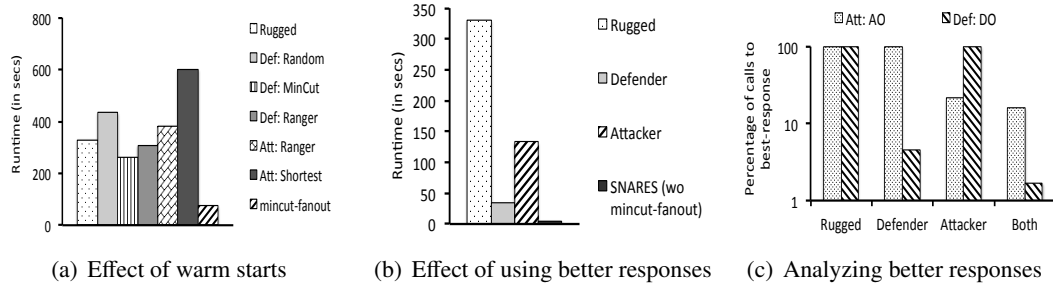


Figure 4.9: The contributions of individual components of SNARES. RUGGED is used as a baseline.

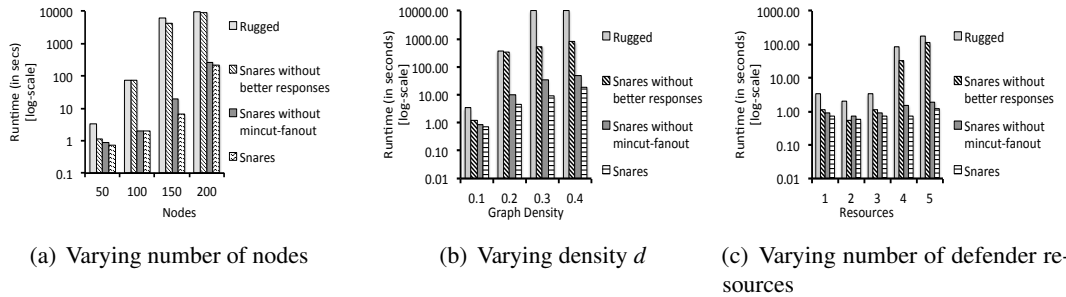


Figure 4.10: The runtime required by SNARES as the input problem size is varied.

Warm Starts without Better Responses: We compare the performance of choosing the `mincut-fanout` warm-start methodology with 5 other methodologies, ranging from random selection to using previously published algorithms for this domain. We also establish the baseline using `RUGGED`.

All data points are averaged over 30 samples for random geometric graphs. We use random geometric graphs since they have been shown to mimic the connectivity properties of real road networks [Eppstein and Goodrich, 2008]. A random geometric graph is generated as follows: nodes or vertices are placed at random uniformly and independently on a 2-D region, and two vertices u, v are connected by an edge if and only if the distance between them is at most a threshold d , i.e., $\|x - y\|_2 \leq d$. In all our experiments, our 2-D region is normalized to a unit square, and the value of d varies from 0 to 1.

These results are shown in Figure 4.9(a). The y-axis shows the runtime in seconds and the x-axis shows the different methodologies for warm starts. These results are averaged over 30 random geometric graphs with 50 nodes, 5 targets, 3 defender resources and $d = 0.2$. The target payoffs were randomly generated between 0 and 100. The first bar of the graph represents the runtime of `RUGGED`. The second, third and fourth bars are results when warm starts are used for the defender. They represent a random choice of k edges, sampling of defender pure strategies from the union of min-cuts between the source s and each target $t \in T$, and pure strategies obtained by sampling the solution obtained using `RANGER` respectively. The fifth and the sixth bars are results when warm-starts are used for the attacker. They use the `RANGER` algorithm and shortest paths from the source s to each target $t \in T$ respectively. The seventh bar in the graph represents the results of using `mincut-fanout` as in `SNARES`. Here, `RUGGED` took 329.69 seconds, random selection of edges for the defender increased the runtime to 435.24 seconds whereas `mincut-fanout` reduced

it to 76.67 seconds. These results show that while `mincut-fanout` is effective, other approaches are not as effective and may even perform worse than `RUGGED`.

Better Responses without Warm Starts: We now present the results of using better responses in `SNARES`. We evaluate the use of better responses for each player independently as well as in conjunction. However, no warm starts were used in these experiments, that is, the full Algorithm 3 was used but with Line 1 disabled. These experiments are also done on the same graphs as before: 30 samples of random geometric 50 node graphs with 5 targets, 3 defender resources and $d = 0.2$. Again, `RUGGED` forms the baseline. These results are shown in Figure 4.9(b). The y-axis shows the runtime in seconds whereas the x-axis shows the different configurations for the experiment. For example, `RUGGED` took 329.69 seconds whereas using better responses for just the defender reduced the runtime to 33.58 seconds. Moreover, `SNARES` required just 4.46 seconds, an improvement of 98%. These results also show that using better responses for any one player provides a boost in performance, and using it for both players simultaneously makes `SNARES` even more effective.

Figure 4.9(c) shows the percentage of times calls to the best response module have to be made on the y-axis (on log-scale) and varies the configuration on the x-axis. The results are shown for all the four configurations from the previous experiment. Each result shows the percentage of iterations better response did *not* generate an improving strategy for both the players (i.e, in Algorithm 3, check in Line 5 failed and Line 6 was called for the defender, and check in Line 9 failed and Line 10 was called for the attacker). The lower the bar, the lower percentage of times the best response module has to be called. `RUGGED` has no better responses, and is hence plotted at 100%. For example, the best response of the attacker and defender were computed in only 15.81% and 1.69% of the iterations in `SNARES`.

4.4.4.2 Scalability in Simulation:

This section evaluates the performance of SNARES as the input problem size is varied. These results are also conducted on random geometric graphs and are averaged over 30 samples. We do not plot error bars in our graphs because the y-axis is on a log-scale; however, SNARES was statistically significantly (with $p < 0.05$) faster than RUGGED for all experiments with more than 100 nodes, or $d \geq 0.2$, or $k \geq 4$, or $|T| \geq 4$.

Vary Number of Nodes: Figure 4.10(a) presents the results when varying the number of nodes in the input problem. The x-axis shows the number of nodes in the graph, whereas the y-axis shows the runtime in seconds (on a log-scale). The four bars in the graph compare the performance of RUGGED with (i) SNARES without better responses, (ii) SNARES without mincut-fanout, and (iii) SNARES. These experiments were conducted on random graphs generated with density $d = 0.1$, 3 targets, 3 source nodes for the attacker, and 3 defender resources. These results show that all configurations are better than the baseline of RUGGED, and that SNARES is the most efficient. RUGGED ran out of memory in 26 out of 30 samples for 200 node graphs, and was killed in another 2 samples since it did not finish execution in 3 hours. For example, for 150 nodes, while RUGGED took 6021.08 seconds, and SNARES without better responses used 4,152.80 seconds. Additionally, SNARES without mincut-fanout reduced the runtime to 19.58 seconds and SNARES required only 6.53 seconds. Thus, the experiment shows that the combination provides the most significant boost in performance, SNARES taking only 1.08% of the time required by RUGGED.

Vary Graph Density: Figure 4.10(b) presents the results when varying the distance d used when generating the random geometric graphs. The x-axis shows the value of d , whereas the y-axis gives the runtime. These experiments were conducted on random graphs generated with

density 50 nodes, 3 targets, 3 source nodes for the attacker, and 3 defender resources. These results show that as the density of the graph is increased, the runtime required by all the algorithms increases. Experiments that did not terminate in 10,800 seconds (3 hours) were terminated (as in the case of most experiments with graph density higher than 0.3 when run with RUGGED). These results also show that SNARES performs much better than RUGGED. For example, for $d = 0.3$, most experiments with RUGGED did not finish in 3 hours, whereas SNARES without better responses took 537.19 seconds. Furthermore, SNARES without mincut-fanout required 32.74 seconds, whereas SNARES required only 9.04 seconds.

Vary Number of Resources: We now present the results when varying the number of defender resources in Figure 4.10(c). These results are shown for random graphs with 50 nodes, 3 targets, 3 sources and graph density $d = 0.1$. The x-axis in this graph shows the number of defender resources, whereas the y-axis shows the runtime in seconds on log scale. The results show that the performance trends remain the same: SNARES scales much better than RUGGED when the problem size is increased and the use of better responses provides a more significant performance boost. For example, for 4 resources, RUGGED required 83.90 seconds whereas SNARES only required 0.72 seconds on average.

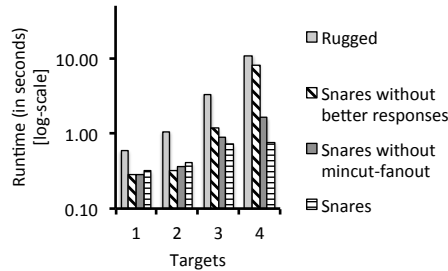


Figure 4.11: Varying Number of targets.

Vary Number of Targets: Figure 4.11 presents the results when varying the number of targets for random graphs 50 nodes, 3 sources, 3 resources and $d = 0.1$. The x-axis shows the number of targets, whereas the y-axis shows the runtime in seconds on log-scale. We observe similar performance trends: SNARES scales better than RUGGED in the number of targets as well. For example, for 4 targets, where RUGGED took 10.97 seconds, SNARES only required 0.77 seconds.

4.4.4.3 Real Data

We also tested the performance of SNARES on real urban road network data. We downloaded the OSM information for the road network of Mumbai [Haklay and Weber, 2008]. We extracted this information for the entire city of Mumbai, that is, the road network existing between latitudes 18.840 and 72.750 and longitudes 19.360 and 73.160.

We first present results in Table 4.3 comparing SNARES with RUGGED on the southern part of the Mumbai road network. RUGGED was only able to solve for a subset of the Mumbai road network, and thus, we can only use a subset of the Mumbai map for this experiment. These experiments were done with 3 targets and 3 sources, whose locations on the map were motivated by the Mumbai attacks of November 2008. These results show that SNARES has a significant improvement over RUGGED; for example, for a subset of the graph with 252 nodes, RUGGED took 34,344.70 seconds to place 4 resources whereas SNARES only 30.77 seconds!

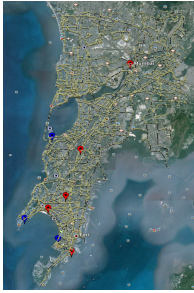
While RUGGED could only compute solutions for the southern tip of the road network of Mumbai, SNARES was able to solve the entire road network. These results are shown in Table 4.4. We ran SNARES varying the number of targets and number of defender resources for 3 sources. The easy-hard-easy pattern in the runtime with the increase in resources is expected based on the runtime properties of security games [Jain et al., 2012]. For example, it took SNARES only 101.09

Map		Resources			
Size	Algorithm	1	2	3	4
45	RUGGED	0.91	6.43	22.58	33.42
	SNARES	1.08	2.62	7.53	7.71
129	RUGGED	6.63	32.55	486.48	3,140.23
	SNARES	2.23	2.99	10.99	21.06
252	RUGGED	17.19	626.25	2,014.14	34,344.70
	SNARES	3.83	4.85	16.19	30.77

Table 4.3: Runtime of RUGGED [6] and SNARES on real Mumbai map. Results of SNARES are averaged over 30 runs.

seconds to find the optimal solution for placing 10 checkpoints when considering 8 targets. Thus,

SNARES is now scalable enough to be applied and used in the real world.



Resources	Number of Targets	
	4	8
1	18.23	27.12
5	1,209.37	7,289.03
10	27.26	129.51
15	12.64	101.09

Runtime Required by SNARES:
All results averaged over 30 samples.

Table 4.4: The image is map of Mumbai road network comprising 9,503 nodes and 20,416 edges. The sources (blue dots) and targets (red dots) are placed arbitrarily for these tests.

Chapter 5: Solving Bayesian Games

In this chapter, I present the hierarchical approach to solving general Bayesian games, Bayesian games with arbitrary scheduling constraints as well as Bayesian games with patrolling constraints.

5.1 Solving Bayesian-SPNSC Problem Instances

I now present Hierarchical Bayesian solver for General Stackelberg games, or HBGS, an algorithm that computes solutions to Bayesian-SPNSC instances. Two main approaches have been proposed in prior work to compute the equilibrium for such Bayesian Stackelberg games, namely DOBSS [Paruchuri et al., 2008a] and Multiple-LPs [Conitzer and Sandholm, 2006] (refer Section 2.9 for details). DOBSS solves the Bayesian game by solving a mixed-integer linear program that internally decomposes the problem by individual follower types, whereas Multiple-LPs works on the Harsanyi transformed version of the game. The exponential number of linear programs that are solved by Multiple-LPs approach, and the exponential possibilities for assigning values for integer variables in DOBSS, does not allow these algorithms to scale well with increasing number of follower types. Indeed, if the optimal solution could be obtained by solving only a few of these linear programs, the performance could be improved significantly — even significantly better than DOBSS. Specifically, if I could construct a smaller tree of the follower’s action choices in the

first place, or obtain bounds on solution quality to perform branch and bound search, significant speed-ups would be obtained. This is the intuition behind HBGS: HBGS reduces the number of linear programs that need to be solved using two main insights: (1) *Feasibility* rules that help eliminate *infeasible* follower strategies in the Bayesian game; and (2) *Bounds* that help prune the follower action space using branch and bound search. HBGS constructs a hierarchical tree of restricted games, the solutions of which provide such feasibility and bounds information. I first discuss the hierarchical structure of HBGS, and then describe the feasibility and bounding techniques.

5.1.1 Bayesian Game Computation

Computing solutions to a Bayesian Stackelberg security game has been shown to be NP-Hard [Conitzer and Sandholm, 2006]. This is chiefly because of the exponentially large attacker action space in a Bayesian Stackelberg security game. The entire action space of the attacker is shown in Figure 5.1. Figure 5.1 shows an *attacker action tree*, i.e., a depiction that represents possible combinations of actions for each attacker type in a tree. A solution to a Bayesian Stackelberg security game requires specifying an action choice for each possible attacker type in the game, since the defender does not know which attacker type it is playing against. In the tree representation shown here, every level corresponds to a different attacker type, whereas every branch corresponds to the possible actions for that type (in our case, the possible targets that can be attacked). Every leaf node represented a complete strategy for the attacker, with an action for each type defined by the choices along the path from the root to the leaf. For example, the pure strategy $[t_2^1, t_1^2]$ where attacker of type 1 attacks target t_2 and attacker of type 2 attacks target t_1 is represented by the leaf $[2, 1]$ in Figure 5.1. In a Bayesian game there are an exponential number

of leaves in this tree (specifically, $|T|^{|\Lambda|}$, where Λ is the set of attacker types). A game with 10 attacker types and just 5 targets would have 9,765,625 leaves.

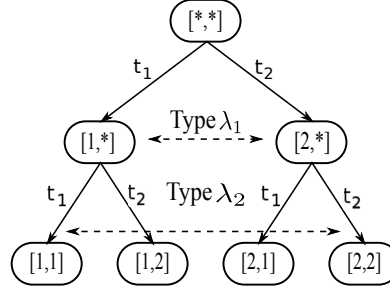


Figure 5.1: Example tree representing the pure strategies for the attacker in a Bayesian Stackelberg security game.

One approach to solving a Bayesian Stackelberg game is to consider the optimal solution for the defender in each of the leaf nodes, and take the maximum over all of these possibilities (this is the approach taken in MultipleLPs [Conitzer and Sandholm, 2006]). The solution for each leaf node is an optimal mixed strategy for the defender, subject to the additional constraints that the attacker choices represented in the path to the leaf node are best-responses for each attacker type to the given defender strategy. For example, the solution for leaf $[2, 1]$ for our example in Figure 5.1 would be the optimal mixed strategy \mathbf{x} for the defender such that the best response of attacker type 1 is target t_2 and for attacker type 2 is target t_1 . Note that it is possible that a leaf has no solution, i.e., there may not exist a mixed strategy for the defender such that the best responses of the attacker are consistent with the leaf node. These nodes are *infeasible*. The optimal solution for the entire problem is the solution among all feasible leaf nodes that gives the defender the highest expected utility.

Any solution algorithm for a Bayesian Stackelberg game must consider all possible leaf nodes to find an optimal solution. The MultipleLPs method [Conitzer and Sandholm, 2006] does this explicitly, enumerating the leaf nodes and solving a linear program to find the optimal strategy for

each one. DOBSS [Paruchuri et al., 2008a] has an implicit formulation based on a mixed-integer program that maps each leaf of the attacker action tree to one unique assignment of values to the integer variables. Depending on the solver used for this optimization problem, this may allow for some pruning of leaf nodes in the solution process. In the following sections, I will present HBGS as using the Multiple-LPs linear program for solving each of the leaf nodes; however, alternate methods could be employed.

5.1.2 HBGS Solution Methodology

The intuition behind HBGS is based on two main insights: (1) *Feasibility* rules that help eliminate *infeasible* attacker strategies in the Bayesian game (an attacker strategy or target is deemed infeasible if it cannot be a best response of the attacker to attack this target for any possible mixed strategy for the defender); and (2) *Generation of tighter bounds* that help prune the attacker pure strategy space during branch and bound search. HBGS constructs a hierarchical tree of *restricted games* with fewer attacker types to provide this information. I first discuss the hierarchical structure of HBGS, and then the rules that help in pruning the attacker action space for the Bayesian-SPNSC game. Finally, I describe how all of these techniques are combined in the full HBGS algorithm.

5.1.2.1 Hierarchical Type Trees

HBGS first constructs a hierarchical structure of *restricted games*. A restricted game is an instantiation of the input Bayesian-SPNSC instance in which only a subset of the attacker types is represented, ignoring the rest. The probability of facing each attacker type is re-normalized in the restricted game. These restricted games are exponentially smaller than the original input instance, since the problem size scales exponentially with the number of attacker types. The objective of

constructing such restricted games is two fold: solutions to these games provides (i) infeasible set of pure strategies per attacker type λ in the original problem, which can then be pruned out; and (ii) corresponding upper bounds \mathcal{B}^λ for the set T^λ of feasible pure strategy for each attacker type λ in the restricted game. For the purposes of computing this feasible set of pure strategies T^λ and the upper bounds \mathcal{B}^λ , the Bayesian Stackelberg game $G(\Theta, \Psi^\Lambda)$ is decomposed into many smaller restricted games, $G(\Theta, \Psi^{\Lambda_i})$ by partitioning the set of types, Λ , into subsets Λ_i . Any partition of Λ into subsets Λ_i is applicable, such that:

$$\cup_i \Lambda_i = \Lambda \quad (5.1)$$

$$\Lambda_i \cap \Lambda_j = \emptyset \quad \forall i, \forall j, j \neq i \quad (5.2)$$

Once a partition has been established, a *hierarchical type tree* is constructed where the root node corresponds to the entire Bayesian-SPARS game $G(\Theta, \Psi^\Lambda)$, and its children correspond to the restricted games, $G(\Theta, \Psi^{\Lambda_i})$. Note that this is a different tree from the one introduced previously to represent the attacker actions; this tree instead represents a partitioning of the types and not the attacker actions. I present and experimentally evaluate three possible partitioning schemes in this article: (1) a *depth-one* partition, (2) a *depth-two* partition, and (2) a *fully branched binary tree* (where children can then be hierarchically decomposed into even more restricted games). An example game of depth-one partitioning with 4 types is shown in Figure 5.2(a). Here, each restricted game has exactly one type and the total depth of the tree is one. Figure 5.2(b) shows a fully branched binary partitioning, where the entire problem is decomposed into two restricted games of two types each, which are in turn decomposed into two sub-games.

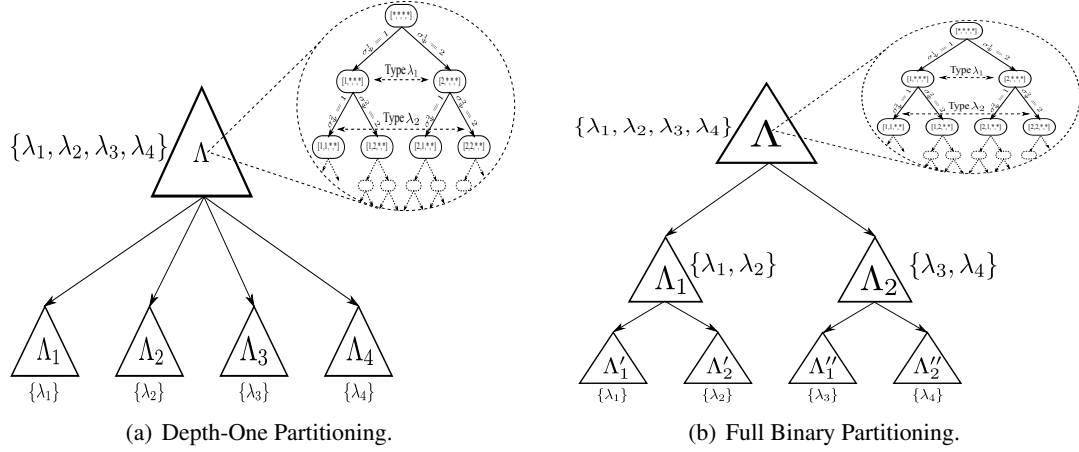


Figure 5.2: Examples of possible hierarchical type trees generated in HBGS. The root node is the original Bayesian-SPARS problem instance, $G(\Theta, \Psi^\Lambda)$. Every other node is a restricted Bayesian game. Figure 5.2(a) shows a depth-one partitioning, where $G(\Theta, \Psi^\Lambda)$ is decomposed into four restricted games $G(\Theta, \Psi^{\Lambda_i}), i \in \{1..4\}$. Figure 5.2(b), on the other hand, shows the full binary partitioning where the original $G(\Theta, \Psi^\Lambda)$ is decomposed into two restricted games, which are then further re-decomposed into two smaller restricted games.

The evaluation of the hierarchical tree is bottom-up, so all children are evaluated before the parent nodes are evaluated. Every node is evaluated using Algorithm 6 (discussed later), and the feasible pure strategies T^{Λ_i} with corresponding bounds \mathcal{B}^{Λ_i} obtained at the i^{th} child are propagated up to the parent. These are used when the parent is evaluated, again using Algorithm 6. This process continues until the root node is solved to obtain the optimal solution for the original game $G(\Theta, \Psi^\Lambda)$.

5.1.2.2 Pruning a Bayesian Game

(1) *Feasibility*: HBGS applies the following theorem to reduce the strategy space T^Λ of the attacker.

Theorem 8. *The attacker's pure strategy $t = [t^\lambda]$ is infeasible in the Bayesian game $G(\Theta, \Psi^\Lambda)$ if the strategy t^λ is infeasible for the attacker of type λ in a restricted game, $G(\Theta, \Psi^{\Lambda'})$, where the attacker can only be of type λ (that is, $\Lambda' = \{\lambda\}$).*

Proof. I prove the theorem by showing the contrapositive. Suppose that the pure strategy t containing t^λ is feasible in the original game $G(\Theta, \Psi^\Lambda)$, with δ being the corresponding defender optimal mixed strategy. Thus, by the definition of SSE and optimal defender strategy, the best response of the attacker of type λ to the defender strategy δ is t^λ even in the restricted game $G(\Theta, \Psi^{\Lambda'})$, which proves the theorem. \square

Theorem 8 states that if t^λ can never be the best response of attacker type λ in the restricted game $G(\Theta, \Psi^{\Lambda'}), \Lambda' = \{\lambda\}$ (that is, a game with only the attacker of type λ), then a pure strategy containing t^λ can never be the best-response of the attacker in *any* Bayesian game $G(\Theta, \Psi^\Lambda), \Lambda = \{\lambda_1, \lambda_2, \dots\}$. Thus, any pure strategy containing t^λ is *infeasible* when computing solutions for the original game $G(\Theta, \Psi^\Lambda)$ and can be omitted. In other words, if some *branches* in the attacker action tree (Figure 5.1) are infeasible, no *leaves* in the subtree connected by that branch need to be evaluated. The theorem can be extended to restricted games with $\Lambda' \subseteq \Lambda$ by considering Λ' as one *hyper-type*. This implies that a pure strategy t can be removed from the Bayesian game if any of its components t^λ is infeasible in the corresponding restricted game.

Consider the possible performance improvement for a sample problem with five attacker types ($|\Lambda| = 5$) and ten pure strategies for attacker of each type ($|T^\lambda| = 10, \lambda \in \Lambda$). The total number of pure strategies for the attacker in the Bayesian Stackelberg game is 10^5 . If an oracle could inform us *a-priori* that two particular pure strategies can be discarded for every type of the attacker, the strategy space would reduce to 8^5 pure strategies, which is roughly 33% of the size of the initial problem.

Hbgs identifies the infeasible strategies in each of the restricted games and applies Theorem 8 to prune out infeasible strategies from $G(\Theta, \Psi^\Lambda)$. This process is applied recursively in the hierarchical tree (refer Figure 5.2) to obtain effective pruning at the root node.

(2) *Bounds*: A pure strategy for the attacker needs not be evaluated if the upper bound on the maximum defender expected utility for the corresponding pure strategy is available, and if this upper bound is not better than the best solution known so far. A naïve upper bound is $+\infty$ which leads to no pruning, and would lead to the conventional Multiple-LPs approach. Hbgs uses techniques for obtaining tighter upper bounds on the defender utility based on Theorem 9.

Theorem 9. *The maximal defender payoff is upper bounded by $\sum_{\lambda \in \Lambda} p^\lambda \mathcal{B}(r^\lambda)$ when the attacker chooses a pure strategy $t = \langle r^\lambda \rangle$, where $\mathcal{B}(r^\lambda)$ is the upper bound on the defender utility in the restricted game $G'(\Theta, \Psi^{\Lambda'}) | \Lambda' = \{\lambda\}$ when the attacker of type λ is induced to choose pure strategy r^λ .*

Proof. $\mathcal{B}(r^\lambda)$ upper-bounds the maximum utility of the defender for any strategy that induces the attacker of type λ to choose r^λ as the best response. Thus, the defender utility against attacker of type λ for any strategy δ is no more than $\mathcal{B}(r^\lambda)$. Therefore, $U_\Theta^\lambda(\delta, r^\lambda) \leq \mathcal{B}(r^\lambda)$. Applying Equation (??),

$$U_\Theta(\delta, t) \leq \sum_{\lambda \in \Lambda} p^\lambda \mathcal{B}(r^\lambda) \quad \forall \delta \quad (5.3)$$

which proves the theorem.¹

□

¹This theorem can also be generalized to restricted games where $\Lambda' \subseteq \Lambda$, just like Theorem 8.

The bounds $\mathcal{B}(t^\lambda)$ are generated for all children and then propagated up the hierarchical tree (Figure 5.2), where they are used by the parent to prune out branches from its own Bayesian game (Figure 5.1).

5.1.2.3 HBGS Description

HBGS solves each node of the hierarchical tree (refer Figure 5.2) using Algorithm 6. This algorithm takes as input a set of attacker types Λ , the defender Θ , the set of feasible pure strategies of the attacker T^Λ ,² upper bounds \mathcal{B}^Λ on the defender payoff for every attacker pure strategy in T^Λ and the utilities U_Θ and U_Ψ for both the players. The output of the algorithm is the optimal defender mixed strategy δ^* for this game, the optimal defender reward r^* and the updated set of feasible pure strategies T^* for the attacker and the updated corresponding upper bounds on the defender's payoff \mathcal{B}^* . These upper bounds \mathcal{B}^* are the exact payoffs r (Line 7, Algorithm 6) computed for all the attacker pure strategies that are explicitly evaluated by the algorithm, and equal the upper bounds \mathcal{B}^Λ for the attacker pure strategies that the algorithm was able to prune without explicit computation. HBGS is used to solve each node of the hierarchical tree (refer Figure 5.2); the hierarchical tree is evaluated in a bottom-up sequence such that the parent nodes gets updated information from its children.

Once HBGS starts its computation for a node of the hierarchical tree (refer Figure 5.2), it constructs a tree representing the attacker actions, as in Figure 5.1. This attacker action tree is then solved using Multiple-LPs linear programming approach. Only the pure strategies in the cross-product of the feasible set of strategies of individual types need to be evaluated for the attacker (Theorem 8). T^* represents this maximal set, as given in Line 2 (and updated later in Line

² T^Λ could contain some infeasible pure strategies of the attacker, but no feasible pure strategy will be omitted. For instance, the algorithm starts by considering the exhaustive set of pure strategies.

10). \mathcal{B}^* represents the bounds for all these strategies, and is obtained in Line 3 (and updated later in Line 9). Lines 2 to 5 are initialization; $T^\lambda(i)$ represents the i^{th} pure strategy in the set T^λ . The main loop of the algorithm starts after Line 6, where one pure strategy (*leaf*) is evaluated after another. The function `solve` (Line 7) in HBSA solves the column generation procedure of Bayesian-ASPEN

Algorithm 6 HBGS ($\Lambda, \Theta, T^\Lambda, \mathcal{B}^\Lambda, U_\Theta, U_\Psi$)

```

// initialize
//  $T^\Lambda$ : pruned feasible pure strategy set for all attacker types
//  $\mathcal{B}^\Lambda$ : bounds for all pure strategies for all attacker types
1.  $\text{FT} := \text{construct-attacker-Action-Tree}(T^\Lambda)$ 
2.  $T^* := \text{leaves-of}(\text{FT})$  // feasible pure strategies of  $\Psi$ 
3.  $\mathcal{B}^*(t) := \text{getBounds}(t, \mathcal{B}^\Lambda) \quad \forall t \in \prod_\lambda T^\lambda$ 
4.  $\text{sort}(T^*, \mathcal{B}^*(t))$  // sort  $t$  in descending order of  $\mathcal{B}^*(t)$ 
5.  $t := [T^1(1), T^2(1), \dots, T^{|\Lambda|}(1)]$  // left-most leaf
6.  $r^* := -\infty$  //  $r^*$ : current best known solution
// start
repeat
  7. (feasible,  $\delta, r$ ) := solve( $\Theta, t$ ) // using Bayesian-ASPEN
  if feasible then
    if  $r > r^*$  then
      // update current best solution
      8a.  $r^* := r$ 
      8b.  $\delta^* := \delta$ 
    9.  $\mathcal{B}^*(t) := r$  //update bound
  else
    10.  $T^* := T^* - t$  //remove infeasible strategy
    11.  $t := \text{getNextStrategy}(t, r^*, T^\Lambda, \mathcal{B}^\Lambda)$ 
until  $t <> \text{NULL}$ 
return ( $\delta^*, r^*, T^*, \mathcal{B}^*$ )

```

(described in Section 5.2.1). The attacker pure strategy t is feasible if this Bayesian-ASPEN has a feasible solution. The maximal defender reward r and the corresponding defender mixed strategy δ are also obtained from Bayesian-ASPEN (Line 7). If the pure strategy is feasible, the bounds \mathcal{B}^* are updated (Line 9). Otherwise, the strategy t is removed from the pure strategy set T^* of the attacker (Line 10).

The function `getNextStrategy()` moves from one *leaf* (pure strategy) to another of this attacker action tree: this is the branching heuristic (Line 11). For example, it would iterate through all the 4 leaves in Figure 5.1 one by one if no leaf was pruned. The defender strategy δ^* to the maximal corresponding defender reward r^* is the optimal defender strategy for this Bayesian game. Algorithm 6 also returns the set of feasible pure strategies, T^* , and the corresponding bounds, \mathcal{B}^* . This feasible strategy set T^* is a subset of the cross-product of T^λ , the feasible strategies per type, since it does not contain the strategies that were computed and found to be infeasible.³ T^* and \mathcal{B}^* are the feasibility sets and bounds that are propagated up the hierarchical tree; however, I first discuss the branch and bound heuristic used in Algorithm 6.

Branch and Bound Heuristics: HBGS sorts $t^\lambda \in T^\lambda$, the pure strategies per type, in decreasing order of their bounds $\mathcal{B}(t^\lambda)$ before the tree in Figure 5.1 is constructed. The branching heuristic prefers that the leaf which can generate the highest defender expected utility. The bounds on each leaf are a direct application of Theorem 9. The function `getBounds` computes the weighted sum of the bounds per attacker type $\mathcal{B}^\lambda(t^\lambda)$ ⁴ to generate the bound $\mathcal{B}(t)$ for this leaf using Theorem 9.

Tree Traversal and Pruning: Algorithm 7 formally defines the tree-traversal strategy. The algorithm traverses the leaves of the attacker action tree from left to right (*lexicographic* tree traversal) with the objective to find the first leaf (pure strategy) whose bound is higher than the current best solution r^* . If no such leaf exists, the optimal solution has been achieved and HBGS can be successfully terminated. This tree is constructed keeping the child nodes sorted in descending order from left to right in every sub-tree. For example, in Figure 5.1, $\mathcal{B}(T^1(1)) \geq \mathcal{B}(T^1(2))$ (children of root) and $\mathcal{B}(T^2(1)) \geq \mathcal{B}(T^2(2))$ where $T^\lambda(i)$ represents the i^{th} pure strategy for attacker

³Some of the strategies in T^* that were not computed may still be infeasible; Algorithm 6 ensures no feasible strategy is removed.

⁴The bounds are weighted by the distribution p^λ over types.

type λ . The leaves are evaluated from left to right, that is, the leaf $[1, 1]$ is evaluated first and leaf $[2, 2]$ last.

If the bound \mathcal{B} for any leaf (pure strategy) t is smaller than the best solution obtained thus far, that leaf need not be evaluated. Additionally, *right* siblings of this leaf t need not be evaluated either, given the sorted nature of every sub-tree. For example, in Figure 5.1, if the bound of leaf $[2, 1]$ is worse than the solution at $[1, 2]$, then the leaf $[2, 2]$ does not need to be evaluated as well.

Algorithm 7 accomplishes this type of pruning of branches as well.

Algorithm 7 getNextStrategy($t, r^*, T^\Lambda, \mathcal{B}^\Lambda$)

```

for  $\lambda = |\Lambda|$  to 1 Step  $-1$  do
   $j := \text{index-of}(T^\lambda, t^\lambda)$ 
  // Fix the pure strategies of parents:  $t^i, i < \lambda$ 
  // Update the pure strategy of type  $\lambda$ :  $T^\lambda(j + 1)$ 
  // Children choose their best pure strategy:  $T^i(1), i > \lambda$ 
   $t := [t^1, \dots, t^{\lambda-1}, T^\lambda(j + 1), T^{\lambda+1}(1), \dots, T^{|\Lambda|}(1)]$ 
  if  $r^* < \text{getBounds}(t, \mathcal{B}^\Lambda)$  then
    return  $t$ 
return NULL

```

Hbgs Summary: The leaves of the hierarchical type tree are solved to identify infeasible strategies and obtain upper bounds on every attacker strategy. This information is propagated up the tree, and the procedure repeated for every node until the optimal solution is obtained at the root. While Hbgs does incur the overhead of solving many smaller restricted games, it outperforms all existing techniques in the overall performance, as shown in the experimental results.

5.1.3 Experimental Results

I provide two sets of experimental results. First, I compare the performance of DOBSS, Multiple-LPs and Hbgs for Bayesian-SPNSC games. Second, I show speedups via approximations. The payoffs for both players for all test instances were randomly generated, and were consistent with

the definition of security games as defined earlier in the thesis. Results were obtained on a standard 2.8GHz machine with 2GB main memory, and are averaged over 30 trials.

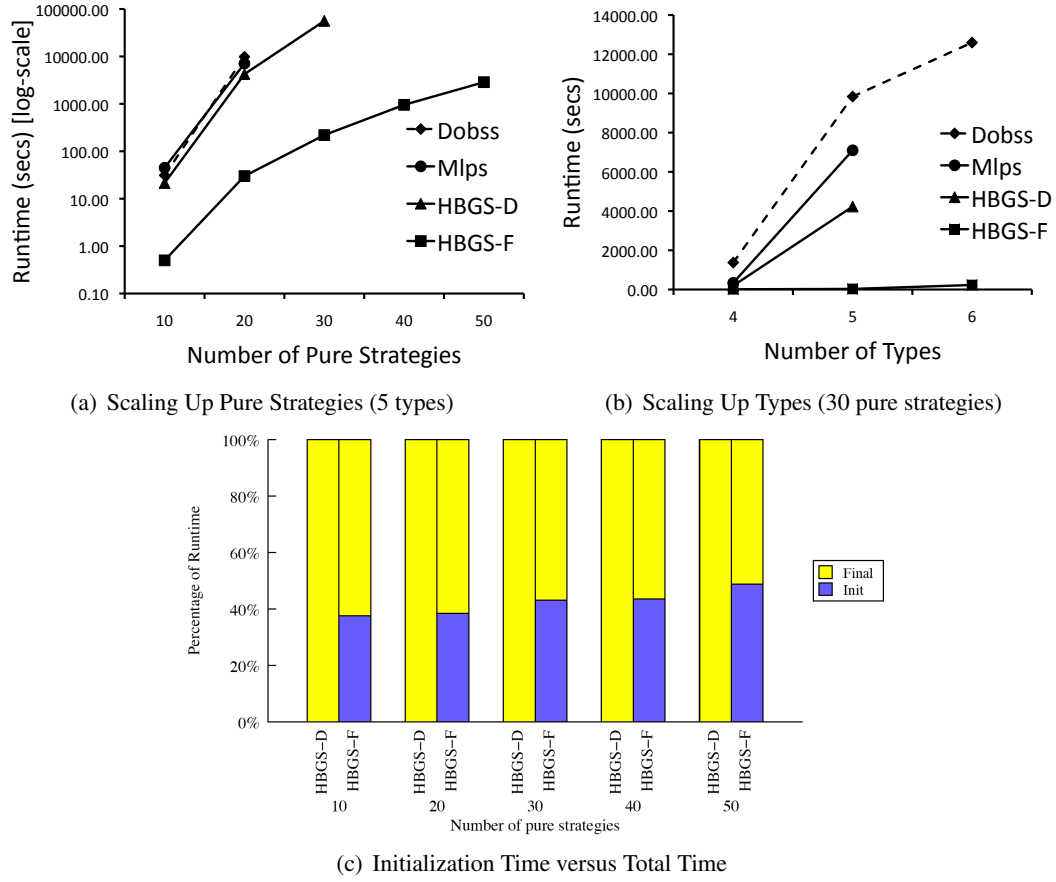


Figure 5.3: This plot shows the comparisons in performance of the four algorithms when the size of the input problem is scaled.

5.1.3.1 HBGS Scale-up

I compare the runtime of HBGS against the runtime of DOBSS and Multiple-LPs, the two chief algorithms for general Bayesian Stackelberg games. I use two variants of HBGS: (1) the first variant, denoted HBGS-D constructed a hierarchical tree of a fixed depth of one where as many restricted games were generated as the number of follower types. (2) The second variant, HBGS-F,

constructed maximally branched binary trees such that each Bayesian game was decomposed into two restricted games with half as many types, until the leaves solved a restricted game with exactly one type. I compared the performance of these algorithms when the number of targets and the number of types were increased. I also show the speed ups obtained when approximation was allowed.

Scale-up of number of strategies: Figure 5.3(a) shows how the performance of the four algorithms scales when the strategy spaces are increased. These tests were done for 5 types. The x-axis shows the number of pure strategies for both players, while the y-axis shows the runtime in seconds on a log scale. For example, for 30 actions and 5 types, Multiple-LPs would solve $30^5 = 2.43e7$ linear programs. The experiments had a time cut-off of 24 hours.

The figure shows that while both variants of HBGS can successfully compute for 5 types and 30 pure strategies, DOBSS and Multiple-LPs cannot. Furthermore, HBGS-F with its fully balanced binary tree scales better than HBGS-D. This is because it solves a much smaller problem at the root node, even though it solves many more restricted problems. Each restricted game provides more pruning (infeasible combinations of follower actions will not be propagated up the tree) and potentially tighter bounds.

Figure 5.3(c) shows an analysis of time required by HBGS-D and HBGS-F in solving all the restricted Bayesian games before the root node of hierarchical type tree is solved. The x-axis shows the number of pure strategies for both the players and the y-axis shows the percentage of runtime. It shows that while HBGS-D spends almost no time in initialization ('Init'), HBGS-F spends almost 40% of its runtime in solving the restricted games. On the other hand, HBGS-F decomposes the problem more finely and thus spends more time solving more of the restricted games. This is because the number of restricted games generated by HBGS-F are more than the

corresponding number in HBGS-D. However, the total time required by HBGS-F is considerably smaller (Figure 5.3(a)) which shows that hierarchical decompositions obtain more pruning and generate better bounds than depth-one hierarchical trees.

Scale-up of number of types: For these experiments, both the row and the column player had 30 pure strategies. The x-axis shows the number of types, whereas the y-axis shows the runtime in seconds. Again, the experiments were terminated after a cut-off time of 24 hours. We can see that HBGS-F scales extremely well as compared to the other algorithms; for example, HBGS-F solved a problem with 6 types in an average 231 seconds whereas DOBSS took an average of 12593.8 for the same problem instances. The other two algorithms didn't even finish their execution in 24 hours. While DOBSS and Multiple-LPs do not scale beyond a few number of types, HBGS-F provides scale-up by an order of magnitude. In Table 5.1, I present the runtime results of HBGS-F for up to 50 types. The experiments in this case had 5 pure strategies for both players (the other algorithms can not solve any instance with more than 20 types in 24 hours). This shows that DOBSS is no longer the fastest Bayesian Stackelberg game solution algorithm, and HBGS-F provides scale-up by *an order of magnitude*.

Table 5.1: Scaling up types (30 pure strategies per type)

Types	Follower Pure Strategy Combinations	Runtime (secs)
10	9.7e7	0.41
20	9.5e13	16.33
30	9.3e20	239.97
40	9.1e27	577.49
50	8.9e34	3321.681

5.1.3.2 Approximations

This section discusses the performance scale-ups that can be achieved when the algorithm was allowed to return approximation solutions. Three parameter settings of approximations were allowed: 1 unit, 5 unit and 10 units⁵. The approximations were tried on HBGS-F (with fully branched binary trees) since that prior experiments had shown it to be the fastest algorithm.

The number of types was fixed to 6 and the number of pure strategies was varied for the results shown in Figure 5.4(a). The number of targets here is shown on the x-axis, whereas the y-axis shows the runtime in seconds. Similarly, Figure 5.4(b) shows the results when the number of types was increased while fixing the strategy space to 50 pure strategies for the leader and all follower types. These figures show that the approximation variants of HBGS scale significantly better. For example, while HBGS-F took 43,727 seconds to solve a problem instance with 50 pure strategies and 6 types, the 1, 5 and 10 unit approximations were able to solve the same problem in 10639, 3131 and 2409 seconds respectively, which is up to 18 times faster.

I also analyzed the difference in solution quality when the approximations were allowed, which is shown in Figure 5.4(c). The y-axis shows the *percentage error* in the *actual* solution quality of the approximate solution while the x-axis shows the number of targets. Lower bar implies lower error. For example, the maximum error in all settings for HBGS with an allowed approximation of five units was less than two percent. These results show that allowing for approximate solutions can dramatically increase the scalability of the algorithms without significant loss in the solution quality.

⁵The maximum reward in the matrix was 100 units, and these were chosen as 1%, 5% and 10% of the maximum possible payoff.

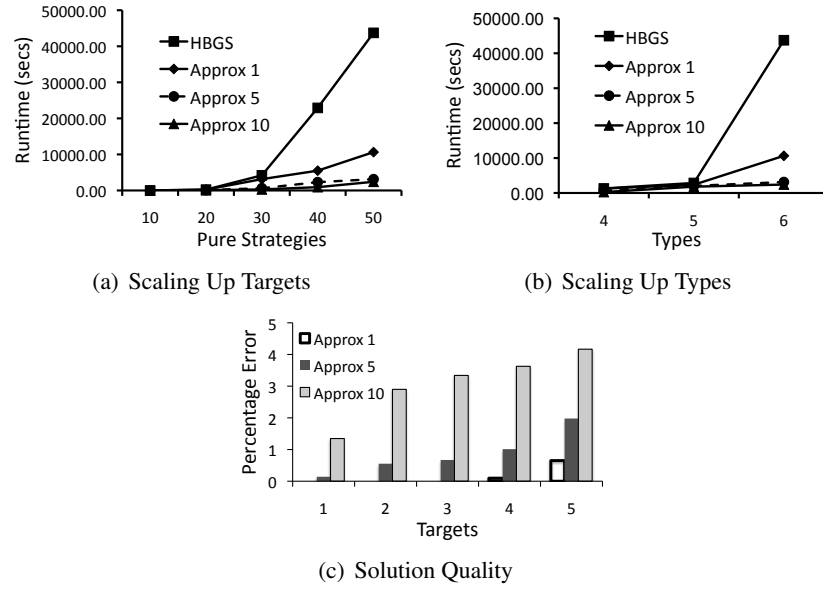


Figure 5.4: This plot shows the comparisons of HBGS and its approximation variants.

5.2 Solving Bayesian-SPARS Problem Instances

I now present Hierarchical Bayesian Solver for Security games with Arbitrary schedules, or HBSA, an algorithm that computes solutions to Bayesian-SPARS instances. First, I extend the basic ASPEN problem formulation to include multiple attacker types so it can be applied to instances of Bayesian-SPARS. HBSA uses the same hierarchical framework as described above in HBGS, however, it uses my new Bayesian-ASPEN formulation to solve each node in the attacker action tree. I now describe Bayesian-ASPEN approach in more detail.

5.2.1 Bayesian-ASPEN

Bayesian-ASPEN computes solutions to instances of the Bayesian-SPARS problem. It uses column generation to evaluate leaves of the *attacker action tree* from Figure 5.1, and I first describe this procedure. Then I describe the methods for using branching and bounding heuristics to reduce the overall computation done on the tree.

5.2.1.1 Bayesian-ASPEN Column Generation

The column generation procedure used in Bayesian-ASPEN is similar to methods used in ASPEN, as described in Section 3.1.1. The primary differences are extensions to the master problem formulation to include multiple attacker types, and updated computations for the reduced cost calculations used in the slave network flow problem.

Master Problem for Bayesian-ASPEN: The defender and the adversary optimization constraints from ASPEN need to be extended over all adversary types, in accordance with the definition of SSE. The master problem, given in Equations (5.4) to (5.8), solves for the probability vector \mathbf{x} that maximizes the defender reward.⁶ Equations (5.5) and (5.6) enforce the SSE conditions for the defender and adversary of each type, such that the attacker of each type chooses his best-responses. Additionally, the chosen defender strategy is such that maximizes the defender's payoff, as given by the objective in Equation (5.4). Here, d_λ refers to the expected utility of the defender when the defender has committed to the mixed strategy \mathbf{x} and the attacker of type λ has chosen the best response \mathbf{a}_λ . The defender expected utility for protecting target t against adversary type λ is given by the t^{th} component of the column vector $\mathbf{D}_\lambda \mathbf{P} \mathbf{x} + \mathbf{U}_\Theta^{\lambda,u}$ (the adversary payoff is defined

⁶Just like in ASPEN, the actual algorithm minimizes the negative of the defender reward for correctness of reduced cost computation, and I show maximization of defender reward only for expository purposes.

analogously). As before, the leaf node (attacker pure strategy \mathbf{a}) is fixed before column generation is executed and is not a variable in this formulation.

$$\max \quad \sum_{\lambda \in \Lambda} d_{\lambda} p_{\lambda} \quad (5.4)$$

$$\text{s.t.} \quad \mathbf{d}_{\lambda} - (\mathbf{D}_{\lambda} \mathbf{P} \mathbf{x} + \mathbf{U}_{\lambda, \Theta}^u) \leq (\mathbf{1} - \mathbf{a}_{\lambda}) M \quad \forall \lambda \in \Lambda \quad (5.5)$$

$$0 \leq \mathbf{k}_{\lambda} - (\mathbf{A}_{\lambda} \mathbf{P} \mathbf{x} + \mathbf{U}_{\lambda, \Psi}^u) \leq (\mathbf{1} - \mathbf{a}_{\lambda}) M \quad \forall \lambda \in \Lambda \quad (5.6)$$

$$\sum_{j \in J} x_j = 1 \quad (5.7)$$

$$\mathbf{x} \geq 0 \quad (5.8)$$

Slave Problem: The slave problem for Bayesian-ASPEN is the same as for ASPEN except that the reduced cost of a joint schedule is updated to take into account all the attacker types. The reduced cost \bar{c}_j of variable x_j , associated with column \mathbf{P}_j for Bayesian-ASPEN is given in Equation (5.9), where \mathbf{w}_{λ} , \mathbf{y}_{λ} , \mathbf{z}_{λ} and h are dual variables of master constraints (5.5), (5.6-rhs), (5.6-lhs) and (5.7) respectively.

$$\bar{c}_j = \sum_{\lambda \in \Lambda} (\mathbf{w}_{\lambda}^T (\mathbf{D}_{\lambda} \mathbf{P}_j) + \mathbf{y}_{\lambda}^T (\mathbf{A}_{\lambda} \mathbf{P}_j) - \mathbf{z}_{\lambda}^T (\mathbf{A}_{\lambda} \mathbf{P}_j)) - h \quad (5.9)$$

Again, the reduced costs \bar{c}_j are decomposed into \hat{c}_t , reduced costs per target:

$$\hat{c}_t = \sum_{\lambda \in \Lambda} (w_{\lambda, t} D_{\lambda, t} + y_{\lambda, t} A_{\lambda, t} - z_{\lambda, t} A_{\lambda, t}) \quad (5.10)$$

The column with the minimum reduced cost is identified using the same minimum cost network flow slave formulation as ASPEN using the new calculation for \hat{c}_t .

5.2.1.2 Improving Branching and Bounds

ASPEN used the ORIGAMI heuristic to arrange the leaves representing the attacker pure strategies for a SPARS problem instance, as shown in Figure 3.1. ORIGAMI-S is designed only for security games with one attacker type, and hence is not directly applicable to Bayesian-ASPEN. However, we can adapt the method for Bayesian-ASPEN by solving ORIGAMI-S for each attacker type λ independently and then using the weighted combination of the solutions as branch and bound heuristics. The solutions are weighted by the probability p^λ of facing the attacker type λ . For example, if the ORIGAMI-S solution for type 1 provides a defender upper bound of $\mathcal{B}(t_2^1)$ for target t_2 , and the ORIGAMI-S solution to type 2 provides a defender upper bound of $\mathcal{B}(t_1^2)$ for target t_1 , then the upper bound used by Bayesian-ASPEN for the leaf $[2, 1]$ in Figure 5.1 would be $\mathcal{B}(t_2^1)p^1 + \mathcal{B}(t_1^2)p^2$, where p^1 and p^2 are the probabilities for attacker type 1 and 2 respectively. This upper bound is valid because if the defender cannot perform better than $\mathcal{B}(t_i^\lambda)$ against each attacker type λ independently, then it cannot perform better than $\mathcal{B}(t_i^\lambda)p^\lambda$ when it is facing the type λ with probability p^λ . Bayesian-ASPEN computes the upper bound for all the leaves, sorts them in decreasing order and then uses column generation to compute the exact solution for each leaf until (i) the exact solution for all the leaves has been computed, or (ii) a solution has been obtained that is better than the upper bound for all remaining leaves.

I now introduce HBSA that builds on Bayesian-ASPEN and further reduces the number of leaves (refer Figure 5.1) that must be evaluated. This section will also clarify the use of Bayesian-ASPEN in HBSA. I will then provide an experimental comparison of HBSA and Bayesian-ASPEN with ORIGAMI-S in the following experimental results section.

5.2.2 Experimental results

In this section, I compare the performance of HBSA for Bayesian-SPARS games. Since no previous algorithms exist to solve Bayesian security games with scheduling constraints, I compare the performance between Bayesian-ASPEN and variants of HBSA. I tested three different algorithms: (1) the first, Bayesian-ASPEN, as explained in Section 5.2.1. (ii) The second, HBSA-D, uses a hierarchical tree with a depth of one (e.g., as shown Figure 5.2(a)), such that each leaf solves a restricted game with exactly one follower type. (2) The third, HBSA-F, uses a fully branched binary tree, as the one shown in Figure 5.2(b).

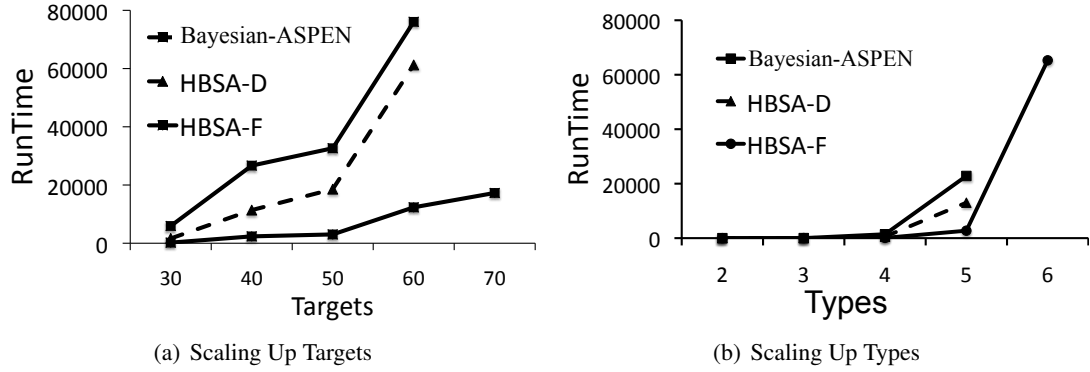


Figure 5.5: This plot shows the comparisons in performance of the three algorithms when the input problem is scaled.

5.2.2.1 Scale-up in number of targets:

In these experiments, the number of targets was varied while keeping the number of adversary types fixed to 5. The number of defender resources was set so that the defender is able to cover 10% of the total number of targets. The results are shown in Figure 5.5(a) where the x-axis shows the number of targets and the y-axis shows the runtime in seconds. The graph shows that HBSA-F is fastest, and scales much better compared to the Bayesian-ASPEN and HBSA-D variants.

The simulations were terminated if they didn't finish in 24 hours. For example, HBSA-D and Bayesian-ASPEN did not finish in 24 hours for the case with 70 targets, while HBSA-F was able to solve the problem instance in less than 5 hours.

5.2.2.2 Scale-up in number of types:

These experiments varied the number of types, while keeping the number of targets fixed to 50. The number of resources was set to 5, so as to cover 10% of the total number of targets. The x-axis shows the number of types whereas the y-axis shows the runtime in seconds. The graph again shows that HBSA-F is the fastest algorithm. Again, the cut-off time for the experiments was 24 hours, and for example, HBSA-D and Bayesian-ASPEN could not solve for 6 types in 24 hours.

5.2.2.3 Effects of using different hierarchies

The objective of these experiments is to further explore the impact of using different tree arrangements in the runtime performance of HBSA. While my previous experiments showed that the full binary tree arrangement was better than using a depth-one arrangement, this experiment is designed to investigate the trade-off between pre-processing and actual computation: a greater depth in the hierarchical tree implies more preprocessing but also better bounds, which are conflicting factors contributing to the total runtime. Specifically, I explore the runtime performance of an intermediate level tree, the depth-two tree. An example of a depth-two tree for 8 attacker types is shown in Figure 5.6. I generate random Bayesian-SPARS instances with 8 attacker types and compare the runtime performance of the depth-two tree with the full binary tree (depth-three for 8 attacker types). I do not show results for the depth-one tree since that took substantially more (more than 5 hours for some instances) when the number of targets was more than 10.

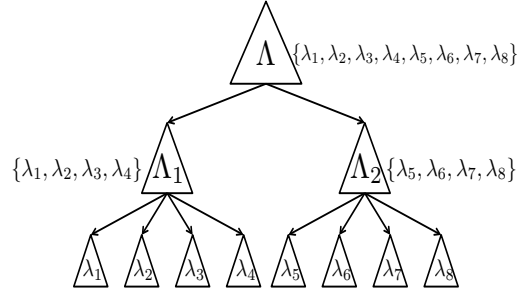


Figure 5.6: A Depth-Two tree for 8 attacker types.

The results are shown in Figure 5.7. The attacker types for these experiments were randomly generated, and were randomly arranged to form the hierarchical structure (in other words, there was no preferential selection of attacker type λ_1 over attacker type λ_2 when constructing the hierarchical tree). The results are averaged over 30 problem instances. The runtime performance is shown in Figure 5.7(a). The y-axis in the figure shows the time in seconds on the log scale, whereas the x-axis shows the number of targets in the problem instance. Each cluster has two sets of results: the first two bars correspond to the results for depth-two hierarchy, whereas the next two bars show the results for a full binary tree hierarchy. The first bar in each set is the time required for pre-processing, i.e. the time required to solve the sub-trees below the root node in the hierarchical type tree (refer Figure 5.2). The second bar shows the total average runtime required by the algorithm. For example, for 20 targets, the pre-processing and total runtime required for the depth-two hierarchy are 107 and 2,288 seconds respectively, whereas the corresponding times for the full-binary hierarchy are 15 and 1,054 seconds respectively.

The results show that shallower hierarchies are better when the number of targets is small, whereas the full binary hierarchy starts to dominate when the number of targets is increased. This result makes intuitive sense since the pre-processing overhead is a more significant fraction of the total runtime for problem instances with a smaller number of targets. I now show the number of pure strategies of the attacker required to be explored at the root node of both the

depth-two and full binary hierarchical type trees (refer (Figure 5.2) in Figure 5.7(b)). Remember that the number of pure strategies evaluated refers to the number of leaves explored in the tree representing the attacker's pure strategies (refer Figure 5.1), and that this directly corresponds to the amount of computation required *after* the pre-processing has been completed. The y-axis of Figure 5.7(b) shows the number of pure strategies evaluated for the attacker, whereas the x-axis shows the number of targets. For example, the number of pure strategies expanded by the depth-two hierarchy for 20 targets is 184,763 whereas for the full binary hierarchy is 88,422. Similarly, for 15 targets, the number of pure strategies expanded by the depth-two hierarchy for 20 targets is 51,096 whereas for the full binary hierarchy is 46,108. Thus, in combination with Figure 5.7(a), the experiment shows (i) the number of pure strategies evaluated for full binary hierarchy is always no greater than the pure strategies evaluated for the depth-two hierarchy (the difference in number of pure strategies evaluated is statistically significant only for 15 and 20 targets in Figure 5.7(b)), and (ii) the depth-two hierarchy is faster for lesser number of targets (for 5, 10 and 15 targets in Figure 5.7(a)) and slower for 20 targets. The results confirms that there exists a trade-off in the choice of the hierarchy: deeper trees are faster only when the number of targets are large otherwise the overhead of pre-processing overwhelms the total runtime required to solve the problem.

5.2.2.4 Different arrangement of types in HBSA

The objective of these experiments is to identify the impact of the distribution of types in the runtime performance of HBSA as the number of targets is increased. I test two arrangements in these experiments: one that puts *similar* types in the same sub-tree whereas other which combines *dissimilar* types. The optimal coverage vectors $\mathbf{c}^\lambda = \mathbf{P}\mathbf{x}$ are computed per type λ by solving

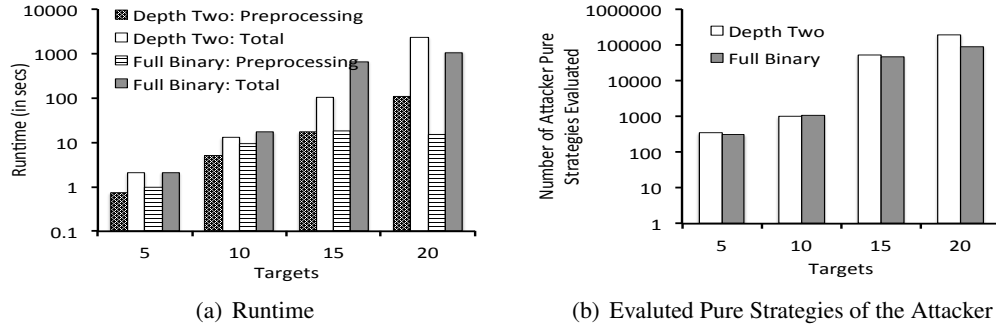


Figure 5.7: The figure shows the impact in runtime when the distribution of trees is varied in the hierarchy used in HBSA. These results are for 8 attacker types. While I do not show the error bars in this figure as well, depth-two hierarchy was faster for 10 and 15 targets whereas full binary hierarchy was faster for 20 targets with statistical significance.

a restricted SPARS game just for type λ , and then the K-L divergence distance [Kullback and Leibler, 1951] between the resulting solutions \mathbf{c}^λ is used as a similarity metric. A smaller K-L distance implies similar marginal coverage vectors; the larger this distance, the more dissimilar the marginals. For this experiment, I generated random instances of the Bayesian-SPARS problems with 8 attacker types, and always arranged them in a full binary tree hierarchy. I conducted experiments with different tree hierarchies like depth-one, depth-two and full binary tree; however, I present results only for the full binary tree hierarchy since it was found to perform (and scale) the best in all my experiments.

The results are shown in Figure 5.8. These results are averaged over 30 problem instances. The runtime performance is shown in Figure 5.8(a). The y-axis in the figure shows the time in seconds on the log scale, whereas the x-axis shows the number of targets in the problem instance. Each cluster has two sets of results: the first two bars correspond to the results when similar types are combined, whereas the next two bars show the results when dissimilar types are combined. The first bar in each set is the time required for pre-processing, i.e. the time required to solve the sub-trees below the root node in the hierarchical type tree (refer Figure 5.2). The second bar shows the total average runtime required by the algorithm. For example, for 20 targets, the

pre-processing and total runtime required for the ‘similar’ arrangement are 12 and 1,028 seconds respectively, whereas the corresponding times for the ‘dissimilar’ arrangement are 21 and 2,578 seconds, respectively.

The results show that combining similar types is always more helpful than combining dissimilar types. This result makes intuitive sense since combining similar types is expected to generate tighter bounds (since the defender is better able to optimize against two similar opponents), resulting in more pruning at every subsequent parent node. To test this hypothesis, I also plot the number of pure strategies of the attacker (refer Figure 5.1) that are expanded at the root node of the hierarchical type tree (refer (Figure 5.2)). Like in the previous experiment, the number of pure strategies of the attacker represents the number of leaves from Figure 5.1 that are expanded by the HBSA algorithm after the pre-processing has been completed. These results are shown in Figure 5.8(b). The y-axis shows the number of pure strategies evaluated for the attacker, whereas the x-axis shows the number of targets. For example, the number of pure strategies expanded by the ‘similar’ arrangement for 20 targets is 80,781 whereas for the ‘dissimilar’ arrangement is 160,502 respectively. The results confirm my hypothesis that combining similar types results in fewer pure strategies of the attacker being evaluated.

5.3 Bayesian SPPC Domain

In this section, I present the solution methodology for solving the Bayesian extension of the SPPC domain. Again, the defender does not know the type of the attacker she would be facing, however, the defender does know a prior probability of facing each type. The attacker knows his type as well the defender strategy, and then computes his best response.

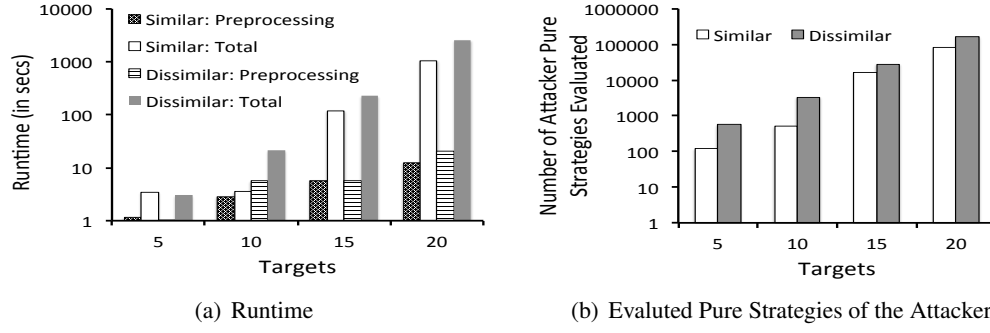


Figure 5.8: The figure shows the impact in runtime when the distribution of types is varied in the hierarchy used in HBSA. We, again, do not show the error bars because of the log scale of the y-axis but the similar type arrangement was faster than the dissimilar type arrangement for 10, 15 and 20 targets with statistical significance.

I again present a branch-and-price formulation to compute optimal solutions for the Bayesian extension of the SPPC domain. Here, again, the branch-and-price formulation is composed of a branch and bound module and a column generation module. Again, the actions of the attacker are modeled as an integer variable. The branch and bound assigns a value (i.e. a specific target to attack) to this integer in every branch. The solution at each node of this tree is computed using the column generation procedure. The master and the slave problems for this column generation procedure are described below.

5.3.1 Master Formulation

The objective of the master formulation is to compute the probability distribution \mathbf{x} over the set of tours \mathbf{T} such that the expected defender utility is maximized. The master formulation is given in Equations (5.11) to (5.16). Λ specifies the set of adversary types, and is subscripted using λ . Again, Equation (5.13) computes the payoff of the defender. Equations (5.14) and (5.15) compute the payoff of the attacker, while ensuring that $q_s^\lambda = 1$ is feasible if and only if attacking target s

is the best response of the attacker of type λ . Equations (5.12) and (5.16) ensure that \mathbf{x} is a valid probability distribution.

$$\min_{x,d,q} - \sum_{\lambda \in \Lambda} d^\lambda \quad (5.11)$$

$$\text{s.t. } \sum_{t \in T} x_t \leq 1 \quad (5.12)$$

$$d^\lambda - \sum_{t \in T} x_t z_{st} (\tau_s^\lambda + R_s^\lambda) + M q_s^\lambda \leq M - R_s^\lambda \quad (5.13)$$

$$-k^\lambda - \sum_{t \in T} x_t z_{st} (P_s^\lambda + R_s^\lambda) + R_s^\lambda \leq 0 \quad (5.14)$$

$$k^\lambda + \sum_{t \in T} x_t z_{st} (P_s^\lambda + R_s^\lambda) + M q_s^\lambda - R_s^\lambda \leq M \quad (5.15)$$

$$x_t \in [0, 1] \quad (5.16)$$

5.3.2 Slave

The objective of the slave formulation is to compute the next best tour to add to the set of tours \mathbf{T} . This is again done using a minimum cost integer network flow formulation. The network flow graph is constructed in the same way as before. The updated reduced costs for this variant of the domain are computed using the same standard techniques and are given in the Equation (5.17). Here, w^λ , y^λ , v^λ and h represent the duals of Equations (5.13), (5.14), (5.15) and (5.12) respectively.

$$\bar{c}_t = \sum_{\lambda \in \Lambda} \sum_{s \in S} (w_s^\lambda (\tau_s^\lambda + R_s^\lambda) + (v_s^\lambda - y_s^\lambda) (P_s^\lambda + R_s^\lambda)) z_{st} - h \quad (5.17)$$

This reduced cost of a tour \bar{c}_t is again decomposed into reduced costs per target in the following manner:

$$\bar{c}_t = \sum_{s \in S} \hat{c}_s z_{st} - h \quad (5.18)$$

$$\hat{c}_s = \sum_{\lambda \in \Lambda} (w_s^\lambda (\tau_s^\lambda + R_s^\lambda) + (v_s^\lambda - y_s^\lambda) (P_s^\lambda + R_s^\lambda)) \quad (5.19)$$

These reduced costs per target, \hat{c}_s , are then put as the costs on the links of the minimum cost network flow formulation.

The results of the runtime of this domain are presented with detailed analysis in Chapter 6.

Chapter 6: $d:s$ and Phase Transition

Software security assistants built on the framework of Stackelberg security games [Kiekintveld et al., 2009] have been deployed by a variety of real-world security agencies. For example, ARMOR [Jain et al., 2010c] has been in use by the police at Los Angeles International Airport since 2007. Similarly, IRIS [Jain et al., 2010c] and PROTECT [An et al., 2011] have been in use by the US Federal Air Marshals Service and the US Coast Guard since 2009 and 2011 respectively. Many different algorithms have been proposed for computing solutions to such problems [Conitzer and Sandholm, 2006; Paruchuri et al., 2008b; Gatti, 2008; Kiekintveld et al., 2009; Jain et al., 2010b; Dickerson et al., 2010b; Letchford and Vorobeychik, 2011; Bosansky et al., 2011] with a focus on scalability to enable the application of these models to newer and more complex real-world domains.

In this chapter, I investigate what properties of Stackelberg security game instances make them hard to solve in practice, across different input sizes and different security domains. I show that this question can be answered using the novel concept of the deployment-to-saturation ($d:s$) ratio. This ratio, which we denote $d:s$, is defined as the number of deployed defender resources divided by the number of resources beyond which additional deployments would not provide any benefit to the defender. I show that the hardest computational instances arise when this ratio is

0.5, independent of the domain representation, model and solver. Specifically, I consider three different classes of security domains, eight different MIP algorithms (including two algorithms actually deployed in practice), five different underlying MIP solvers, two different variations on the Stackelberg equilibrium concept, and a variety of domain sizes and conditions.

I identify two important implications of my findings. First, new algorithms should be compared on the hardest problem instances; I show that most previous research has compared the runtime performance of algorithms only at low $d:s$ ratios, where problems are comparatively easy. Second, I argue that this computationally hard region is the point where optimization offers the greatest benefit to security agencies, implying that problems in this region deserve increased attention from researchers.

Finally, I leverage the concept of *phase transitions* to better understand this algorithm-independent, computationally hard region. This approach to understanding algorithm-independent structural properties was pioneered by [Cheeseman et al., 1991] and [Mitchell et al., 1992]. They showed that the probability that a uniform-random 3-SAT instance will be satisfiable exhibits a phase transition when the number of variables is fixed and the number of clauses crosses roughly 4.3 times the number of variables, which corresponds to the point where the probability that the instance will be solvable crosses 0.5. Phase transitions have also been used to understand the computational impact of problem structure in optimization problems, such as MAX-SAT [Slaney and Walsh, 2002] and TSP [Gent and Walsh, 1996; Frank et al., 1998]. The approach taken in this work is to identify a phase transition in the decision version of the optimization problem (i.e., asking whether or not a solution exists with a given objective function value). I show that security games exhibit a phase transition at 0.5 for random Stackelberg security game instances, and that this phase transition corresponds to the computationally hardest instances at the $d:s$ ratio of 0.5.

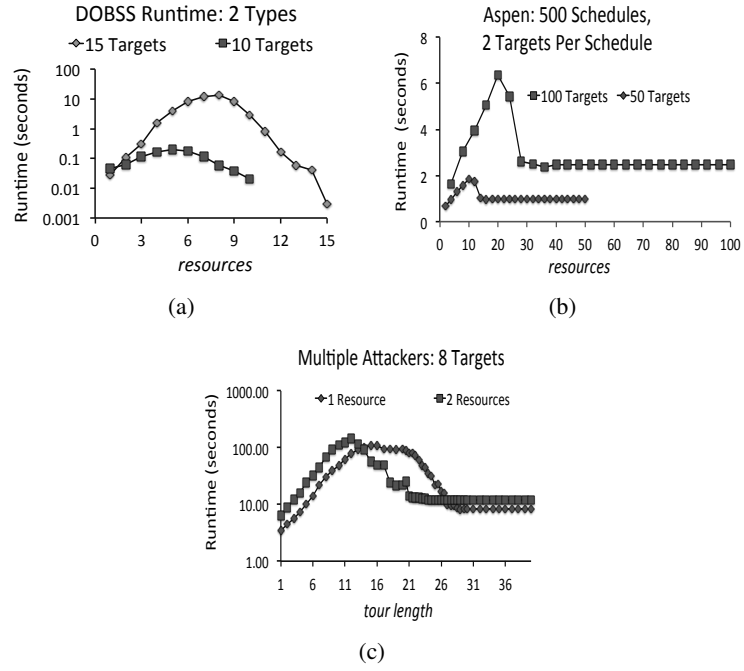


Figure 6.1: Average running time of DOBSS, ASPEN and multiple-attacker branch-and-price algorithm for SPNSC, SPARS and SPPC domains respectively.

As mentioned previously, this chapter focuses on the runtime required by the different algorithms that compute solutions for instances of security games for the three domains described above. Figure 6.1 shows the runtime for computing solutions using DOBSS, ASPEN and multiple-attacker branch-and-price algorithm for the SPNSC, SPARS and SPPC domains respectively. (Recall that these three configurations are particularly interesting, as they are the ones that have been deployed in practice.) The x -axis in each figure shows the number of available resources to the defender, and the y -axis shows the runtime in seconds. In the SPNSC and the SPARS domains I define the number of resources as the number of officers available to the defender; in the SPPC domain, I define it as the maximum feasible tour length. These graphs show that there is no unified value of the number of defender resources which makes security game instances hard to solve. I

also tried normalizing the number of resources by the number of targets, however, I found similar inconsistencies across different domains even with that normalization.

6.1 Deployment to Saturation Ratio

I now propose the novel concept of the *deployment-to-saturation* ($d:s$) ratio, a concept that unifies the domain independent properties of problem instances across different security domains. Specifically, I consider the three security domains introduced before, eight different MIP algorithms (including two deployed algorithms), five different underlying MIP solvers, two different equilibrium concepts in Stackelberg security games, and a variety of domain sizes and conditions. I show experimentally that the hardest problem instances occur when the $d:s$ ratio is about 0.5. (Specifically, in my experiments, the hardest problem instances occurred at the $d:s$ ratios between 0.48 and 0.54. However, because of discretization, I was not able to test all $d:s$ ratios in all domains. Without exception, the hardest value was the feasible value closest to 0.5. This fact, in combination with my phase transition arguments presented at the end of the chapter, lead me to conclude that the hardest region is precisely $d:s = 0.5$.)

More specifically, the deployment-to-saturation ($d:s$) ratio is defined in terms of *defender resources*, a concept whose precise definition differs from one domain to another. Given this definition, *deployment* denotes the number of defender resources available to be allocated, and *saturation* denotes the minimum number of defender resources such that the addition of further resources beyond this point yields no increase in the defender's expected utility. For the SPNSC and the SPARS domain, deployment denotes the number of available security personnel, whereas saturation refers to the minimum number of officers required to cover all targets with a probability

of 1. For the SPPC domain, deployment denotes the maximum feasible tour length, while saturation denotes the minimum tour length required by the team of defender resources such that the team can tour all the targets with a probability of 1.

I now present results for all the three security domains. All the results shown below are averaged over 100 samples, and were collected on a machine with a 2.7GHz Intel Core i7 processor and 8GB main memory. In all graphs, the x -axis shows the $d:s$ ratio and the y -axis shows the runtime in CPU-seconds. Experiments were conducted using CPLEX 12.2 unless otherwise noted.

6.1.1 SPNSC Domain

For this domain, I considered both the general-sum and security game compact representations.

6.1.1.1 General sum representation.

I conducted experiments varying the algorithm, number of attacker types and number of targets. The results for the general sum representation are plotted in Figures 6.2(a), 6.2(b) and 6.2(c). The payoffs for the two players were selected uniformly at random: the payoffs for success and failure were selected from the ranges $[1, 10]$ and $[-10, -1]$ respectively.

Figure 6.2(a) shows that the runtime required by all three algorithms (MultipleLPs, DOBSS and HBGS) peaks at $d:s = 0.53$. (While I would like to have observed peaks at $d:s = 0.5$ in all of my experiments, I typically observed values that were slightly different. The explanation that might come first to mind is variance due to having measured an insufficient number of samples. However, there is also a more critical issue: because the numbers of resources and targets are discrete, I was not able to measure every $d:s$ value. Here, 8 resources and 15 targets corresponded

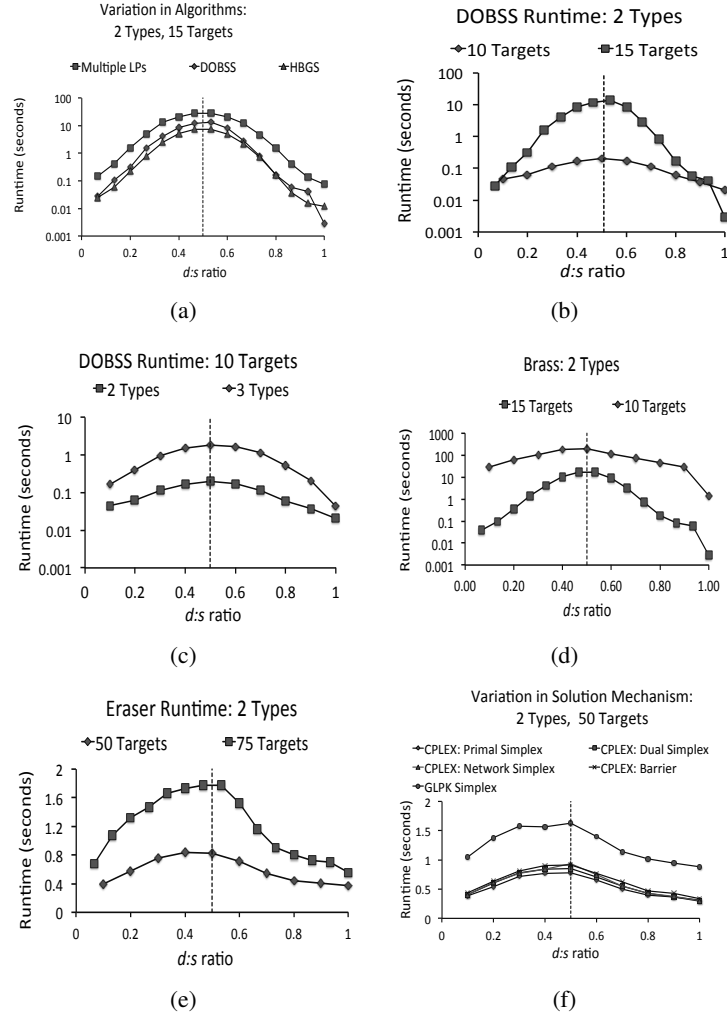


Figure 6.2: Average runtime of computing the optimal solution for a SPNSC problem instance. The vertical dotted line shows $d:s = 0.5$.

to $d:s = 0.53$.) This set of experiments considered 2 attacker types and 15 targets. Moreover, all the three algorithms required the maximum runtime when the $d:s$ ratio was 0.53. For example, MultipleLPs required 27.9 seconds to compute the optimal solution. This experiment shows that computation is hardest for the SPNSC problem instances when the $d:s$ ratio is about 0.5.

The next two experiments study runtime variation when the number of targets and the number of types in the domain vary. Figure 6.2(b) varies the number of targets in the domain from 10 to

15. Similarly, Figure 6.2(c) varies the number of types from 2 to 3 in the security domain. For example, DOBSS took 1.8 seconds on average for instances with 3 attacker types at the $d:s$ ratio of 0.5 (5 resources and 10 targets),

I also ran experiments with BRASS, which computes an ϵ -Stackelberg equilibrium [Pita et al., 2010]. These results are shown in Figure 6.2(d). The hardest instances for BRASS in a domain with 15 targets corresponded to a $d:s$ ratio of 0.53 (8 resources), with BRASS taking 17 seconds.

6.1.1.2 Security game compact representation.

I conducted experiments with ERASER that varied the number of targets and the number of attacker types. I generated payoffs for the players as before. Figure 6.2(e) shows the results for problem instances with 2 attacker types and both 50 and 75 targets. For example, the runtime required for 75 targets for the $d:s$ ratio of 0.49 (37 resources) was 1.8 seconds. This was the computationally hardest point for 75 targets. I also varied the number of types, and those results also confirmed my claim.

Our next experiment investigated the effect on ERASER's runtime of changing its underlying solver and solution mechanism. I plot the runtime required by ERASER with CPLEX Primal Simplex, CPLEX Dual Simplex, CPLEX Network Simplex, CPLEX Barrier and GLPK Simplex methods. Again, I generated the payoffs and game instances as before. A sample result is that, for the $d:s$ ratio of 0.50 (25 targets), the runtime required by CPLEX Dual Simplex was 0.9 seconds and the runtime required by GLPK Simplex was 1.6 seconds. These experiments again show that the $d:s$ ratio of 0.5 corresponds with the computationally hardest instances across a range of underlying solver and solution mechanisms for the SPNSC domain.

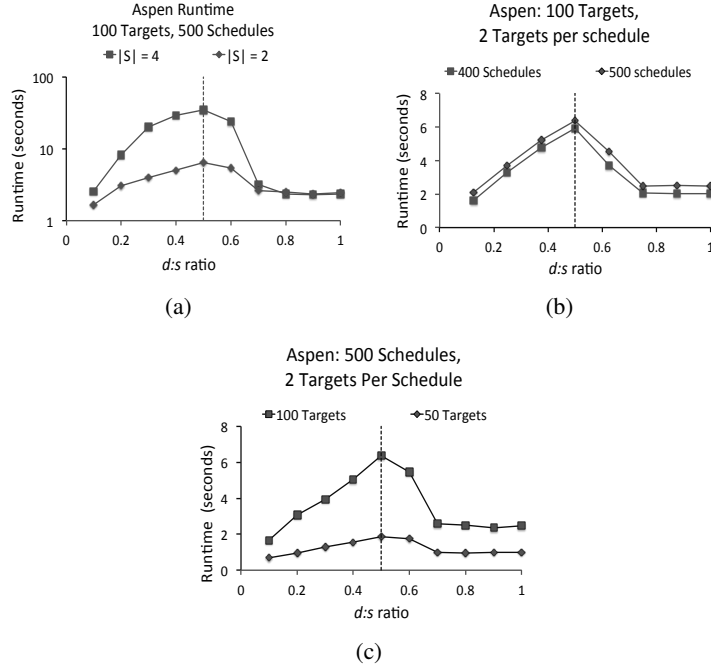


Figure 6.3: Average runtime of computing the optimal solution for a SPARS game using ASPEN. The vertical dotted line shows $d:s = 0.5$.

6.1.2 SPARS Domain

I conducted experiments varying the length of a schedule, the number of targets and the number of schedules in SPARS problem instances. ASPEN was used to compute solutions. As before, payoffs for the two players were selected uniformly at random; the rewards for success were selected uniformly at random from the interval $[1, 10]$, and the penalty for failure uniformly at random from the interval $[-10, -1]$.

Figure 6.3(a) shows the results for SPARS problem instances with 100 targets and 500 schedules, when the number of targets covered by each schedule, denoted by $|S|$, was varied. For example, the runtime required for $|S| = 2$ at the $d:s$ ratio of 0.50 (20 deployed resources, 40 required for saturation) was 6.4 seconds. This was computationally the hardest point for $|S| = 2$.

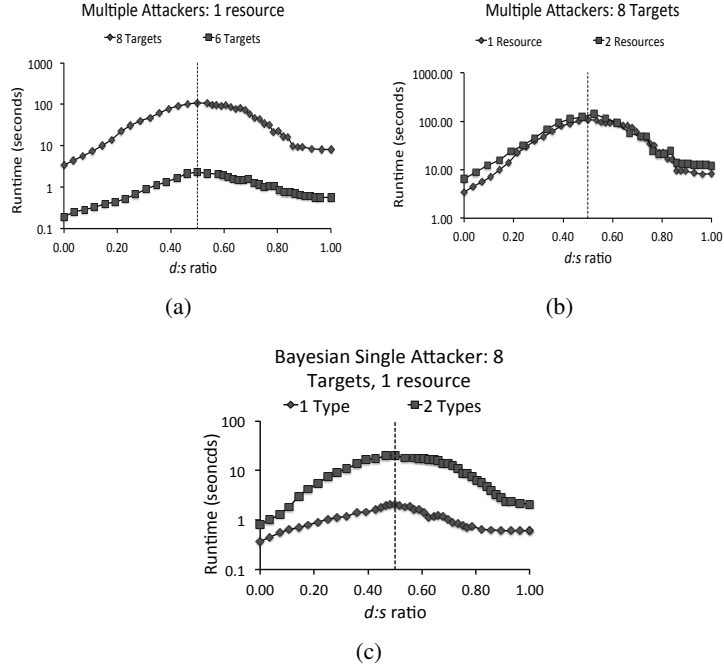


Figure 6.4: Average runtime for computing the optimal solution for a patrolling domain. The vertical dotted line shows $d:s = 0.5$.

For $|S| = 4$, the computationally hardest point required 28.9 seconds at $d:s = 0.5$ (10 available resources, 20 required for saturation).

Figure 6.3(b) shows the results for SPARS problem instances with 100 targets and 2 targets per schedule, considering 400 and 500 schedules. For example, the runtime required for 500 schedules for the $d:s$ ratio of 0.50 (20 resources, 40 required for saturation) was 6.4 seconds. Figure 6.3(c) shows the results for SPARS problem instances with 500 schedules, 2 targets per schedule for 50 and 100 targets. For example, the runtime required for 50 targets for the $d:s$ ratio of 0.50 (10 resources, 20 required for saturation) was 1.9 milliseconds which, again, was the computationally hardest point for 50 targets.

6.1.3 SPPC Domain

I present results for both the multiple attacker and the Bayesian single attacker variants in Figure 6.4. Figure 6.4(a) shows the results for the multiple attacker SPPC domain with 1 defender resource, and with the number of targets varying from 6 to 8. For example, for the $d:s$ ratio of 0.50, the algorithm took 108.2 seconds to compute the optimal solution. Figure 6.4(b) shows the runtime required to compute the optimal solution for the multiple attacker SPPC domain with 8 targets. It varies the number of defender resources from 1 to 2. For example, for the $d:s$ ratio of 0.50, the algorithm took 144.0 seconds to compute the optimal solution for 2 resources. This was again the computationally hardest point.

Similarly, Figure 6.4(c) shows the runtime required for our branch-and-price based algorithm to compute an optimal solution for the Bayesian single attacker SPPC domain with 8 targets and 1 defender resource, along with the probability p that the decision problem is solvable. It varies the number of types from 1 to 2. For example, for the $d:s$ ratio of 0.50, the algorithm took 2.0 seconds to compute the optimal solution for 1 type.

6.2 Implications of the findings

I have provided evidence that the hardest random Stackelberg game instances occur at a deployment-to-saturation ratio of 0.5. This finding has two key implications.

First, it is important to compare algorithms on hard problems. If random data is used to test algorithms for security domains, it should be generated at a $d:s$ ratio of 0.5. There has indeed been a significant research effort focusing on the design of faster algorithms for security domains. Random data has often been used; unfortunately, I find that it tends not to have come

from the $d:s = 0.5$ region. (Of course, the concept of a deployment-to-saturation ratio did not previously exist; nevertheless, I can assess previous work in terms of the $d:s$ ratio at which data was generated.) For example, [Jain et al., 2011a] compared the performance of HBGS with DOBSS and MultipleLPs, but they only compared $d:s$ ratios between 0.10 and 0.20. Similarly, [Pita et al., 2010] presented runtime comparisons between different algorithms, varying the number of attacker types in the security domain; all experiments in this chapter were fixed at $d:s = 0.30$ (10 targets, 3 resources). [Jain et al., 2011b] showed scalability results for RUGGED, testing at $d:s$ ratios of 0.10 and (mostly) 0.20. Runtime results have also been presented in other security settings [Dickerson et al., 2010b; Vanek et al., 2011; Bosansky et al., 2011]; these algorithms compute defender strategies for networked domains. Their experiments keep the number of resources fixed and increase the size of the underlying network; however, none of these papers provides enough detail about how instances were generated to allow us to accurately compute the $d:s$ ratio.

To make it easier for future researchers to test their algorithms on hard problems, I have written a benchmark generator for security games that generates instances from $d:s = 0.5$. This generator is written in Java, and is available for download at <http://teamcore.usc.edu/DTS>. It allows users to generate instances for all domains described above, as well as to compute solutions for all the algorithms mentioned in this research. It also allows switching between GLPK and CPLEX.

Second, I observe that intermediate values of the $d:s$ ratio, the computationally hard region, is also the region where optimization is most valuable and hence where security officials are most likely to seek help in optimizing their resource deployment. If the $d:s$ ratio is large, there are enough resources to protect almost all targets, and performing a rigorous optimization offers little additional benefit. If $d:s$ is small, there are not enough resources for optimized deployment to have a significant impact. To make this intuition concrete, I show an example from random data

from the SPNSC domain in Figure 6.5. I present results for 50 and 75 targets, each averaged over 100 random instances. The x -axis plots the $d:s$ ratio, and the y -axis shows the difference between the defender utilities obtained by the optimal strategy and a naïve randomization strategy. A low utility difference implies that the naïve strategy is almost as good as the optimal strategy, whereas a high difference shows that it is worthwhile to invest in computing the optimal strategy. The naïve strategy I use here prioritizes targets based on the attacker’s payoff for successfully attacking a target, and then uniformly distributes its resources over twice as many top targets as the number of resources. For example, at a $d:s$ ratio of 0.5, for 50 targets, the difference in utilities between the optimal solution and the solution from the randomized strategy was 5.07 units, whereas it was 0.21 units at a $d:s$ ratio of 1. This suggests that computationally hard settings are also those where security forces would benefit the most from adopting nontrivial strategies; hence, researchers should concentrate on these problems.

6.3 Phase Transitions

All the runtime results show an easy-hard-easy computational pattern as the $d:s$ ratio increases from 0 to 1, with the hardest problems at $d:s = 0.5$. Such easy-hard-easy patterns have also been observed in other NP-complete problems, most notably 3-SAT [Cheeseman et al., 1991; Mitchell et al., 1992]. In 3-SAT, the hardness of the problems varies with the clause-to-variable (c/v) ratio, with the hardest instances occurring at about $c/v = 4.26$. The SAT community has used the concept of *phase transitions* to better understand this hardness peak.

Phase transitions have also been used to study properties of optimization problems. Specifically, one can derive the decision version of an optimization problem by asking “does there exist a

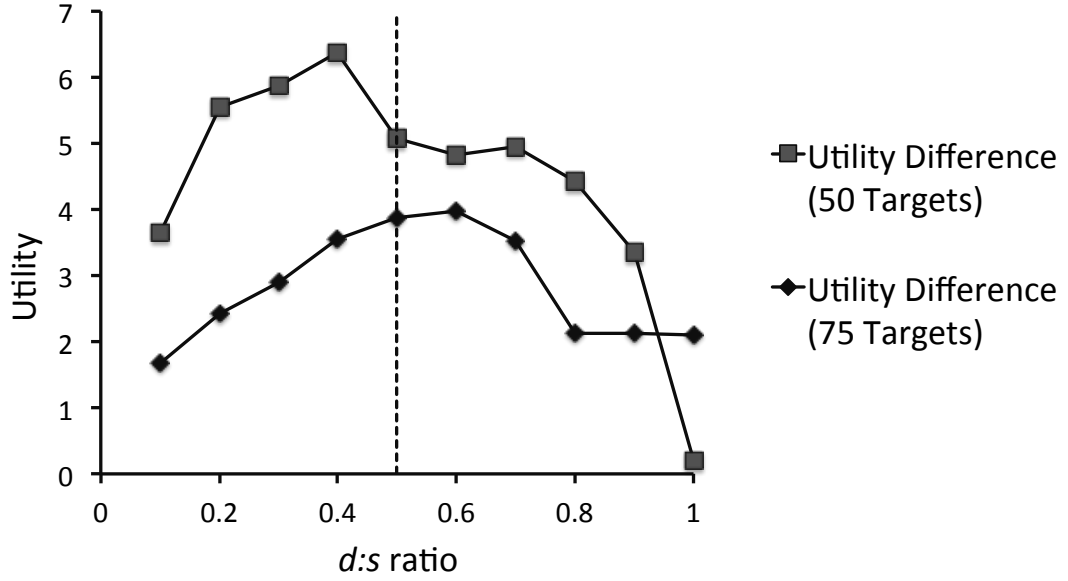


Figure 6.5: The difference between expected defender utilities from ERASER and a naïve randomization policy. The vertical line shows $d:s = 0.5$.

solution with objective function value $\geq k$ ”, and then looking for a phase transition in the decision problem. This approach was pioneered by Gent et al. [Gent and Walsh, 1995], who studied the properties of four different optimization problems including TSP and Boolean circuit synthesis. They computed the optimal tour length from the TSP optimization problem, and then used this value as k to define the decision version of the TSP instance. They showed that a phase transition in the solubility of this problem corresponded to the computationally hardest region. The same approach was later also used by Gent and Walsh [Gent and Walsh, 1996].

In the context of game theory, phase transitions have been used to analyze the efficiency of markets in adaptive games [Savit et al., 1999] and the probability of cooperation in evolutionary game theory [Hauert and Szab, 2005]. To my knowledge, this work is the first that identifies such structural properties in the context of Stackelberg security games.

6.3.1 Phase Transitions in Security Games

I begin by defining the decision version of the SSE optimization problem, which I denote $SSE(D)$. $SSE(D)$ asks whether there exists a defender strategy that guarantees expected utility of at least the given value D . I want to claim that a phase transition in the decision problem correlates with the hardest random problem instances. However, I obtain different phase transitions for different values of D . Following Gent et al. [Gent and Walsh, 1995], I define D^* as the median objective function value achieved in the SSE optimization problem when the $d:s$ ratio is set to 0.5. (Observe that this definition guarantees that at a $d:s$ ratio of 0.5, exactly 50% of problem instances will have a feasible solution. On the other hand, it does not guarantee that there will be a phase transition—i.e., a sharp change—in the probability of solvability.) I estimated D^* by sampling 100 random problem instances at $d:s = 0.5$, and computing the sample median of their objective function values.

Claim 1. *As the $d:s$ ratio varies from 0 to 1, the probability p that a solution exists to $SSE(D^*)$ exhibits a phase transition at $d:s = 0.5$. This phase transition is independent of the security domain or its representation. Furthermore, this phase transition aligns with the computationally hardest instances.*

To support this claim, I computed the probability of solvability of the decision problem $SSE(D^*)$ for all the security domains and algorithms mentioned above. The phase transition results are shown in Figures 6.6 for the SPNSC domain, in Figure 6.7 for the SPARS domain, whereas results for the SPPC domain are shown in Figure 6.8 respectively. In the all figures, the x -axis shows the $d:s$ ratio as before, the primary y -axis shows the runtime in seconds, and the secondary y -axis shows the probability p of finding a solution to $SSE(D^*)$. I plot runtimes

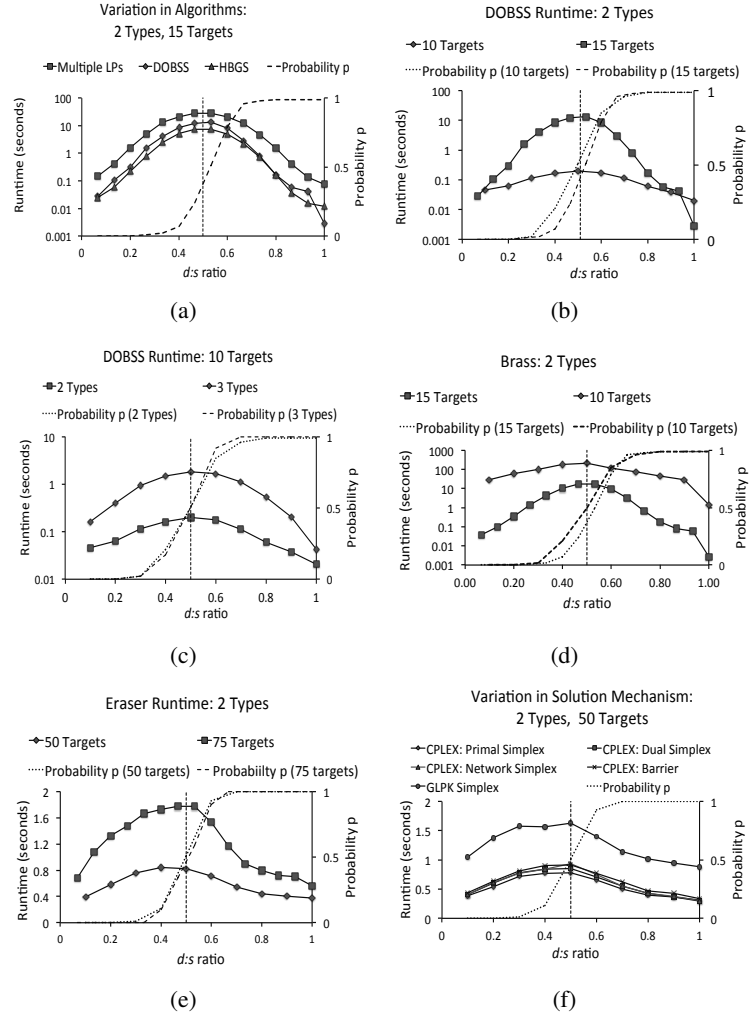


Figure 6.6: Average runtime of computing the optimal solution for a SPNSC problem instance. The vertical dotted line shows $d:s = 0.5$.

using solid lines, as before, and plot p using a dashed line. Figure 6.6(c) presents results for the DOBSS algorithm for the SPNSC domain for 10 targets and 2 and 3 attacker types. As expected, the $d:s$ ratio of 0.5 corresponds with $p = 0.51$ as well as the computationally hardest instances; more interestingly, I observe that p undergoes a phase transition as the $d:s$ grows. Similarly, Figure 6.7(b) shows results for the ASPEN algorithm for the SPARS domain with 100 targets, 2 targets per schedule and 400 and 500 schedules, and Figure 6.8(a) shows results for the multiple

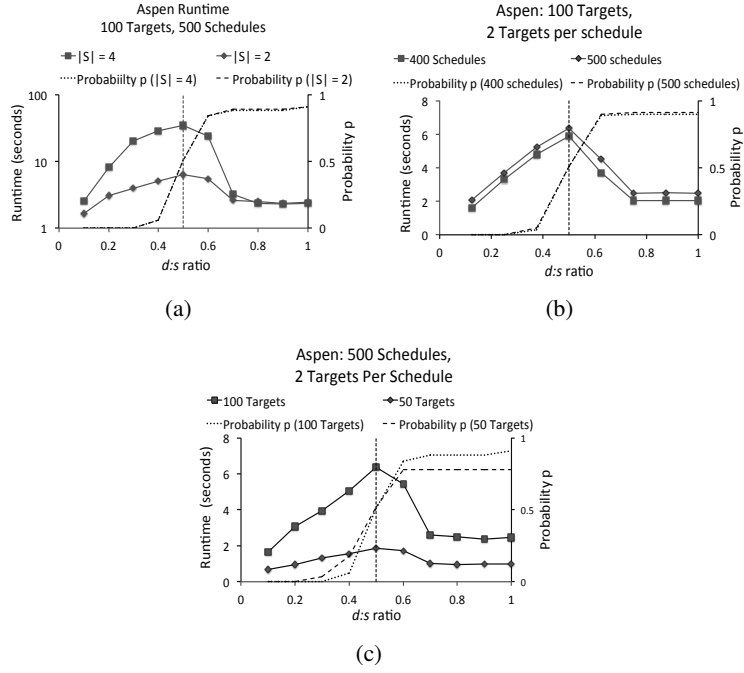


Figure 6.7: Average runtime of computing the optimal solution for a SPARS game using ASPEN. The vertical dotted line shows $d:s = 0.5$.

attacker SPPC domain for 1 defender resource. In both cases, I again observe a phase transition in p . The runtime results of ERASER varying the number of attacker types are shown in Figure 6.9. The x-axis shows the $d:s$ ratio, whereas the y-axis shows the runtime in seconds.

One might wonder how I can decide that the increase in p is steep enough to be called a phase transition. I know from both the experimental and theoretical literature on phase transitions in decision problems that the transition becomes steeper as problem size increases, approaching a step function in the limit [Kirkpatrick and Selman, 1994; Friedgut, 1998]. This is a property that I can check for experimentally. I conducted experiments in the SPNSC domain, since it is the easiest to solve at widely varying problem sizes; the results are shown in Figure 6.10. The x -axis shows the $d:s$ ratio, and the y -axis shows the probability p of finding a feasible solution to the decision version of a corresponding SPNSC problem; I plot results for problem instances with 50,

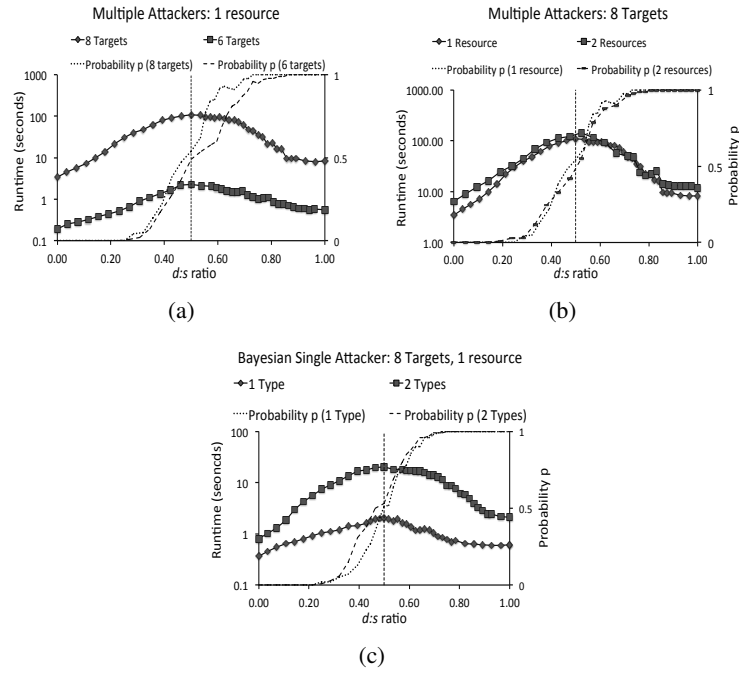


Figure 6.8: Average runtime for computing the optimal solution for a patrolling domain. The vertical dotted line shows $d:s = 0.5$.

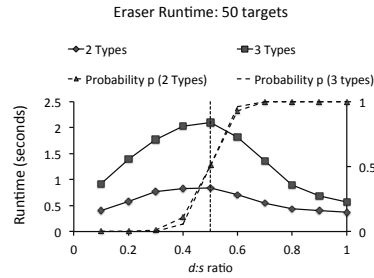


Figure 6.9: ERASER results with varying number of attacker types.

100 and 150 targets. I observe the desired result: the phase transition indeed becomes sharper as the number of targets increases.

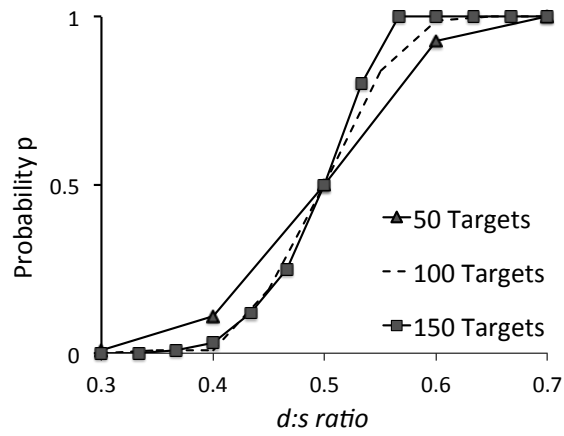


Figure 6.10: Probability that the decision problem $SSE(D^*)$ is soluble for SPNSC instances of three problem sizes. The phase transition gets sharper as the problem size increases.

Chapter 7: Related Work

There exists related work both in game-theoretic as well as non-game theoretic literature studying the security domain. Much of this work is theoretical analysis of hypothetical scenarios, while my thesis focuses on algorithms designed for use in real-world security operations. There are three main areas of related work:

1. The first area is on computation for Stackelberg security games.
2. The second area of related work applies Stackelberg games to other security scenarios.
3. The third area of related work applies other optimization techniques to model the security domain.

I now explore these three areas in detail.

7.1 Computation in Stackelberg Security Games

The first area of related work is on efficient algorithms for Stackelberg security games, such as the ones studied in this paper. Game-theoretic models have been applied in a variety of homeland security settings, such as protecting critical infrastructure [Brown et al., 2006; Pita et al., 2008; Nie et al., 2007; Kiekintveld et al., 2009] and computer network security [Lye and Wing, 2005;

Srivastava et al., 2005], and different algorithms have been developed for such models. The related work on these game-theoretic approaches for security can be broadly sub-divided into three categories:

1. Algorithms on computing Stackelberg equilibria,
2. Algorithms to account for human behavior, and
3. Algorithms for computing *robust* defender strategies.

7.1.1 Efficient computation of Stackelberg equilibria

Within this area of efficient algorithms, the MultipleLPs approach [Conitzer and Sandholm, 2006] was the first to propose optimal computation of leader strategies in a Stackelberg game. While this paper did not envision a security scenario, security domains led to a requirement of Bayesian Stackelberg games. A Bayesian Stackelberg game can be converted to a Stackelberg game by using the Harsanyi transformation [Harsanyi and Selten, 1972]; however, the size of the Harsanyi transformed matrix would grow exponentially with the number of attacker types, inhibiting application for large input problems. The MultipleLPs approach [Conitzer and Sandholm, 2006] computed optimal defender strategies by operating on the Harsanyi transformed matrix [Harsanyi and Selten, 1972]; while it did not explicitly represent the Harsanyi transformed matrix in memory, it required computing solutions to exponentially many linear programs. DOBSS [Paruchuri et al., 2008b] avoided this Harsanyi transformation, and was the first mixed-integer linear program proposed for computing optimal defender strategies for the Stackelberg security games. While DOBSS was much faster than Multiple LPs [Conitzer and Sandholm, 2006], it still requires the

input to explicitly represent all the pure strategies of the defender and hence does not scale to domains with thousands of targets and tens of resources.

Continuing with the first area of related work, **ORIGAMI** is a polynomial time algorithm that computes optimal defender strategies for a security game when no scheduling constraints are present (an example of scheduling constraints is the logistical constraints faced by a federal air marshal). **ERASER-C**, then, a mixed-integer linear program [Kiekintveld et al., 2009] was developed for larger and more complex Stackelberg security games. **ERASER-C** focuses on games with large numbers of defenders with scheduling constraints, handling the combinatorial explosion in the defender’s joint schedules. Unfortunately, as the authors note, **ERASER-C** may fail to generate a correct solution in cases where arbitrary schedules with more than two flights (e.g., multi-city flight tours) are allowed in the input, or when the set of flights cannot be partitioned into distinct sets for departure and arrival flights. **ERASER-C** avoids enumerating joint schedules to gain efficiency, but loses the ability to correctly model arbitrary schedules. Furthermore, **ERASER-C** only outputs a coverage vector \mathbf{c} , where c_t is the probability of the defender protecting target t . It does not provide the mixed strategy \mathbf{x} over joint schedules \mathbf{J} of all defender resources, which is necessary to implement the coverage \mathbf{c} in practice. Additionally, no other algorithm has yet been provided to convert marginals to probabilities over joint schedules, and in Section 3.2, we present the first efficient algorithm that addresses this challenge for arbitrary scheduling constraints.

The most recent algorithm employing large-scale optimization methods to solve Bayesian Stackelberg games is **HUNTER** [Yin and Tambe, 2012]. It employs Benders decomposition [Bertsimas and Tsitsiklis, 1994] and cut-generation, however, it is not designed to compute optimal strategy for a defender with scheduling constraints. Double-oracle based approaches that use both cut and column generation have also been proposed for security games [Halvorson et al.,

2009a; Jain et al., 2011b], however, they have only been applied for zero-sum settings. We present algorithms that are not restricted to the strict zero-sum requirement of the previous algorithms, but instead operate on Stackelberg *security* games [Kiekintveld et al., 2009]. In a security game, protecting a target is always beneficial for the defender and worse for the attacker, however, the payoffs need not be zero-sum.

In contrast, ASPEN employs the technique of branch-and-price [Barnhart et al., 1994] and computes solutions for a Stackelberg security game with arbitrary scheduling constraints. Additionally, hierarchical decomposition methods like the one employed by HBSA have also not seen much application towards obtaining optimal solutions in Bayesian Stackelberg games, although similar techniques have been proposed to obtain approximate Nash equilibrium for symmetric games [Wellman et al., 2005].

Game theory has also been applied to a wide range of problems where one player — the evader — tries to minimize the probability of detection by and/or encounter with the other player — the patroller; the patroller wants to thwart the evader’s plans by detecting and/or capturing him. The formalization of this problem led to a family of games, often called *pursuit-evasion games* [Adler et al., 2002]. As there are many potential applications of this general idea, more specialized game types have been introduced, e.g., *hider-seeker games* [Flood, 1972; Halvorson et al., 2009b] and *infiltration games* [Alpern, 1992] with mobile patrollers and mobile evaders; *search games* [Gal, 1980] with mobile patrollers and immobile evaders; and *ambush games* [Ruckle et al., 1976] with the mobility capabilities reversed. In the game model proposed in this paper, the evader is mobile whereas the patroller is not, just like in ambush games. However, in contrast with ambush games, we consider *targets* (termed *destinations* in ambush games) of varying importance.

The network security game model described in this thesis is most similar to that of *interdiction games* [Washburn and Wood, 1995], where the evading player — the attacker — moves on an arbitrary graph from one of the origins to one of the destinations (aka. *targets*); and the interdicting player — the defender — inspects one or more edges in the graph in order to detect the attacker and prevent him from reaching the target. As opposed to interdiction games, we do not consider the detection probability on edges, but we allow different values to be assigned to the targets, which is crucial for real-world applications.

Recent work has also considered scheduling multiple-defender resources using cooperative game-theory, as in *path disruption games* [Bachrach and Porat, 2010], where the attacker tries to reach a single known target. In contrast with the static asset protection problem [Dickerson et al., 2010a], we attribute different importance to individual targets and unlike its dynamic variant [Dickerson et al., 2010a], we consider only static target positions. Recent work in security games and robotic patrolling [Basilico et al., 2009; Jain et al., 2010b] has focused on concrete applications. However, they have not considered the scale-up for both defender and attacker strategies. For example, in ASPEN, the attacker’s pure strategy space is polynomially large, since the attacker is not following any path and just chooses exactly one target to attack. Our game model was introduced by Tsai et al. [Tsai et al., 2010]; however, their approximate solution technique can be suboptimal. We discuss the shortcomings of their approach in Section 4.1, and provide an optimal solution algorithm for the general case.

Finally, algorithms that model security domains using Stackelberg games have seen many real-world deployments. ARMOR [Pita et al., 2008; Jain et al., 2010c] is a software assistant deployed at the Los Angeles International Airport since August 2007 that casts the scheduling problem of vehicular checkpoints and canine patrols as a Stackelberg game and uses the DOBSS

algorithm to compute these schedules. Similarly, the IRIS [Jain et al., 2010c] scheduling system, in use by the United States Federal Air Marshal Service since October 2009, generates schedules over international flights for the air marshals using the ASPEN algorithm presented in this thesis. Similarly, GUARDS [Pita et al., 2011b] is also a game-theoretic scheduling system in use by the United States Transport Security Administration to randomize behind-the-scenes activities conducted by the security agency. In the same way, PROTECT [An et al., 2011], another software scheduling system based on Stackelberg games, has been in use by the Boston Coast Guard since April 2011 to generate patrol routes for the boats and other resources available to the Boston Coast Guard. Finally, TRUSTS [Yin et al., 2012c] is another software scheduling system based on Stackelberg games that has been in use by the Los Angeles Sheriff's Department since May 2012 to generate strategies for the officers to inspect passengers towards reducing crime and suppressing fare evasion on the Los Angeles metro transit system.

7.1.2 Stackelberg equilibria modeling humans

The second category of related work that applies game-theory to security domains computes defender strategies when faced against human adversaries. This work takes into account the biases and bounded rationality of a human opponent. COBRA is one such algorithm that considers *anchoring-bias* of humans [Pita et al., 2009], as well as attacker indifference between pure strategies that are at most ϵ away from the optimal. Alternate solution techniques grounded in psychological concepts like Quantal Response Equilibrium (QRE) have also been proposed [Yang et al., 2011]. The focus of these algorithms has been to develop algorithms that perform well against humans; indeed they have been evaluated against human subjects. My research is complimentary to this

work; and my techniques of column generation are now being combined with Quantal response and other models of human-decision making.

7.1.3 Computation of robust solutions

The third category of related work aims at computing robust solutions. Kiekintveld et. al [Kiekintveld et al., 2011] model distributions over preferences of an attacker using infinite Bayesian games, and propose an algorithm to generate approximate solutions for such games. Yin et. al [Yin et al., 2012a] also provide robust solutions in the presence of execution and observation errors. The COBRA algorithm [Pita et al., 2009] mentioned before focuses on ϵ -rationality of the attacker, specifically for human subjects. In contrast, Yin et. al [Yin et al., 2010a] consider the limiting case where an attacker has no observations and thus investigate the equivalence of Stackelberg vs Nash equilibria. Even earlier investigations have emphasized the value of commitment to mixed strategies in Stackelberg games in the presence of noise [van Damme and Hurkens, 1997]. Secrecy and deception have also been modeled for Stackelberg games [Zhuang and Bier, 2011]. Outside of Stackelberg games, models for execution uncertainty in game-theory have been separately developed [Archibald and Shoham, 2009]. Robust solution methods for simultaneous move games have also been studied [Aghassi and Bertsimas, 2006; Porter et al., 2002].

7.2 Stackelberg games in other security scenarios

The second area of related work applies Stackelberg games to other security scenarios. Lawrence et al [Wein, 2008] apply Stackelberg games in the context of screening visitors entering the US. In their work, they model the U.S. Government as the leader who specifies the biometric identification

strategy to maximize the detection probability using finger print matches, and the follower is the terrorist who can manipulate the image quality of the finger print. Stackelberg games have also been used for studying missile defense systems [Brown et al., 2005a] and for studying the development of an adversary’s weapon systems [Brown et al., 2005b]. A family of Stackelberg games known as inspection games is closely related to the security games we are interested in and includes models of arms inspections and border patrols [Avenhaus et al., 2002]. Another line of recent work is on randomized security and robotic patrolling using Stackelberg games for generic “police and robbers” scenario [Gatti, 2008; Amigoni et al., 2008; Basilico et al., 2009]. These models use extensive form games to model the domain and present alternative algorithms to patrolling domains.

7.3 Other optimization techniques for security domains

The third area of related work applies other optimization techniques to model the security domain, but does not address the strategic aspects of the problem. These methods provide a randomization strategy for the defender, but they do not take into account the fact that the adversaries can observe the defender’s actions and then adjust their behavior. Examples of such approaches include [Ruan et al., 2005; Paruchuri et al., 2006] which are based on learning, Markov Decision Processes (MDPs) and Partially Observable Markov Decision Processes (POMDPs). As part of this work, the authors model the patrolling problem with locations and varying incident rates in each of the locations and solve for optimal routes using a MDP framework. Another example is the “Hypercube Queueing Model” [Larson, 1974] which is based on queueing theory and depicts the detailed spatial operation of urban police departments and emergency medical services. It has

found application in police beat design, in allocation of patrolling time, etc. Babu et al [Babu et al., 2006] have worked on modeling passenger security system at US airports using linear programming approaches, however, their objective is to classify the passengers in various groups and then screen them based on the group they belong to. Similarly, Agmon et. al [Agmon et al., 2008] analyze the performance of an attacker with zero-knowledge, and an attacker with partial knowledge in a perimeter patrolling domain. Such frameworks can address many of the problems we raise, including different target values and increasing uncertainty by using many possible patrol routes. However, they fail to account for the possibility that an intelligent attacker will observe and exploit patterns in the security policy. If a policy is based on the historical frequency of attacks, it is essentially a reactive policy and an intelligent attacker will always be one step ahead.

Chapter 8: Conclusions

Game-theoretic approaches have shown their usefulness in deployed security applications such as ARMOR for the Los Angeles International Airport Pita et al. [2008], IRIS for the Federal Air Marshal Service Jain et al. [2010a], GUARDS for the Transportation Security Administration Pita et al. [2011a], PROTECT for the Boston Coast Guard Shieh et al. [2012], and TRUSTS for the Los Angeles Metro Rail System Yin et al. [2012b]. At the core of these applications is the Stackelberg game model. A solution to these Stackelberg games yields the optimal mixed strategy, or the optimal allocation of the defender's resources.

However, game theoretic models for real-world problems can have trillions of pure strategies for both players. Thus, scalable algorithms to solve these game-theoretic models are thus required to obtain solutions for real-world domains: e.g., scheduling 10 air marshals to protect 100 flights yields $\binom{100}{10} \approx 1.7 \times 10^{13}$ unique assignments (or pure strategies) for the defender. Such large models cannot even be stored in the memory of computers today, let alone be solved by existing algorithms. I have provided algorithms especially designed to scale-up to exponentially many pure strategies for both players, as required to compute solutions for large real-world domains. My research on computational game theory provides algorithms that have enabled optimal solutions to

be computed for domains with: (i) trillions of strategies for the defender, (ii) trillions of strategies for the attacker, and (iii) Bayesian Stackelberg games with many adversary types.

These algorithms avoid representing the entire game in memory, while computing solutions for the *entire large problem*. These algorithms are built on the following insights: (i) Real-world domains have exponentially many *pure strategies for the defender* (e.g. a combination of checkpoints), and so, an incremental approach of generating pure strategies of the defender is required. This will avoid enumerating all the pure strategies, and will only add a pure strategy if the pure strategy would help increase defender payoff. (ii) In domains with exponentially many attacker pure strategies, an incremental approach to generate pure strategies for the attacker (e.g. attack paths) should be used to avoid enumeration of the pure strategy set of the attacker. (iii) A Bayesian Stackelberg game can be decomposed into *hierarchically*-organized smaller games, each with smaller number of attacker types, providing heuristics which can be used to eliminate the never-best-response (that is, dominated) pure strategies of the attacker. I also provide mathematical guarantees for the obtained solutions: the algorithms can compute the *globally optimal solution* and can also be tuned to return an approximate solution with quality guarantees.

These insights provide speed-ups by reducing the size of the game: while insights on strategy generation restrict the game size by efficiently generating sub-games that include a pure strategy only if it improves the player's payoff, the hierarchical approach pre-processes the input Bayesian Stackelberg game instance and removes the attacker pure strategies that cannot be part of the optimal solution. Furthermore, I have investigated what properties of Stackelberg security game instances make them hard to solve in practice, across different input sizes and different security domains. The algorithms developed in my thesis have also been deployed in the real-world.

8.1 Contributions

While previous algorithms could not scale to domains with more than 1000 pure strategies in Stackelberg games, my thesis provides novel algorithms built on large-scale optimization techniques that scale to billions of pure strategies for both players. My thesis made the following contributions:

- **ASPEN:** I designed ASPEN [Jain et al., 2010b] for large security problems with arbitrary scheduling constraints, e.g., the problem of scheduling air marshals on board flights. ASPEN builds on the large-scale optimization approach of *branch-and-price*, which uses a combination of branch-and-bound, linear programming and network flows to efficiently compute the solution. In fact, ASPEN is the algorithm that powers the IRIS system.
- **RUGGED and SNARES:** I designed RUGGED for domains where both the defender and the attacker have billions of pure strategies and they operate on a network [Jain et al., 2011b], e.g., when considering cyber-security or protection of an urban road network. The RUGGED algorithm uses a *double-oracle* methodology, which is similar to column/cut generation approaches proposed in operations research. The RUGGED algorithm laid the foundation for SNARES, which exploiting sub-modularity properties in the problem, built on RUGGED, and provided orders of magnitude speed-ups [Jain et al., 2013]. We are, in fact, in discussions with the police force of Mumbai, India to see how SNARES may be made available to them for deploying checkpoints on the roads of Mumbai.
- **HBSG and HBSA:** Furthermore, modeling uncertainty is an important challenge when focusing on real-world domains. Uncertainty is modeled through the *Bayesian* extension of Stackelberg games. I thus developed an efficient computational approach for solving large

Bayesian Stackelberg games, or Stackelberg games with many attacker types. I proposed a hierarchical methodology of decomposing large *Bayesian* Stackelberg games into many smaller Bayesian Stackelberg games, and provided a framework to use the solutions to these smaller games to efficiently apply *branch-and-bound* on the original large Bayesian Stackelberg game. Using this hierarchical methodology, I have provided two algorithms: HBGS and HBSA tailored to compute efficient solutions with and without arbitrary scheduling constraints respectively [Jain et al., 2011a].

- **Deployment-to-Saturation ratio:** I have studied problem instances for Stackelberg games broadly to identify the properties that make a *problem instance* computationally challenging. I formalized the concept of the *deployment-to-saturation* ($d:s$) ratio in Stackelberg security games, and showed that problem instances for which $d:s = 0.5$ are computationally harder than instances with other $d:s$ ratios for a wide range of different domains, algorithms, solvers or equilibrium computation methods [Jain et al., 2012]. This work also provides evidence that the computationally hard region is also one where optimization is most beneficial to the real-world security agencies, corroborating the need for algorithmic advances. Furthermore, I use the concept of phase transitions to better understand this computationally hard region.
- **Deployments – ARMOR and IRIS:** My work has also been deployed in the real-world: I have developed algorithms for and subsequently led the building of the IRIS system that is used by the Federal Air Marshals Service (FAMS) to schedule air marshals on board international commercial flights since October 2009 [Jain et al., 2010c]. I also worked on the ARMOR system, which is in use by the Los Angeles airport police [Pita et al., 2008]. Furthermore, the success of IRIS and ARMOR systems has led to newer deployments

of such algorithms in other real-world security domains, like the PROTECT system for the U.S. Coast Guard [Shieh et al., 2012], and the TRUSTS system for the LA Sheriff Department [Yin et al., 2012b].

8.2 Future Plans

The research described in this thesis is driven by the vision of a world where agent technologies are widespread, and working to assist decision makers in critical domains, with emphasis on (i) *security*, e.g., protecting cyber-networks and transportation systems, (ii) *sustainability*, e.g., forest and wildlife conservation, and (iii) *safety*, e.g., health care and disaster response.

The mathematical framework of game theory is appropriate for analyzing decision making for all these domains. However, there are three significant research areas that need to be developed towards my vision: (i) Scalable behavioral game theory: computing solutions for large real-world domains in the presence of humans, who may be boundedly rational or have limited computationally capability; (ii) Stochastic coalitional game theory: analyzing decision making for a team of agents in an uncertain environment; and (iii) Spatiotemporal game theory: performing computations over continuous space and time. My current research has focused on addressing these challenges, with the focus of my Ph.D. thesis being scalable game theoretic algorithms. I briefly describe these pillars of game theory below.

8.2.1 Scalable behavioral game theory

Scalable algorithms that incorporate human decision making are required to obtain game-theoretic solutions for real-world domains. This is required since real human adversaries do not necessarily

act according to abstract models of rationality, since they may have cognitive biases, limited computational ability and uncertain or incomplete information. Instead, humans may rely on heuristics and simplified abstractions for their decision making, which is not captured in traditional game-theoretic models. The insights proposed in my thesis have led to algorithms that can scale to real-world sizes; now these algorithms are being extended with models of human decision making. I have earlier co-developed game-theoretic algorithms that exploit insights from behavioral models like anchoring bias [Pita et al., 2009], and algorithms using strategy generation for achieving scalability and using quantal response for human decision making are forthcoming. However, much more remains to be done in developing scalable algorithms that perform better against humans individually or in groups.

8.2.2 Stochastic coalitional game theory

Many real-world domains have multiple teams of agents, where agents in one team cooperate and coordinate to jointly achieve a common goal. This coordination between agents leads to coalition structures; however, in real-world domains, such coalitions may face uncertainty and adversaries. Payoffs to the team depend on the combination of actions taken by the individual team members, and these payoffs may also vary over time.

Distributed Constraint Optimization Problems (DCOPs) framework is proposed in literature for coordinating between multiple agents, and provides a basis for coalition games. However, DCOPs are limited since they do not handle stochasticity. Thus, I have defined a new class of Distributed Coordination of Exploration and Exploitation (DCEE) [Jain et al., 2009; Taylor et al., 2010] problems, that balance the exploration and exploitation of multiple mobile agents (e.g.,

for robot navigation in buildings for post disaster recovery); I developed novel algorithms and implemented them on actual iRobot Creates.

Coalition formation among agents is a key aspect of real-world decision making, in both non-adversarial as well as adversarial domains. A coalition of adversaries who may not have perfectly-aligned goals must negotiate with each other on who pays which cost or who receives what benefits. Similarly, a coalition of defenders may have teams with different skill sets and goals. It is also critical to understand the dynamic nature of how these relationships form and change. I plan to use DCEE for analyzing defender coalitions in adversarial settings by researching equilibrium analysis of such games, as well as investigate strategic adaptation over time, based on both sound mathematical principles and human behavioral models.

8.2.3 Spatiotemporal game theory

Adversarial domains in the real world require both the defenders and the attackers to act in a geographical space, and in continuous time. Incorporating spatiotemporal modeling in game theory requires novel research — current work often does not model continuous spaces and continuous time. Incorporating spatiotemporal reasoning will improve our ability to address domains such as protection of large forest areas or fisheries of the world or protecting endangered species, and help us generate more effective strategies for the defender. This field has not seen much focus; a situation that I would like to redress.

In summary, for my future work, inspired by real-world challenges of security, sustainability and safety, my vision is to take on fundamental challenges that arise in taking computational game theory into the real world: in problem domains that range from physical security to cybersecurity to forest protection to conservation of wildlife to disaster rescue and management. To address

these fundamental challenges, I would like to conduct basic research built on foundations of interdisciplinary connections to economics, operations research, psychology, health, and law among other disciplines.

Bibliography

- Air Traffic Control: By the Numbers. <http://www.natca.org/mediacenter/bythenumbers.msp>, 2011.
- Micah Adler, Harald Räcke, Naveen Sivadasan, Christian Sohler, and Berthold Vöcking. Randomized pursuit-evasion in graphs. In *ICALP*, pages 901–912, 2002.
- Michele Aghassi and Dimitris Bertsimas. Robust Game Theory. *Math. Program.*, 107:231–273, June 2006.
- Noa Agmon, Vladimir Sadov, Gal A. Kaminka, and Sarit Kraus. The Impact of Adversarial Knowledge on Adversarial Planning in Perimeter Patrol. In *Proceedings of the International Conference on Autonomous Agents and Multiagent Systems (AAMAS)*, volume 1, pages 55–62, 2008.
- S. Alpern. Infiltration Games on Arbitrary Graphs. *Journal of Mathematical Analysis and Applications*, 163:286–288, 1992.
- Francesco Amigoni, Nicola Gatti, and Antonio Ippedico. A game-theoretic approach to determining efficient patrolling strategies for mobile robots. In *Proceedings of the 2008 IEEE/WIC/ACM International Conference on Web Intelligence and Intelligent Agent Technology - Volume 02, WI-IAT '08*, pages 500–503, Washington, DC, USA, 2008. IEEE Computer Society. ISBN 978-0-7695-3496-1. doi: 10.1109/WIIAT.2008.324. URL <http://dx.doi.org/10.1109/WIIAT.2008.324>.
- Bo An, James Pita, Eric Shieh, Milind Tambe, Chris Kiekintveld, and Janusz Marecki. Guards and protect: next generation applications of security games. *SIGecom Exch.*, 10(1):31–34, March 2011. ISSN 1551-9031. doi: 10.1145/1978721.1978729. URL <http://doi.acm.org/10.1145/1978721.1978729>.
- Christopher Archibald and Yoav Shoham. Modeling Billiards Games. In *Proceedings of the International Conference on Autonomous Agents and Multiagent Systems (AAMAS)*, 2009.
- Rudolf Avenhaus, Bernhard von Stengel, and Shmuel Zamir. Inspection Games. In Robert J. Aumann and Sergui Hart, editors, *Handbook of Game Theory*, volume 3, chapter 51, pages 1947–1987. North-Holland, Amsterdam, 2002.
- L. Babu, L. Lin, and R. Batta. Passenger Grouping Under Constant Threat Probability in an Airport Security System. In *European Journal of Operational Research*, volume 168, pages 633 – 644, 2006.

Yoram Bachrach and Ely Porat. Path Disruption Games. In *AAMAS*, pages 1123–1130, 2010.

C. Barnhart, E.L. Johnson, G.L. Nemhauser, M.W.P. Savelsbergh, and P.H. Vance. Branch and Price: Column Generation for Solving Huge Integer Programs. In *Operations Research*, volume 46, pages 316–329, 1994.

Tamer Basar and Geert Jan Olsder. *Dynamic Noncooperative Game Theory*. Academic Press, San Diego, CA, 2nd edition, 1995.

N. Basilico, N. Gatti, and F. Amigoni. Leader-Follower Strategies for Robotic Patrolling in Environments with Arbitrary Topologies. In *Proceedings of the International Conference on Autonomous Agents and Multiagent Systems (AAMAS)*, pages 500–503, 2009.

Dimitris Bertsimas and John N. Tsitsiklis. *Introduction to Linear Optimization*. Athena Scientific, 1994.

Mikel Blanco, Aurelia Valino, Joost Heijs, Thomas Baumert, and Javier Gonzalez Gomez. The Economic Cost of March 11: Measuring the direct economic cost of the terrorist attack on March 11, 2004 in Madrid. *Terrorism and Political Violence*, 19(4):489–509, 2007.

Branislav Bosansky, Viliam Lisy, Michal Jakob, and Michal Pechoucek. Computing Time-Dependent Policies for Patrolling Games with Mobile Targets. In *Tenth International Conference on Autonomous Agents and Multiagent Systems*, pages 989–996, 2011.

Michele Breton, A. Alg, and Alain Haurie. Sequential Stackelberg Equilibria in Two-Person Games. *Optimization Theory and Applications*, 59(1):71–97, 1988.

G. Brown, M. Carlyle, J. Kline, and K. Wood. A Two-Sided Optimization for Theater Ballistic Missile Defense. In *Operations Research*, volume 53, pages 263–275, 2005a.

G. Brown, M. Carlyle, J. Royset, and K. Wood. On The Complexity of Delaying an Adversary’s Project. In B. Golden, S. Raghavan, and E. Wasil, editors, *The Next Wave in Computing, Optimization and Decision Technologies*, pages 3–17. Springer, 2005b.

Gerald Brown, Matthew Carlyle, Javier Salmeron, and Kevin Wood. Defending Critical Infrastructure. In *Interfaces*, volume 36, pages 530 – 544, 2006.

Rina Chandran and Greg Beitchman. Battle for Mumbai Ends, Death Toll Rises to 195. *Times of India*, 29 November 2008.

Peter Cheeseman, Bob Kanefsky, and William M. Taylor. Where the Really Hard Problems are. In *Proceedings of the International Joint Conference on Artificial Intelligence*, pages 331–337, 1991.

CNN. Sources: Air Marshals missing from almost all flights. 2008.
http://articles.cnn.com/2008-03-25/travel/siu.air.marshals_1.air-marshals-federal-air-

Vincent Conitzer and Tuomas Sandholm. Computing the Optimal Strategy to Commit to. In *Proceedings of the ACM Conference on Electronic Commerce (ACM-EC)*, pages 82–90, 2006.

- John Dickerson, Gerardo Simari, V.S. Subrahmanian, and Sarit Kraus. A Graph-Theoretic Approach to Protect Static and Moving Targets from Adversaries. In *AAMAS*, pages 299–306, 2010a.
- J.P. Dickerson, G.I. Simari, V.S. Subrahmanian, and Sarit Kraus. A Graph-Theoretic Approach to Protect Static and Moving Targets from Adversaries. In *Proceedings of the Ninth International Conference on Autonomous Agents and Multiagent Systems (AAMAS-2010)*, pages 299–306, 2010b.
- David Eppstein and Michael T. Goodrich. Studying (Non-Planar) Road Networks Through an Algorithmic Lens. *CoRR*, abs/0808.3694, 2008.
- Merrill M. Flood. The Hide and Seek Game of Von Neumann. *MANAGEMENT SCIENCE*, 18 (5-Part-2):107–109, 1972.
- Jeremy Frank, Ian P. Gent, and Toby Walsh. Asymptotic and Finite Size Parameters for Phase Transitions: Hamiltonian Circuit as a Case Study. *Inf. Process. Lett.*, 65:241–245, March 1998. ISSN 0020-0190. doi: [http://dx.doi.org/10.1016/S0020-0190\(97\)00222-6](http://dx.doi.org/10.1016/S0020-0190(97)00222-6). URL [http://dx.doi.org/10.1016/S0020-0190\(97\)00222-6](http://dx.doi.org/10.1016/S0020-0190(97)00222-6).
- Ehud Friedgut. Sharp thresholds of graph properties, and the k-sat problem. *J. Amer. Math. Soc.*, 12:1017–1054, 1998.
- Shmuel Gal. *Search Games*. Academic Press, New York, 1980.
- Nicola Gatti. Game Theoretical Insights in Strategic Patrolling: Model and Algorithm in Normal-Form. In *Proceedings of the European Conference on Artificial Intelligence (ECAI)*, pages 403–407, 2008.
- Ian P. Gent and Toby Walsh. Phase transitions from real computational problems. In *Proceedings of the 8th International Symposium on Artificial Intelligence*, pages 356–364, 1995.
- Ian P. Gent and Toby Walsh. The TSP Phase Transition. *Artificial Intelligence*, 88(12):349 – 358, 1996.
- M. Haklay and P. Weber. Openstreetmap:user-generated street maps. *Pervasive Computing, IEEE*, 7(4):12–18, 2008.
- E. Halvorson, V. Conitzer, and R. Parr. Multi-step multi-sensor hider-seeker games. In *IJCAI*, pages 336–341, 2009a.
- Erik Halvorson, Vincent Conitzer, and Ronald Parr. Multi-step Multi-sensor Hider-Seeker Games. In *Proceedings of the International Joint Conference on Artificial Intelligence (IJCAI)*, pages 159–166, 2009b.
- J.C. Harsanyi and R. Selten. A Generalized Nash Solution for Two-person Bargaining Games with Incomplete Information. In *Management Science*, volume 18, pages 80–106, 1972.
- Christoph Hauert and Gyrgi Szab. Game theory and Physics. *Am. J. Phys.*, 73(5):405–414, 2005. doi: 10.1119/1.1848514.

- M. Jain, J. Tsai, J. Pita, C. Kiekintveld, S. Rathi, M. Tambe, and F. Ordóñez. Software assistants for randomized patrol planning for the LAX Airport Police and the Federal Air Marshals Service. *Interfaces*, 40:267–290, 2010a.
- Manish Jain, Matthew E. Taylor, Milind Tambe, and Makoto Yokoo. Dcop meets the real world: Exploring unknown reward matrices with applications to mobile sensor nets. In *IJCAI*, 2009.
- Manish Jain, Erim Kardes, Christopher Kiekintveld, Fernando Ordóñez, and Milind Tambe. Security Games with Arbitrary Schedules: A Branch and Price Approach. In *Proceedings of the AAAI Conference on Artificial Intelligence (AAAI)*, 2010b.
- Manish Jain, Jason Tsai, James Pita, Christopher Kiekintveld, Shyamsunder Rathi, Milind Tambe, and Fernando Ordóñez. Software Assistants for Randomized Patrol Planning for the LAX Airport Police and the Federal Air Marshals Service. *Interfaces*, 40:267–290, 2010c.
- Manish Jain, Christopher Kiekintveld, and Milind Tambe. Quality-bounded Solutions for Finite Bayesian Stackelberg Games: Scaling up. In *Proceedings of the International Conference on Autonomous Agents and Multiagent Systems (AAMAS)*, 2011a.
- Manish Jain, Dmytro Korzhuk, Ondrej Vanek, Vincent Conitzer, Michal Pechoucek, and Milind Tambe. A Double Oracle Algorithm for Zero-Sum Security Games on Graphs. In *Proceedings of the International Conference on Autonomous Agents and Multiagent Systems (AAMAS)*, 2011b.
- Manish Jain, Kevin Leyton-Brown, and Milind Tambe. The deployment-to-saturation ratio in security games. In *AAAI*, 2012.
- Manish Jain, Vincent Conitzer, Michal Pechoucek, and Milind Tambe. Security scheduling for real-world networks. In *AAMAS*, 2013.
- Albert Jiang and Kevin Leyton-Brown. A polynomial-time algorithm for action-graph games. In *Artificial Intelligence*, pages 679–684, 2006.
- Armen Keteyian. TSA: Federal Air Marshals. 2010. <http://www.cbsnews.com/stories/2010/02/01/earlyshow/main6162291.shtml>, retrieved Feb 1, 2011.
- Christopher Kiekintveld, Manish Jain, Jason Tsai, James Pita, Milind Tambe, and Fernando Ordóñez. Computing Optimal Randomized Resource Allocations for Massive Security Games. In *Proceedings of the International Conference on Autonomous Agents and Multiagent Systems (AAMAS)*, pages 689–696, 2009.
- Christopher Kiekintveld, Janusz Marecki, and Milind Tambe. Approximation Methods for Infinite Bayesian Stackelberg Games: Modeling Distributional Payoff Uncertainty. In *Proceedings of the International Conference on Autonomous Agents and Multiagent Systems (AAMAS)*, 2011.
- Scott Kirkpatrick and Bart Selman. Critical behavior in the satisfiability of random boolean formulae. *Science*, 264:1297–1301, 1994.

- Daphne Koller and Brian Milch. Multi-agent influence diagrams for representing and solving games. *Games and Economic Behavior*, 45(1):181–221, 2003.
- D. Korzhyk, V. Conitzer, and R. Parr. Complexity of Computing Optimal Stackelberg Strategies in Security Resource Allocation Games. In *Proceedings of the AAAI Conference on Artificial Intelligence (AAAI)*, pages 805–810, 2010.
- Solomon Kullback and Richard A. Leibler. On Information and Sufficiency. *The Annals of Mathematical Statistics*, 22(1):79–86, 1951.
- R.C. Larson. A Hypercube Queueing Modeling for Facility Location and Redistricting in Urban Emergency Services. In *Journal of Computers and Operations Research*, volume 1, pages 67–95, 1974.
- George Leitmann. On Generalized Stackelberg Strategies. *Optimization Theory and Applications*, 26(4):637–643, 1978.
- Joshua Letchford and Yevgeniy Vorobeychik. Computing Randomized Security Strategies in Networked Domains. In *Proceedings of the Workshop on Applied Adversarial Reasoning and Risk Modeling (AARM) at AAAI*, 2011.
- Joshua Letchford, Vincent Conitzer, and Kamesh Munagala. Learning and Approximating the Optimal Strategy to Commit To. In *Proceedings of the International Symposium on Algorithmic Game Theory (SAGT)*, pages 250–262, 2009.
- Robert Looney. Economic Costs to the United States Stemming From the 9/11 Attacks. *Strategic Insights*, 1(6), August ”2002”.
- Kong-wei Lye and Jeannette M. Wing. Game strategies in network security. *International Journal of Information Security*, 4(1–2):71–86, 2005.
- H. Brendan McMahan, Geoffrey J. Gordon, and Avrim Blum. Planning in the Presence of Cost Functions Controlled by an Adversary. In *Proceedings of the International Conference on Machine Learning (ICML)*, pages 536–543, 2003.
- D. Mitchell, B. Selman, and H. Levesque. Hard and Easy Distributions of SAT Problems. In *Proceedings of the American Association for Artificial Intelligence*, pages 459–465, 1992.
- G. L. Nemhauser, L. A. Wolsey, and M. L. Fisher. An Analysis of Approximations for Maximizing Submodular Set Functions–I. *Mathematical Programming*, 14(1):265–294, Dec 1978.
- Nie, R. Batta, Drury, and Lin. Optimal Placement of Suicide Bomber Detectors. In *Military Operations Research*, volume 12, pages 65–78, 2007.
- Martin J. Osborne and Ariel Rubinstein. *A Course in Game Theory*. MIT Press, 1994.
- Praveen Paruchuri, Milind Tambe, Fernando Ordonez, and Sarit Kraus. Security in Multiagent Systems by Policy Randomization. In *Proceedings of the International Conference on Autonomous Agents and Multiagent Systems (AAMAS)*, 2006.

- Praveen Paruchuri, Jonathan P. Pearce, Janusz Marecki, Milind Tambe, Fernando Ordóñez, and Sarit Kraus. Playing games with security: An efficient exact algorithm for Bayesian Stackelberg games. In *AAMAS-08*, pages 895–902, 2008a.
- Praveen Paruchuri, Jonathan P. Pearce, Janusz Marecki, Milind Tambe, Fernando Ordóñez, and Sarit Kraus. Playing Games with Security: An Efficient Exact Algorithm for Bayesian Stackelberg games. In *Proceedings of the International Conference on Autonomous Agents and Multiagent Systems (AAMAS)*, pages 895–902, 2008b.
- J. Pita, C. Kiekintveld, M. Tambe, E. Steigerwald, and S. Cullen. GUARDS - game theoretic security allocation on a national scale. In *AAMAS*, pages 37–44, 2011a.
- James Pita, Manish Jain, Craig Western, Christopher Portway, Milind Tambe, Fernando Ordóñez, Sarit Kraus, and Praveen Paruchuri. Deployed ARMOR Protection: The Application of a Game-theoretic Model for Security at the Los Angeles International Airport. In *Proceedings of the International Conference on Autonomous Agents and Multiagent Systems (AAMAS), Industry Track*, pages 125–132, 2008.
- James Pita, Manish Jain, Fernando Ordóñez, Milind Tambe, Sarit Kraus, and Reuma Magorichen. Effective solutions for real-world Stackelberg games: When agents must deal with human uncertainties. In *Proceedings of the International Conference on Autonomous Agents and Multiagent Systems (AAMAS)*, 2009.
- James Pita, Manish Jain, Fernando Ordóñez, Milind Tambe, and Sarit Kraus. Robust Solutions to Stackelberg Games: Addressing Bounded Rationality and Limited Observations in Human Cognition. *Artificial Intelligence Journal*, 174(15):1142–1171, 2010, 2010.
- James Pita, Christopher Kiekintveld, Milind Tambe, Erin Steigerwald, and Shane Cullen. GUARDS - Game Theoretic Security Allocation on a National Scale. In *Proceedings of the International Conference on Autonomous Agents and Multiagent Systems (AAMAS)*, 2011b.
- R. Porter, A. Ronen, Y. Shoham, and M. Tennenholtz. Mechanism Design with Execution Uncertainty. In *Proceedings of the Conference on Uncertainty in Artificial Intelligence (UAI)*, 2002.
- S. Ruan, C. Meirina, F. Yu, K. R. Pattipati, and R. L. Popp. Patrolling in a Stochastic Environment. In *10th Intl. Command and Control Research and Tech. Symp.*, 2005.
- William Ruckle, Robert Fennell, Paul T. Holmes, and Charles Fennemore. Ambushing Random Walks I: Finite Models. *Operations Research*, 24:314–324, 1976.
- Todd Sandler and Daniel G. Arce M. Terrorism and Game Theory. *Simulation and Gaming*, 34(3): 319–337, 2003.
- Robert Savit, Radu Manuca, and Rick Riolo. Adaptive Competition, Market Efficiency, Phase Transitions and Spin-Glasses. *University of Michigan*, 82:2203–2206, 1999.
- E. Shieh, B. An, R. Yang, M. Tambe, C. Baldwin, J. DiRenzo, B. Maule, and G. Meyer. PROTECT: An application of computational game theory for the security of the ports of the United States. In *AAAI*, pages 2173–2179, 2012.

- John Slaney and Toby Walsh. Phase Transition Behavior: from Decision to Optimization. In *Proceedings of the 5th International Symposium on the Theory and Applications of Satisfiability Testing, SAT*, 2002.
- Vivek Srivastava, James Neel, Allen B. MacKenzie, Rekha Menon, Luiz A. Dasilva, James E. Hicks, Jeffrey H. Reed, and Robert P. Gilles. Using Game Theory to Analyze Wireless Ad Hoc Networks. *IEEE Communications Surveys and Tutorials*, 7(4), 2005.
- D. Stevens and et. al. Implementing Security Improvement Options at Los Angeles International Airport. 2006. http://www.rand.org/pubs/documented_briefings/2006/RAND_DB499-1.pdf.
- Milind Tambe. *Security and Game Theory: Algorithms, Deployed Systems, Lessons Learned*. Cambridge University Press, 2011.
- Matthew E. Taylor, Manish Jain, Yanqin Jin, Milind Tambe, and Makoto Yokoo. When should there be a "me" in "team"? distributed multi-agent optimization under uncertainty. In *AAMAS*, 2010.
- TSA. TSA: Federal Air Marshals. 2008. <http://www.tsa.gov/lawenforcement/programs/fams.shtm>.
- Jason Tsai, Zhengyu Yin, Jun young Kwak, David Kempe, Christopher Kiekintveld, and Milind Tambe. Urban Security: Game-Theoretic Resource Allocation in Networked Physical Domains. In *Proceedings of the AAAI Conference on Artificial Intelligence (AAAI)*, 2010.
- LAWA. General Description: Just the Facts. 2007. <http://www.lawa.org/lax/justTheFact.cfm>.
- TSA. Transportation Security Administration — U.S. Department of Homeland Security. 2011a.
- TSA. Layers of Security: What We Do. 2011b.
- Eric van Damme and Sjaak Hurkens. Games with Imperfectly Observable Commitment. *Games and Economic Behavior*, 21(1-2):282 – 308, 1997.
- Ondrej Vanek, Michal Jakob, Viliam Lisy, Branislav Bosansky, and Michal Pechoucek. Iterative Game-theoretic Route Selection for Hostile Area Transit and Patrolling. In *Tenth International Conference on Autonomous Agents and Multiagent Systems*, pages 1273–1274, 2011.
- H. von Stackelberg. *Marktform und Gleichgewicht*. Springer, 1934.
- Bernhard von Stengel and Shmuel Zamir. Leadership with Commitment to Mixed Strategies. Technical Report LSE-CDAM-2004-01, CDAM Research Report, 2004.
- Alan Washburn and Kevin Wood. Two-person Zero-sum Games for Network Interdiction. *Operations Research*, 43(2):243–251, 1995.
- Lawrence M. Wein. Homeland Security: From Mathematical Models to Policy Implementation. In *Operations Research*, 2008.

Michael P. Wellman, Daniel M. Reeves, Kevin M. Lochner, Shih-Fen Cheng, and Rahul Suri. Approximate Strategic Reasoning through Hierarchical Reduction of Large Symmetric Games. In *Proceedings of the AAAI Conference on Artificial Intelligence (AAAI)*, 2005.

Wiki. Federal Air Marshal Service. 2008. http://en.wikipedia.org/wiki/Federal_Air_Marshal_Service.

Rong Yang, Christopher Kiekintveld, Fernando Ordóñez, Milind Tambe, and Richard John. Improved Computational Models of Human Behavior in Security Games. In *Proceedings of the International Conference on Autonomous Agents and Multiagent Systems (AAMAS), Extended Abstract*, 2011.

Z. Yin and M. Tambe. A unified method for handling discrete and continuous uncertainty in Bayesian Stackelberg games. In *AAMAS*, pages 855–862, 2012.

Z. Yin, M. Jain, M. Tambe, and F. Ordóñez. Risk-averse strategies for security games with execution and observational uncertainty. In *AAAI*, pages 758–763, 2012a.

Z. Yin, A. Jiang, M. Johnson, M. Tambe, C. Kiekintveld, K. Leyton-Brown, T. Sandholm, and J. Sullivan. TRUSTS: Scheduling randomized patrols for fare inspection in transit systems. In *IAAI*, 2012b.

Zhengyu Yin, Dmytro Korzhyk, Christopher Kiekintveld, Vincent Conitzer, and Milind Tambe. Stackelberg vs. Nash in security games: interchangeability, equivalence, and uniqueness. In *Proceedings of the International Conference on Autonomous Agents and Multiagent Systems (AAMAS)*, 2010a.

Zhengyu Yin, Dmytro Korzhyk, Christopher Kiekintveld, Vincent Conitzer, and Milind Tambe. Stackelberg vs. Nash in Security Games: Interchangeability, Equivalence, and Uniqueness. In *AAMAS*, pages 1139–1146, 2010b.

Zhengyu Yin, Albert Jiang, Matthew Johnson, Milind Tambe, Christopher Kiekintveld, Kevin Leyton-Brown, Tuomas Sandholm, and John Sullivan. Trusts: Scheduling randomized patrols for fare inspection in transit systems. In *Conference on Innovative Applications of Artificial Intelligence (IAAI)*, 2012c.

Jun Zhuang and Vicki Bier. Secrecy and Deception at Equilibrium, with Applications to Anti-Terrorism Resource Allocation. *Defence and Peace Economics*, 22:43–61, 2011.